ADVANCES IN INORGANIC CHEMISTRY, VOL. 37

STRUCTURES OF ORGANONITROGEN–LITHIUM COMPOUNDS: RECENT PATTERNS AND PERSPECTIVES IN ORGANOLITHIUM CHEMISTRY

KARINA GREGORY,* PAUL von RAGUÉ SCHLEYER,* and RONALD SNAITH†

* Institut für Organische Chemie der Universität Erlangen-Nürnberg, W-8520 Erlangen, Germany
† Department of Chemistry, University Chemical Laboratory, University of Cambridge, Cambridge CB2 1EW, England

I. Introduction

The first X-ray crystal structure of an organolithium compound [$(EtLi)_4$] was published (*1*) just over a quarter of a century ago. These intriguing compounds have received increasing attention ever since (*2, 3*). The definition of "organolithium" has broadened. The term now means not only compounds with C—Li bonds [e.g., alkyl- and aryllithiums, RLi; and alkynyllithiums (lithium acetylides), RC≡CLi], but also lithium derivatives of organic molecules in general, e.g., N—Li species such as amidolithiums (R_2NLi, lithium amides) and O—Li species such as lithium enolates [RC ($=CH_2$)OLi]. Indeed, the two most recently published reviews have been largely concerned with lithium enolates (*4*) and with lithiated sulfones (*4a*). A very thorough review now in press (*5*) describes the syntheses and structures of carbanions of alkali (and alkaline earth) metal cations, and includes related species with organic anions such as amide, enolate, and alkoxide. This present review concentrates on compounds with N—Li bonds. These are chiefly lithium imides [iminolithiums $(RR'C{=}NLi)_n$] and their complexes with added Lewis bases (L), and lithium amides [amidolithiums $(RR'NLi)_n$] and their complexes. For the lithium amide species in particular, we discuss only those whose R,R′ groups do not contain additional functionalities, i.e., the R,R′ groups remain largely uninvolved with lithium centers. These species are termed "simple" lithium amides (see Section III,A). Lithium amide structures exhibiting R,R′-group involvement will be covered in a (pending) follow-up review.

A. Uses of N—Li Compounds; Scope of the Review

Organonitrogen–lithium compounds, and particularly lithium amides (R_2NLi), are widely used both in organic and in organometallic syntheses. For the former, these strong bases are employed as proton abstractors (*5–8*), to generate new organolithiums. These can then be derivatized with so-called electrophiles, e.g., alkyl and acyl halides ($E^+ = R^+$ and $R{-}C^+{=}O$) and trimethylsilylchloride ($E^+ = Me_3Si^+$) [Eq. (1)].

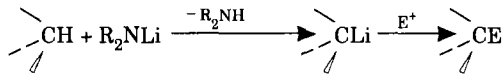

(1)

Alternatively, the newly generated organolithium can be first added to an unsaturated organic electrophile (notably, to a carbonyl compound) prior to "quenching" [Eq. (2)].

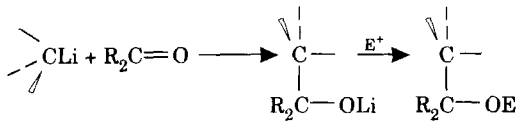

(2)

These R_2NLi bases, especially those with bulky R groups, have the advantage over C—Li reagents (Bu^{n}Li, MeLi, etc.) of having lower nucleophilic character. Proton abstraction is favored over addition to unsaturated functional groups in the organic precursor. Furthermore, such proton abstractions are often not only regiospecific but are also enantiospecific. Hence, there is considerable interest in the use of these bases [including chiral lithium amides (*9*)] in asymmetric syntheses (*10*).

Several R_2NLi bases are now available commercially, e.g., bis(trimethylsilyl)amidolithium, *N*-lithiohexamethyldisilazide [$(Me_3Si)_2NLi$], diisopropylamidolithium [Pr^i_2NLi (LDA)], and (2,2,6,6-tetramethylpiperidinato)lithium, [$Me_2C(CH_2)_3CMe_2NLi$], in the form of solutions of specified molarity in polar solvents such as Et_2O or tetrahydrofuran (THF). These reagents actually are quite specific complexes, $(R_2NLi \cdot xL)_n$, with x defining the degree of solvation and with n defining the degree of association. The preparations and use of reagents of this type have been described in a short article (*11*) and in two recent texts (*12, 13*). These also include details of solvent purification, reagent solubilities, and safety precautions. Procedures for the syntheses of specific lithium reagents also can be found in compilations such as King and Eisch (*14*), whereas Shriver and Drezdzon (*15*) cover all the practical aspects of manipulating oxygen- and moisture-sensitive materials (i.e., all organic lithium compounds).

Lithium amides and lithium imides (iminolithiums) ($R_2C{=}NLi$) have also been used to prepare amides and imides of other metals and metalloid elements, M (*16*), e.g., by reaction with precursors having M—X bonds [e.g., X = Hal, OR, or H; Eq. (3)].

$$\left.\begin{matrix} M{-}X \\ R_2C{=}NLi \end{matrix}\right\} + R_2NLi \longrightarrow \left\{\begin{matrix} M{-}NR_2 \\ M{-}N{=}CR_2 \end{matrix}\right\} + LiX \qquad (3)$$

Despite their extensive synthetic use, it is only quite recently that the NLi species have been isolated and examined. The first single-crystal structure of a lithium amide was the $[(Me_3Si)_2NLi]_3$ trimer. This structure was fully described in 1978 (*17*) [although a powder diffraction study in 1969 also indicated a trimer to be present (*18*)]. Some synthetic advantages of isolating crystalline lithium amides

prior to use were first described in 1983 (*19*). Isolation can ensure reagent purity and allows nonpolar solvents to be used as the reaction medium. For example, $[(Me_3Si)_2NLi{\cdot}OEt_2]_n$, a dimer ($n = 2$) in the solid state, can be prepared by lithiation of $(Me_3Si)_2NH$ in Et_2O. The crystalline solid isolated from such a medium can then be weighed and dissolved in a hydrocarbon solvent for reaction with an organic substrate. As has been pointed out more recently (*20, 21*), prior isolation of not only lithium amides but also of *all* organic lithium reagents generated in solution allows their proper *identification*. Such species are generally solvated, e.g., *not* $(R_2NLi)_n$, but $(R_2NLi{\cdot}xL)_n$, where L is the polar solvent employed during the lithiation of the amine. Isolation often also allows structural characterization of the reagent, in the solid state by X-ray diffraction and in nonpolar solvents (e.g., benzene or toluene) by variable-concentration colligative measurements (cryoscopy, vapor-pressure barometry, etc.) as well as by multinuclear (chiefly, ^6Li, ^7Li, ^{13}C, and ^{15}N) nuclear magnetic resonance (NMR) spectroscopy. The extent of ligand complexation (the value of x) and the concentration- and temperature-dependent degrees of association (the values of n) in solutions of the reagent can thus be ascertained. These are essential data for the full understanding of the reactions of these reagents.

Although synthetic uses have dominated the interest in NLi compounds, our primary concern in this review is the *structures*. The compounds considered usually originate *via* lithiations of organic precursors with N—H bonds (chiefly imines and amines) or *via* additions of organolithiums to CN double or triple bonds, e.g., imines and nitriles. Two other classes of species, with so-called dative NLi linkages, are not treated here and are only mentioned for completeness. First, there are many examples of lithiated organic compounds with central bonds from lithium to anions such as R^- (alkyl, aryl), $RC{\equiv}C^-$ (alkynyl), and RO^- (alkoxy, enolato), whose lithium centers also interact with polar N compounds such as bidentate TMEDA, TMPDA, TMHDA [$Me_2N(CH_2)_nNMe_2$, with $n = 2$, 3, and 6, respectively], and tridentate PMDETA [$Me_2N(CH_2CH_2NMe_2)_2$] ligands. In general, these result in linked cubanelike tetramer, ring dimer, or monomer structures. Schematic representations of these structures, with selected examples, are given in Fig. 1 (*22–27*). Many other examples can be found in recent reviews of the structures of organolithium compounds (*2, 4, 5*). Second, there are a growing number of examples of organic lithium compounds whose anions (R^-, $RC{\equiv}C^-$, RO^-) also contain one or more NMe_2 groups, i.e., in effect, *internal* coordination sites. These also often give rise to tetramers (these are truly isolated, because all Me_2N—Li coordinations take place intramolecularly) and to ring dimers, as illustrated in Fig. 2 (*28–33*).

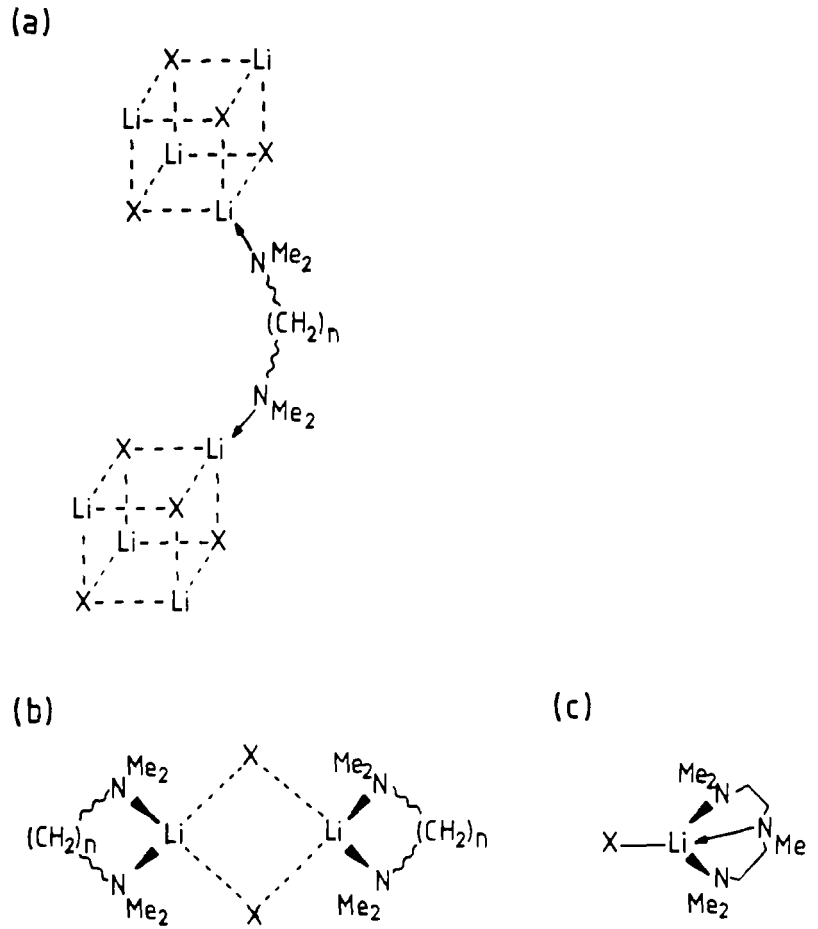

FIG. 1. Structural types found for organolithiums containing neutral N donors: (a) linked tetrameric cubanes, e.g., X = alkyl, n = 2 [$(MeLi)_4$·2TMEDA (*22*)]; X = alkynyl, n = 6 [$(PhC{\equiv}CLi)_4$·2TMHDA (*23*)]; (b) ring dimers, e.g., X = aryl, n = 2 [$(PhLi{\cdot}TMEDA)_2$ (*24*)]; X = alkynyl, n = 3 [$(Ph{\equiv}CLi{\cdot}TMPDA)_2$ (*25*)]; X = enolato, n = 2 {$[Bu^tOC(=CMe_2)OLi{\cdot}TMEDA]_2$ (*26*)}; (c) monomers, e.g., X = aryl [PhLi·PMDETA (*27*)].

Other examples of intramolecularly coordinated (by O as well as by N groups) organolithium compounds can be found in Setzer and Schleyer (*2*) and Seebach (*4*). Two recent reviews are also pertinent. Klumpp (*34*) deals with O- and N-assisted lithiation and carbolithiation of non-aromatic compounds, and Snieckus (*34a*) deals with directed (by amide and carbamate groups) ortho metalation in polysubstituted aromatics.

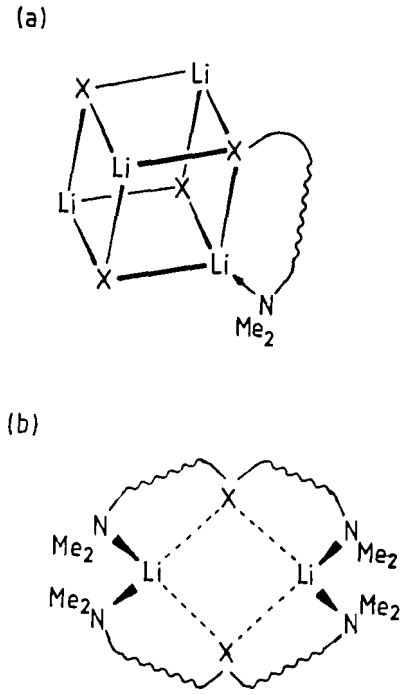

FIG. 2. Structural types found for organolithiums containing internal—NMe_2 donor centers: (a) discrete tetrameric cubanes, e.g., an alkyllithium $[(Me_2NCH_2CH_2CH_2Li)_4$ (*28, 29*)], an aryllithium $\{[(2\text{-}Me_2NCH_2)C_6H_4Li]_4$ (*30*)}, and an enolatolithium $\{[(2\text{-}Me_2NCH_2)C_6H_4\cdot C(=CH_2)OLi]_4$ (*31*)}; (b) ring dimers, e.g., an alkyllithium $\{[(Me_2NCH_2)_2CH\cdot CH(Me)Li]_2$ (*32*)} and an aryllithium $\{[(2,3,5,6\text{-}Me_2NCH_2)_4C_6HLi]_2$ (*33*)}.

Selected NMR studies of aryllithium compounds with *ortho*-NMe_2 and -CH_2NMe_2 groups have also been described (*35*).

We will also include the recently determined structures of imides and amides of other alkali metals (*viz.* Na, K, Rb, and Cs). Only a few structures of derivatives of the heavier alkali metals are known (*3*), but this area can be expected to develop rapidly.

B. Structure and Bonding

Many textbooks still state that organic lithium compounds have appreciable covalent character. This misconception arises from physical properties such as relatively low melting points and solubility in hydrocarbons or other nonpolar solvents. It is true that these properties

are usually associated with covalent, discrete molecular species rather than with typical ionic, three-dimensional latticed "salts" such as $(LiCl)_\infty$. However, such comparisons are misleading. Most of the physical properties of organolithium compounds (the marked exception being conductance) arise due to the overall size and shape of the units making up these materials, and the nature of the peripheries of these units. The lithium bonding within the clusters and rings does not influence these properties. It is now generally agreed that C—Li bonds are essentially ionic (*2, 36, 37*). On electronegativity grounds alone, N—Li bonds must also be similar. For example, natural population analysis of H_3CLi and H_2NLi indicates the C—Li bond to have 89%, and the N—Li bond 90%, ionic character (*38*). Results of MO calculations on N—Li species, presented later in this review, agree in revealing large positive charges on lithium. However, these electrostatic predilections do not necessarily result in polymeric three-dimensional latticed structures. These characterize many common inorganic lithium salts, e.g., $(LiCl)_\infty$, because the anions have spherically symmetrical negative charge distributions and only are constrained by radius ratio criteria (i.e., cation–anion attractions are optimized vis-à-vis cation–cation and anion–anion repulsions). However, there is a crucial difference for organolithium salts. The anions (with C^-, N^-, O^-, etc. centers) are generally large groups whose bulk limits the directionality of the electrostatic interactions. These limitations are increased if the organic lithium compounds are complexed by polar solvents or ligands. These add yet further steric constraints and often decrease the degree of aggregation from that of the pure organolithium.

For the above reasons, organolithium compounds and complexes have been termed "supramolecules" ["complex molecules held together by noncovalent bonds" (*4*)]. What we have here are ionically bonded (at least as far as the central metal–organic anion linkages are concerned) yet often discrete molecular species. Most of their physical properties reflect their limited aggregation and their organic peripheries. These points are stressed in Fig. 3, a schematic presentation of the major structural types of uncomplexed organic lithium compounds.

Several previous reviews have also considered some of these structural generalities (*2, 3, 39–41*). The structural options include polymers. Lithiation of organics (e.g., an "acidic" hydrocarbon, an imine, and a methyl ketone) in nonpolar media (benzene, toluene, and hexanes) often leads to precipitation of amorphous, insoluble products. These can be thought of as arising from continuous vertical association of $(LiX)_n$ rings ("stacking," Fig. 3a) or from continuous lateral association ("laddering" or "fencing," Fig. 3b; $n = 2$ is shown for reasons

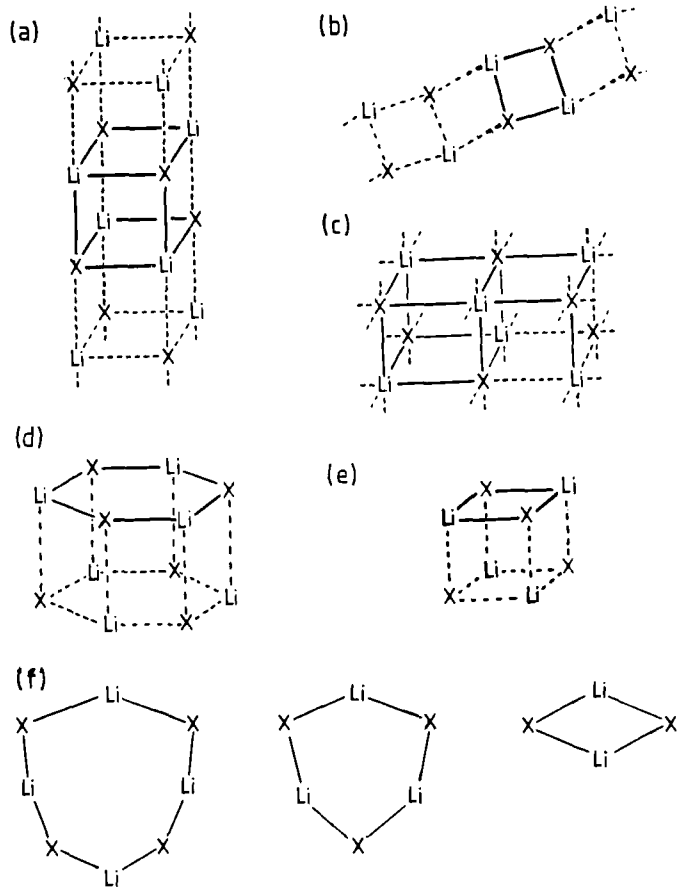

FIG. 3. Structural options for uncomplexed organolithiums: (a) infinite stack of $(LiX)_2$ rings, (b) infinite ladder of $(LiX)_2$ rings, (d) hexamer, a limited stack of two $(LiX)_3$ rings, (e) tetramer, a limited stack of two $(LiX)_2$ rings, and (f) isolated $(LiX)_4$, $(LiX)_3$, and $(LiX)_2$ rings. For contrast, (c) illustrates a segment of an infinite three-dimensional lattice, X being an inorganic "atomic" anion such as Cl^-.

explained later). The reasons for the preference for stacked or laddered structures depend upon the precise stereochemical requirements and orientations of the organic groups (R) in the anion. This will be discussed later, but the crucial point here is the restricted three-dimensional nature of these polymers. In contrast, a typical inorganic lithium salt having a point-charge "atomic" anion (e.g., Cl^-, Fig. 3c) forms a three-dimensional lattice that can be viewed as a stereochemically allowed combination of $(LiX)_2$ ring stacking and laddering. Stereochemical features can also rationalize the other structural types

represented in Fig. 3. Particularly large, sterically demanding R groups within X^- can prevent continuous association, and so result in oligomeric (usually crystalline and organically soluble) materials. For example, stacking can then be limited to just two rings (trimeric ones giving a hexamer, Fig. 3d; dimeric ones giving a tetrahedral tetramer, Fig. 3e). In the limit, stacking and laddering can be prevented altogether, so giving the isolated rings themselves [$(LiX)_n$, with $n = 2, 3$, or 4, Fig. 3f]. The effects of complexation have been illustrated in Figs. 1 and 2. Whether complexation is achieved by addition of neutral Lewis bases or by the presence of base functions within the organic anion, in general it can be said that extensive stacking or laddering is then prevented. This is due largely to the increased steric constraints within the system. The result is that the complexed structures found have limited aggregation. Two-ring stacks of usually dimeric rings, and not of trimeric ones (Figs. 1a and 2a), dimeric rings themselves (significantly, not usually trimeric or tetrameric ones; Figs. 1b and 2b), and, in the limit, monomers (Fig. 1c) are found.

The still quite widespread representations of organolithium reagents as isolated carbanions (R^-) or as organoanions (RO^-, R_2N^-, etc.) are inappropriate if one wishes to understand the nature of these reagents. "Carbanions" must be monomers, but monomeric organolithiums are quite rare. Even for the few known monomers, it is still quite unusual to find totally ion-separated species, even in solution (solvent-separated ion pairs, SSIP). Linked to these points, a general feeling is that many of these structures are in fact in part dictated by the electronic requirements of the metal. However, such dictates are tempered by the steric demands of the organic ligands, both the anionic ones and any Lewis bases present. If this is so, one consequence is that many organic reactions commonly represented as proceeding *via* carbanionic/nucleophilic attack of R^- (of the RLi reagent) on an electrophile or electrophilic center (e.g., the carbon center of a carbonyl

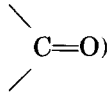

may in fact proceed in the reverse manner, i.e., nucleophilic attack (better termed coordination) of the organic on the electrophilic (Li^+) center of the organolithium. Detailed discussion of this area is beyond the scope of this review, but note that *ab initio* molecular orbital (MO) calculations on the mechanisms and energetics of additions of MeLi and of $(MeLi)_2$ to formaldehyde show that end-on $H_2C{=}O{-}(LiMe)_{1,2}$ complexes form first, prior to $H_2C{-}CH_3$ bond formation *via* a cyclic transition state (*42*). We stress a major point. None of the structures discussed

in this review make much sense if the lithium is excluded. The reactions of these species depend intimately on the metal cation.

Two other bonding features of organolithiums in general require a preliminary note. In addition to their central bonds (Li—C, Li—N, Li—O, etc.), numerous such species appear to have additional and stabilizing Li···H—C interactions. These usually occur when the organic groups restrict association, so leaving lithium centers with low coordination numbers (in general, two or three; e.g., structural types illustrated in Fig. 3d, e, and f). In this sense, they can be considered as compensatory interactions. They were first manifested in short Li···H—C distances found in several crystal structures, some of which are represented in Fig. 4. Indeed, such distances were remarked upon (*43*) regarding the structure of $(MeLi)_4$ [(*44*); Fig. 4a] long before the importance of transition metal and hydrocarbon "agostic" interactions was recognized (*45*).

In methyllithium, the individual tetramers associate further through these intermolecular Li—H—C contacts. Short Li to hydrocarbon group distances are also apparent in the linked structures of several lithium'ates, e.g., $(LiBMe_4)_\infty$ [(*46*); Fig. 4b], and, intramolecularly, in the hexamers (cyclohexylLi)$_6$[(*47*); Fig. 4c] and $(Me_3SiCH_2Li)_6$ (*48*). Full structural details are given in Barr *et al.* (*49*), concerning semiempirical MO calculations on these and related species. Such interactions have also been pinpointed by minimum neglect of differential overlap (MNDO) calculations and by ^6Li–^1H two-dimensional HOESY NMR experiments (*50–51a*). For example, these methods revealed a close Li···H(C_8) contact in a complexed mixture of MeLi and 1-lithionaphthalene (but not in the latter alone), and indeed second lithiation does occur specifically at this 8-(peri) position (*51*). Interactions such as these can also be important in N—Li structures, as will be discussed later. The second bonding feature concerns the importance or otherwise of Li···Li interactions. In many organolithium crystal structures, relatively short Li—Li distances are observed, usually much shorter than the distance found in lithium metal (3.04 Å) and frequently shorter than that found in the Li_2 molecule (2.74 Å). For example, in $(MeLi)_4$ this distance is 2.68 Å (*44*), whereas in $(LiX)_2$ dimers in general (X = R^-, $RC{\equiv}C^-$, R_2N^-, RO^-, etc.), which characteristically have rather acute angles (~75°) at the bridging X groups, the Li—Li cross-ring distance can be as small as 2.30 Å (*2*). The key question is, do such short contacts reflect metal–metal bonding? Most MO calculations indicate not; for example, recent optimizations and topological analyses of 23 RLi structures found no Li—Li bond paths (*52*). NMR experiments can give only somewhat inconclusive results. Thus, using the COSY

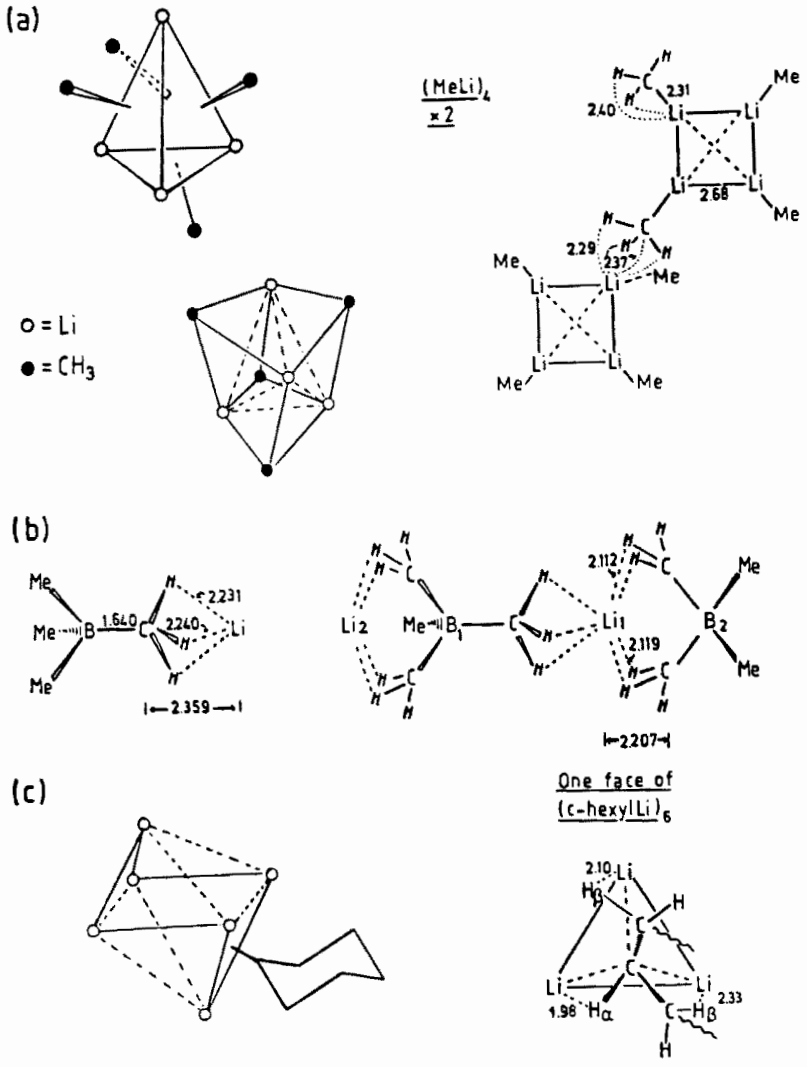

FIG. 4. Lithium compounds exhibiting short Li···H—C contacts in the solid state: (a) representations of $(MeLi)_4$, and of the intercubane contacts found, (b) Li—H_3C and Li—H_2C contacts found in $(LiBMe_4)_\infty$ and (c) part of the structure of (cyclohexyllithium)$_6$, and Li—αHC, —βHC contacts found over its Li_3 faces.

technique, the first homonuclear $^6Li,^6Li$ coupling (~0.1 Hz) was recently detected in tetrahydrofuran (THF) solutions of 3,4-dilithio-2,5-dimethyl-2,4-hexadiene (a tetramer in the solid, with four inner and four outer Li atoms). However, it is not known if such coupling is direct or if it occurs *via* the lithiated carbon atoms (*50, 53*). For several reasons, it is likely that short Li—Li contacts in organolithiums have little or no bonding significance. First, there is the problem that it is not possible to find a proper reference distance for a "single" lithium–lithium bond within such species. Cross-references over very disparate bonding situations, ionic (organolithiums), to metallic (Li metal), to covalent (the Li_2 molecule), are hardly valid. Second, in organolithiums, which are essentially ionically bonded species, the Li centers bear quite substantial $\delta+$ charges. By inference, the essential interaction between such centers is a repulsive/antibonding one. Of course, Li^+ centers are found in lithium metal, but there they have ($1e^-$) electron density between them, so mediating against repulsions. In organolithiums this $1e^-$ per metal atom is largely transferred to, and used in bonding to, the organic groups. A final point is that, even if a fair proportion of the $1e^-$ available to each Li atom was concentrated between the metal centers, the thermodynamic value of a resulting fractional Li—Li bond would be small in comparison with the value of the $Li^{\delta+}$–organic anion$^{\delta-}$ bonding; witness the weak single metal–metal bonds found in lithium itself.

The above discussion of the types of organic lithium compounds, their synthetic uses, and the structural and bonding features they possess sets the scene for the bulk of the review. Here we turn our attention specifically to the structures of NLi compounds.

II. Lithium Imides (Iminolithiums) and Their Complexes; Ring Stacking

A. Uncomplexed Lithium Imides ($RR'C{=}NLi)_n$: Solid-State Structures

Lithium imides [$(RR'C{=}NLi)_n$] have until recently been used without prior isolation. Such use has been as reagents in the syntheses of iminoderivatives of many other metals and metalloids (M) *via* reactions with M—X bonds [X = halide, in particular; see Eq. (3)]; e.g., of main group metals and metalloids Be (*54*), B (*55, 56*), Al (*57, 58*), Si (*59*), and P (*60*), and of transition metals Mo, W (*61*), and Fe (*62*). Addition of organolithiums to nitriles [Eq. (4)] and the lithiation of imines, commonly by Bu^nLi [Eq. (5)], are the most common preparative routes to lithium imides.

$$RLi + R'C{\equiv}N \longrightarrow 1/n(RR'C{=}NLi)_n \quad (4)$$

$$Bu^nLi + RR'C{=}NH \longrightarrow 1/n(RR'C{=}NLi)_n + Bu^nH \quad (5)$$

The lithium imides, produced, e.g., by PhLi additions to PhC≡N, *p*-$ClC_6H_4C{\equiv}N$ (*63*), and $Me_2NC{\equiv}N$ (*64*), have been reacted with organosilylchlorides [R''_3SiCl, to give $Ph(R)C{=}NSiR''_3$ derivatives] or have been hydrolyzed [to give, e.g., the imine $Ph(Me_2N)C{=}NH$]. The imine precursors for Eq. (5) have generally been prepared by addition of Grignard reagents to nitriles, followed by hydrolysis [Eq. (6)].

$$RMgHal + R'C{\equiv}N \longrightarrow RR'C{=}NMgHal \xrightarrow{H_2O} RR'C{=}NH \quad (6)$$

Examples include imines with R = R′ = Bu^t, Ph, and *p*-MeC_6H_4 (*65*). For an imine in which R ≠ R′, e.g., $Ph(Bu^t)C{=}NH$, successful syntheses have employed either PhC≡N + Bu^tMgBr (*65*) or $Bu^tC{\equiv}N$ + PhMgBr (*61*) additions, for example.

The first isolation and characterizations (largely by elemental analyses and infrared (IR) spectroscopy) of lithium imides were described in 1968 (*66*). $(Ph_2C{=}NLi)_n$, a yellow amorphous solid, was prepared from reactions in ether of PhLi + PhC≡N or of MeLi + $Ph_2C{=}NH$. $[Ph(Me)C{=}NLi)]_n$, also a yellow powder was obtained by reacting MeLi and PhC≡N in ether. $[(Me_2N)_2C{=}NLi]_n$, a crystalline hydrocarbon-soluble material, was produced by MeLi lithiation of the imine $(Me_2N)_2C{=}NH$. The syntheses of crystalline $(Bu^t_2C{=}NLi)_n$ (*55, 67*) from Bu^tLi + $Bu^tC{\equiv}N$ in hexane, and of (incompletely characterized) $[Ph(Me_2N)C{=}NLi]_n$ and $\{Ph[(Me_3Si)_2N]C{=}NLi\}_n$ from additions to PhC≡N of the lithium amides Me_2NLi and $(Me_3Si)_2NLi$, respectively (*68*), were described shortly afterward.

In the last decade, the syntheses, characterization, and solid-state structures of four crystalline iminolithiums have been published. All of them are hexamers: $(Bu^t_2C{=}NLi)_6$ (**1**) (*69–72*), $[(Me_2N)_2C{=}NLi]_6$ (**2**) (*70–72*), $[Bu^t(Ph)C{=}NLi]_6$ (**3**) (*71, 72*), and $[Me_2N(Ph)C{=}NLi]_6$ (**4**) (*71, 72*). Both of the methods shown in Eqs. (4) and (5) gave over 80% yields (*72*). The structures of (**1**)–(**4**) are all extremely similar. One typical view, emphasising the six lithium atoms, is shown in Fig. 5 for hexamer (**4**). The metal core can be viewed as a folded chair-shaped Li_6 ring, or as a pseudooctahedron with the apical lithium atoms extended slightly. The dihedral angles between the chair "seat" and "back" in the Li_6 cores of (**2**)–(**4**) average 80 ± 2° [(**1**) is excluded, because its structure was rather imprecisely determined (*69*)]. This contrasts with the 130.7° value for the chair form of cyclohexane and 54.7° for a pure octahedron. In the related hexameric structures of $(cyclohexylLi)_6$ (*47*) and of $(trimethylsilylLi)_6$ [$(Me_3SiLi)_6$] (*73*), these mean angles are 72.9° and

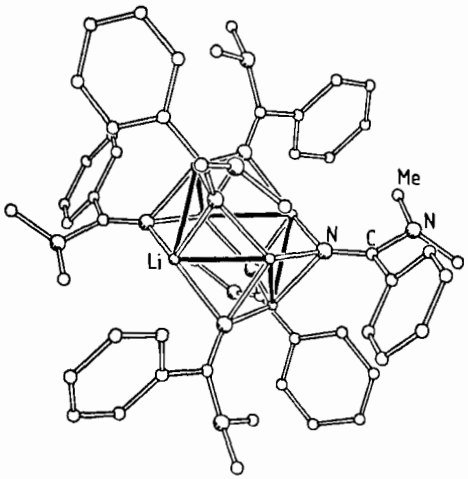

FIG. 5. Molecular structure of the iminolithium hexamer $[Ph(Me_2N)C{=}NLi]_6$ (**4**), highlighting the Li_6 core.

70.5°, respectively, so that the $(iminoLi)_6$ chairs are rather more upright. Each of the six smaller Li_3 triangular faces is bridged by a μ_3-imide ligand; the two larger faces are vacant. Each Li atom then has two short contacts to other Li atoms [mean Li—Li distance 2.48 ± 0.03 Å for (**2**)–(**4**)], two longer Li contacts that form part of each open face (3.21 ± 0.05 Å), and one cross-ring distance (4.05 ± 0.05 Å). As noted in Section I,B, even the shortest contacts do not imply Li—Li bonding.

These hexameric $(RR'C{=}NLi)_6$ molecules are highly ionic. The best quantitative evidence for this comes from *ab initio* MO calculations (6-31G level) on $H_2C{=}NLi$, $(H_2C{=}NLi)_2$, and $(H_2C{=}NLi)_3$ (*72*, *74*). [Calculational results are discussed in full later (see Section II,D)]. A Mulliken population analysis (which tends to underestimate the ionicity) for all three species gave charges on Li of +0.62 to +0.65, and on N of −0.74 to −0.81*e*. When the dimer calculation was repeated with only Li^+ centers present (i.e., the 2s and 2p orbitals were omitted in the lithium basis set) the optimized geometry was very similar (angles within 1°, bond lengths within 0.02 Å) to that using the full basis set. The calculated dimerization energies also were quite close, 73.3 kcal mol^{-1} for the partial basis set and 66.0 kcal mol^{-1} for the full basis set. Furthermore, the lengths of the C=N bonds in the RR'C=N ligands of (**2**)–(**4**) (averaging 1.244, 1.255, and 1.261 Å, respectively) are like those of double bonds in imines. The ν(C=N) stretching frequencies for these compounds also are similar to those of the precursor imines [e.g.,

1615 cm^{-1} for (**4**) and 1590 cm^{-1} for $Me_2N(Ph)C{=}NH$]. Clearly, the imide ligands do not use the π electron density within their C=N linkages. But the largely electrostatic interactions between the Li^+ cations and the imide ligands, $RR'C{=}N^-$, do not explain why hexamers of a certain type form. This problem extends beyond iminolithiums; such hexamers are found for the uncomplexed $(c\text{-}C_6H_{11}Li)_6$ (*47*) and $(Me_3SiLi)_6$ (*73*), as well as for (tetramethylcyclopropylmethylLi)$_6$ [$(Me_2CMe_2CCHCH_2Li)_6$] (*75*) and several lithium enolates (see Sections II,E and I,B and Fig. 3e).

Reasons for the formation of hexameric organolithium "clusters" have emerged from an analysis of the geometries of the (iminoLi)$_6$ species (**2**)–(**4**) (*71, 72*). When these hexamers [e.g., (**4**), Fig. 5] are viewed through unbridged Li_3 faces, the perspective [as shown in Fig. 6, also for (**4**)] is quite striking; the hexamer appears to be constructed from two vertically associated ("stacked") puckered trimeric rings [$(RR'C{=}NLi)_3$]. The metal atoms of one ring nearly eclipse the nitrogen atoms of the other. This has some physical meaning. Figure 7a shows the orientation of an imino ligand over one Li_3 face of (**4**) (the view direction being approximately along the C=N bond). The basal Li atoms in this Li_3 face belong to the same trimeric ring, and the apical Li atom is in the other ring. This orientation is typical for all the Li_3 faces of (**4**), and indeed for all such faces of hexamers (**2**) and (**3**). This

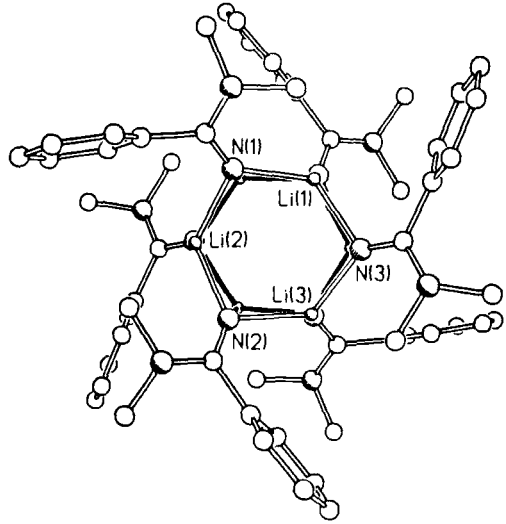

FIG. 6. View of [$Ph(Me_2N)C{=}NLi]_6$ through the unbridged Li_3 faces.

(a)

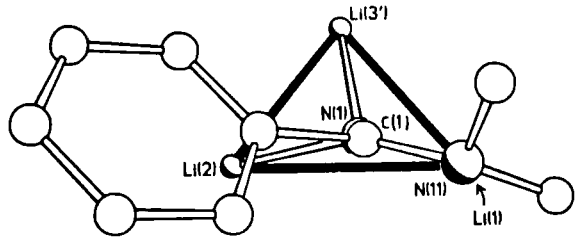

*view direction along C(1)=N(1) bond is inclined at 12.8° to the normal of this Li_3 plane

(b)

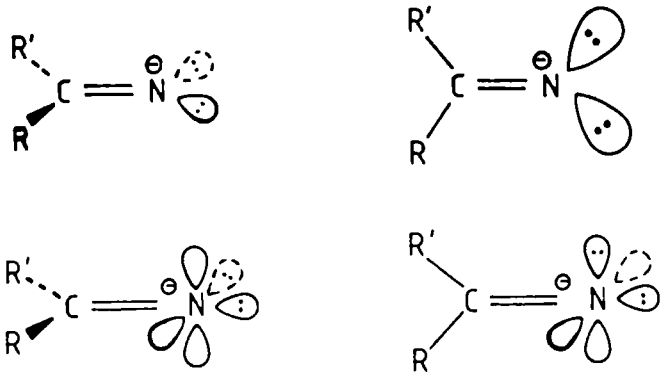

(c)

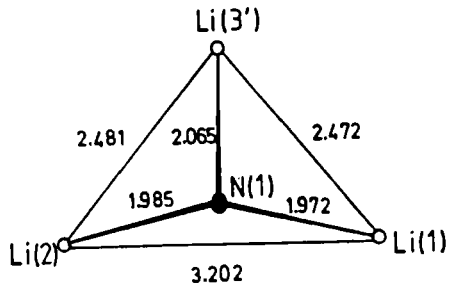

FIG. 7. (a) Orientation of an imino ligand over one Li_3 face of $[Ph(Me_2N)C{=}NLi]_6$ (4); (b) representations depicting the electron density at the imino nitrogens; though there is cylindrical character in this distribution, the in-plane trigonal density is highest; (c) N—Li bond lengths in the Li_3 face shown in (a).

amounts to 24 faces in all, because (**3**) has two independent molecules in its unit cell. Why does the imino ligand tilt with regard to its skeletal plane [e.g., as defined in Fig. 7a, α-C of phenyl·C(1)=N(1)·N(11) of NMe_2]? One possible answer comes from consideration of Fig. 7b. Due to the sp character of the imino N and C atoms, the orientation of the ligands signals the electrostatic directionality (i.e., the dispositions of the lone-pair electron densities on the imino N center). The Li atom which lies very close to the ligand skeletal plane [Li(1) in Fig. 7a] has one lobe on N very much directed toward it. The electrostatic attraction should be strong, and this N-Li link should be relatively short. The other lobe on N bisects the remaining Li centers, but the second basal one [Li(2), which is in the same trimeric ring as Li(1); see Fig. 6] is favored over the apical one [Li(3′), which is in the ring below]. Hence N—Li bonds of unequal lengths are expected, longer and longer still than the more direct N(1)—Li(1) bond. These expectations are confirmed for the face of (**4**) being especially considered (Fig. 7a). As shown in Fig. 7c, quite distinct relatively short [N(1)—Li(1)], medium-length [(N(1)—Li(2)], and long [N(1)—Li(3′)] N—Li bonds are indeed found. A similar relationship between the imino ligand orientations and the N—Li bond lengths is found, without exception, for all the (imino)Li_3 faces of hexamers (**2**)–(**4**).

The N—Li bond lengths given in Table I show that each hexamer has three quite distinct sets of distances, one of each set being found in each of its bridged Li_3 faces: a short bond and a medium-length bond (involving basal Li atoms in terms of Li_3 faces; *cf.* Fig. 7a, involving Li atoms within a given trimeric ring; *cf.* Fig. 6), and a longer bond (to an apical Li atom; an intertrimer bond). Figure 8 emphasises these N—Li bond lengths for (**4**); the perspective and atom labeling are the same as in Fig. 6. During a traverse of each trimer, all the RR′C=N ligands are twisted the same way. This gives alternating short and medium-length bonds. On comparing the trimers, it is seen that every short bond in a given trimer lies above or below a medium-length bond in the other trimer. The result is idealized local D_3, rather than D_6, symmetry. This arrangement is obviously adopted so as to minimize R,R′ repulsions both within and between the trimers.

The above detailed analysis shows that iminolithium hexamers can be regarded as being composed of two stacked trimeric rings. Figure 9 helps explain how the constituent rings associate. Figure 9a shows part of an uncomplexed trimeric ring; the key feature is the general flatness of the system. The $(NLi)_3$ ring is fully planar, and the imino C and (at least) the primary (α) atoms of the groups R,R′ lie also in this plane. [Reasons for this preference for pseudoplanar systems, and for trimeric

TABLE I

N–Li DISTANCES IN THE IMINOLITHIUM HEXAMERS (**2**), (**3**), AND (**4**)[a]

Hexamer	Range of N—Li distances Å	Range of N—Li distances in each trimer[b]		Range of N—Li distances between trimers[b]
		Short bonds	Medium-length bonds	Long bonds
(**2**)[$(Me_2N)_2C{=}NLi]_6$	1.97–2.04	1.97–1.99 (1.98)	2.00–2.01 (2.00)	2.01–2.04 (2.02)
(**3**) $[Bu^t(Ph)C{=}NLi]_6$[c]	1.98–2.05	1.98–1.99 (1.99)	2.01–2.02 (2.02)	2.04–2.05 (2.05)
(**4**)$[Me_2N(Ph)C{=}NLi]_6$	1.96–2.08	1.96–1.98 (1.97)	1.99–2.02 (2.01)	2.03–2.08 (2.06)

[a] From Shearer *et al.* (*69*), Clegg *et al.* (*70*), Barr *et al.* (*71*), and Armstrong *et al.* (*72*).

[b] Mean values in parentheses. Compare Figs. 6 and 8, specifically for hexamer (**4**).

[c] Values given are for one of the two independent molecules found in the unit cell of hexamer (**3**).

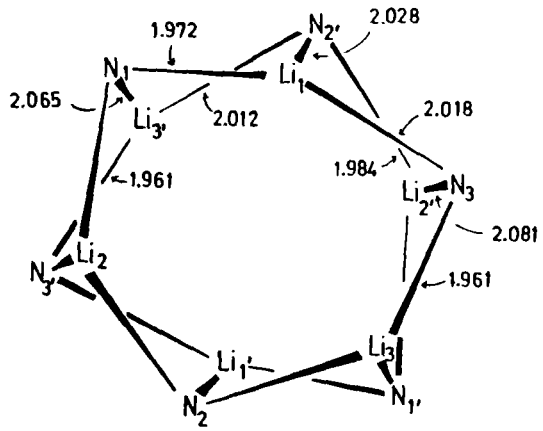

outer N_6 ring	N··N 3.178–3.187 Å	av. LiN̂Li in trimers	107.5°
inner Li_6 ring	Li··Li 2.472–2.487 Å	av. NL̂N „	124.4°
		av. Σ ring angles	695.7°

FIG. 8. N—Li bond lengths in $[Ph(Me_2N)C{=}NLi]_6$ (4), viewed as two stacked trimeric rings.

over dimeric rings, will be substantiated in Section II,B, where the results of MO calculations on $(H_2C{=}NLi)_2$ and $(H_2C{=}NLi)_3$ are presented.] The Li centers in such rings are merely two coordinate. The N atom of each imide anion bears a high charge density. Hence, each ring is set up perfectly to associate further (by stacking). When two or more such rings come together, the coordination number of their Li cations will increase (Fig. 9b). The imino ligands will tilt (and the rings pucker) so that the N-centered regions of electron density are directed toward three Li centers, two in the original ring and the other in the second (*cf.* Fig. 7a and b). As noted above [see Table I and, specifically for hexamer (**4**), Fig. 8], the result is alternating short and medium-length bonds within each constituent ring, and longer N—Li distances between rings.

No iminolithium trimers are known experimentally (the R,R′ substituents would need to be very bulky to prevent stacking). However, two amidolithium trimeric rings have been structurally characterized in the solid state. The lengths of their N—Li bonds give some indication of the strength of the bonding within the hexamers: the mean N—Li bond lengths in $[(PhCH_2)_2NLi]_3$ (*20, 76*) and in $[(Me_3Si)_2NLi]_3$ (*17*) are

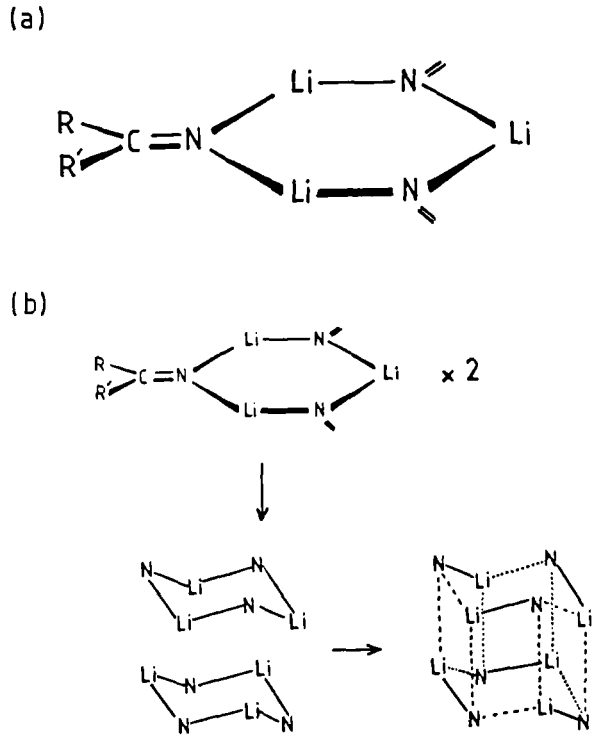

FIG. 9. (a) An isolated, flat (iminoLi)$_3$ trimeric ring (one imide ligand shown); (b) a representation of how two such rings associate, giving a hexamer.

1.95 and 2.01 Å, respectively. Hence the shorter, well-directed N—Li bonds in the constituent trimers of (**2**)–(**4**) (*cf.* Table I) are barely affected by further association: their average length is 1.98 Å. The same is true for the intermediate bonds in each trimer [average length 2.01 Å in (**2**)–(**4**)]. Furthermore, even the bonds between the rings remain quite strong (average, 2.04 Å). This reflects the limited degree of twisting of the RR'C=N ligands [and hence the limited puckering of the (NLi)$_3$ rings] needed to facilitate association. The sum of the angles within the (NLi)$_3$ rings in hexamers (**2**)–(**4**) average 697.5°, 699.0°, and 695.7°, respectively (720° defines total planarity). Nonetheless, even this restricted ligand tilting and ring puckering projects R,R' groups outward from the central (NLi)$_6$ cluster [note the diagonal view of the structure of (**4**), as shown in Fig. 5]. This is sufficient to preclude the stacking of more than two trimeric rings (at least in the solid state).

This ring-stacking concept, used to explain (iminolithium)$_6$ hexa-

mers, can be applied widely, for example, to higher aggregates in solution (Section II,C) and to the widespread occurrence of clustered species (hexamers and tetramers) and rings for the majority of organolithium compounds (Section II,E). Two further experimental observations can be rationalized. First, none of the crystalline hexamers (**1**)–(**4**) are di*aryl*iminolithiums (R,R′ are both Bu^t, both Me_2N, or combinations of these with a single Ph group); in fact, when R,R′ are *both* aryl groups [e.g., Ph (*63, 65, 66*) and *p*-MeC_6H_4 (*65*)], amorphous, seemingly polymeric materials result. These $(RR'C{=}NLi)_n$ ring systems (trimeric or otherwise) are flat. This allows their extensive or continuous association (as illustrated in Fig. 10). Second, the crystal structure of the first uncomplexed mixed-metal imide has recently become available (*77*). This also is a hexamer, $[Bu^t(Ph)C{=}N]_6Li_4Na_2$ (**5**). However, as shown in Fig. 11, it consists of a *triple*-layered stack of *dimeric* $(N{\cdot}metal)_2$ rings, the two outer rings containing essentially Li and the inner one containing Na. It may be that smaller, homocyclic $(NLi)_2$ and $(NNa)_2$ rings provide a better fit for stacking than would mixed (N_3Li_2Na) cycles. However, the considerable substitutional disorder of Li and Na precludes detailed geometric analysis.

B. Iminolithium Complexes: Solid-State Structures

As the lithium centers in the iminolithium hexamers (**1**)–(**4**) are only three coordinate, they might be expected to add monodentate complexing agents (e.g., Et_2O, THF, or pyridine) and, with bi- and tridentate donors (e.g., TMEDA or PMDETA), to give trimers, dimers, or even monomers. In fact, the hexamers are recovered intact after treatment with these various bases (*78*). This possibly reflects a combination of their seemingly quite strong N—Li bonds (including those between the trimeric rings) and the relative steric unavailability of the Li centers in

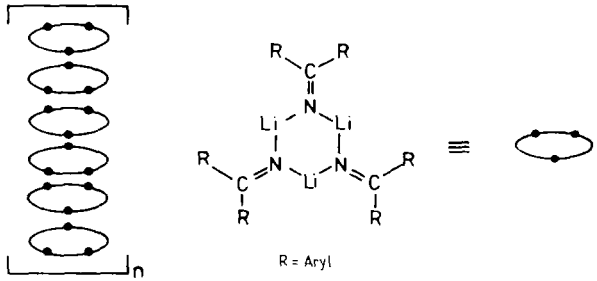

Fig. 10. Association of diaryliminolithium rings into continuous, polymeric stacks.

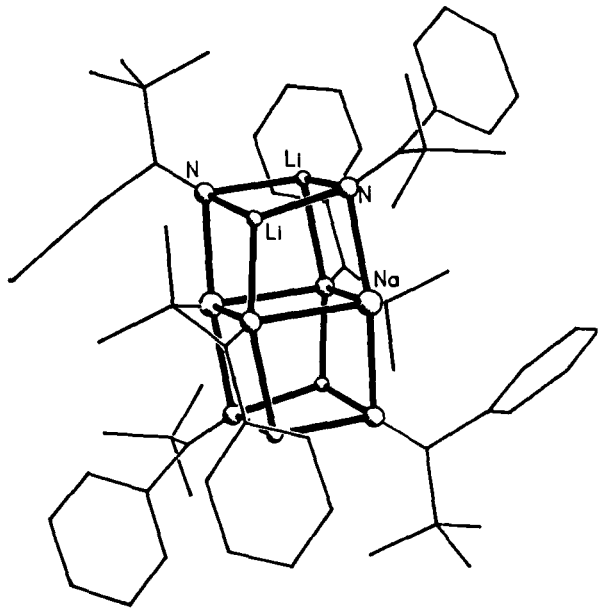

FIG. 11. Molecular structure of the mixed-metal imide $[Bu^t(Ph)C{=}N]_6Li_4Na_2$ (**5**).

these hexamers [e.g., for (**4**), as shown in Fig. 8, the inner Li_6 ring (mean Li—Li distance, 2.48 Å) is surrounded by a larger N_6 ring (mean N—N distance, 3.18 Å)]. Only hexamer (**1**), $(Bu^t_2C{=}NLi)_6$, which on steric grounds might be expected to give the most labile stack, has so far given a complex, and then only with the strong donor HMPA. This complex, the solid-state dimer $(Bu^t_2C{=}NLi{\cdot}HMPA)_2$ (**6**), is shown in Fig. 12 (*78, 79*). Its structure raises two questions. Why is there a switch from a cyclic trimer [as found in (**1**) and in all other hexamers] to a dimer on complexation? Why does this dimer not stack to give a tetrameric pseudocubane structure (as found for many kinds of organolithiums complexed by effectively monodentate donors; *cf.* Figs. 1 and 2, and see also Section II,E)?

A qualitative answer to the first question is provided by consideration of Fig. 13. This shows that $(RR'C{=}NLi)_2$ dimers (Fig. 13a) provide much more room (a larger coordination arc) for further complexation than do $(RR'C{=}NLi)_3$ trimers (Fig. 13b). Moreover, the former require minimal reorganization in terms of bond angle modification at their Li centers. The angles given at Li, ~105° for both a bare dimer and a complexed one and ~145° for a bare trimer, come from several sources. *Ab initio* optimized structures of $(H_2C{=}NLi)_2$ and

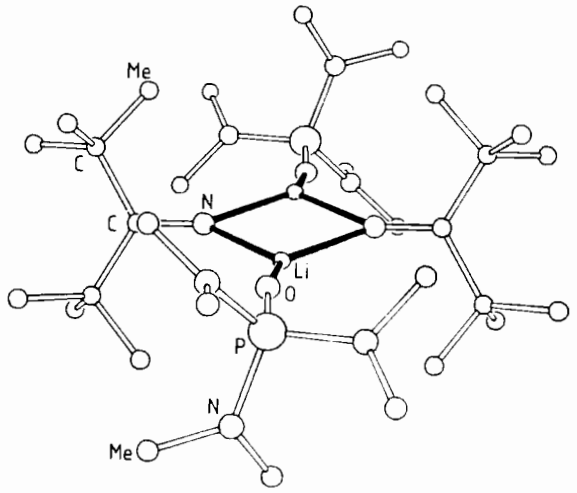

FIG. 12. Molecular structure of the complexed iminolithium ring dimer ($Bu'_2C=NLi\cdot HMPA)_2$ (**6**).

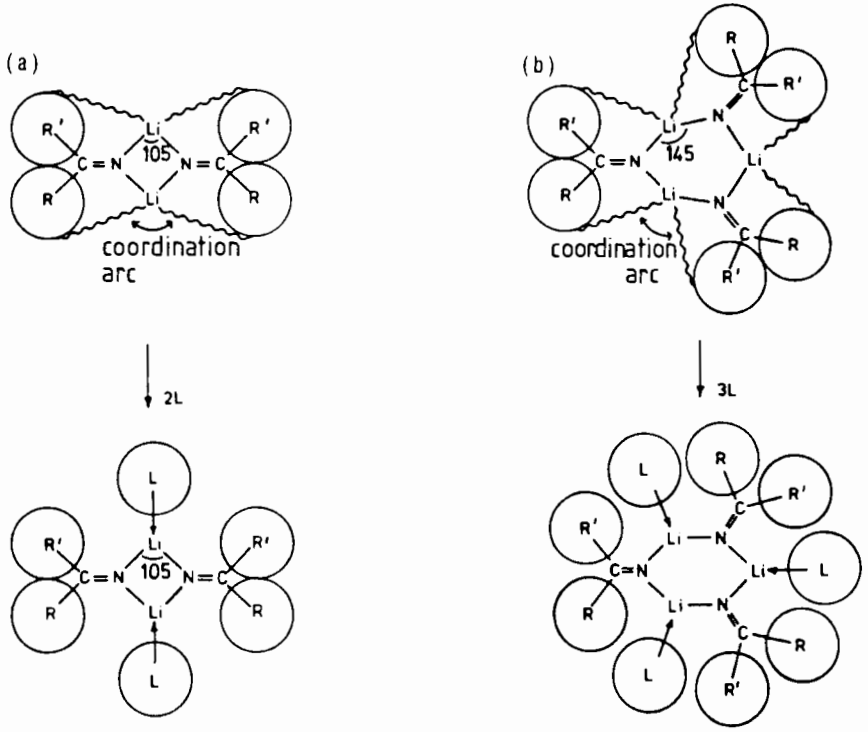

FIG. 13. The steric and geometric consequences of complexing (a) $(iminoLi)_2$ and (b) $(iminoLi)_3$ rings.

$(H_2C{=}NLi)_3$ (*72, 74, 78;* see also Section II,D) have Li angles of 104.4° and 141.2°, respectively. Although uncomplexed iminolithium dimers and trimers are not known experimentally (stacks are favored), a limited number of amidolithiums [$(RR'NLi)_n$, n = 2 and 3] have been reported. Thus [$(Me_3Si)_2NLi]_n$ is a dimer (n = 2) in the gas phase with a ring Li angle of ~100° (*80*), and a trimer (n = 3) in the solid (Li angle 148°) (*17*). In the trimer [$(PhCH_2)_2NLi]_3$, the angle at Li averages 144° (*20, 76*). Numerous solid-state structures of complexed amidolithium ring dimers also are available. A typical example, [$(Me_3Si)_2NLi{\cdot}OEt_2]_2$ has angles at Li of 105° (*19, 81*). In the complexes [$(PhCH_2)_2NLi{\cdot}L]_2$, L = Et_2O or HMPA, these angles average 103° (*20, 76*). In (**6**), the ring angle at Li is 104.6°.

The failure of (**6**) to associate further is due to the severe twisting (58.6°) of the $C_2C{=}N$ moiety of the $Bu^t{}_2C{=}N$ ligands with respect to the $(NLi)_2$ ring plane. The resulting projection of the Bu^t groups above and below the ring plane precludes stacking. Such twisting is needed to avoid a steric clash between the Me groups of the HMPA ligands and those of the Bu^t groups. Yet, somewhat perplexingly, this sterically required realignment of the imino ligands away from their usually preferred orientations seems to have little effect on resulting N—Li bond strengths; indeed these N—Li bonds are the shortest (1.92 and 1.95 Å) known in the solid state. This is due to the largely electrostatic nature of the interaction and is discussed further in the computational section (Section II,D).

The structure of the α-cyanobenzyllithium complex [Ph(H)C⋯C≡≡NLi·TMEDA]$_2$ (*82*) is related to (**6**). This also is a $(NLi)_2$ ring dimer (there are no Li—C bonding contacts). The near-planar anions are at angles of 95.7° and 103.7° to the least-squares plane of the slightly puckered $(NLi)_2$ ring. Hence, as in (**6**), the C substituents (H, Ph) project above and below this ring. The same is true of the chelating TMEDA ligands, so that stacking is doubly prevented. Judging from the bond lengths (C—C, 1.38 Å; C=N, 1.15 Å) within the near-linear anions, $Ph(H)C^-{-}C{\equiv}N$ is a better formulation than $Ph(H)C{=}C{=}N^-$. In any event, the N—Li bond lengths (average 2.04 Å) are much longer than in (**6**). A $(NLi)_2$ ring is also found in the structure of the THF complex of 1-cyano-2,2-dimethylcyclopropyllithium. $[Me_2\overline{CCH_2C}(CN)Li{\cdot}THF]_\infty$ (*4a, 83*). However, the CN groups are now attached to tetrahedral αC^- (of *c*-propyl) centers, and these centers form short (2.14 Å) contacts to Li^+ cations. In this way, each $(NLi)_2$ ring is also part of an $(\overline{C{-}C{-}N{-}Li{\cdot}C{-}C{-}N{-}Li})$ eight-membered ring. These repeating four- and eight-membered rings constitute the polymer. The crystal structure of a complex *di*lithiated trimethylsilylacetonitrile has also

been reported (*4a, 84*). This species crystallizes from ether–hexane solutions as a hexane solvate of $[Me_3Si{\cdot}C(CN)Li_2]_{12}{\cdot}(Et_2O)_6$. Twelve dianions, 24 Li^+ cations, and six Et_2O molecules form, not surprisingly, "an aggregate of unusual size." This contains N—Li, αC—Li, *and* cyano—C—Li bonds.

The general intransigence of the crystalline iminolithium hexamers toward further interaction with Lewis bases is not shown by the amorphous diaryliminolithiums. This may reflect their extensively stacked nature (Section II,A; Fig. 10), which, while raising the lithium coordination number to four in all but the outer rings of the polymer, will presumably weaken individual N—Li bonds. These materials dissolve quite readily in several polar solvents, e.g., THF (*66*), pyridine (*66, 78, 85*), and HMPA (*86*). Crystalline complexes can be recovered from these solutions. Two of these, both derivatives of $(Ph_2C{=}NLi)_n$, have been characterized structurally in the solid state. The tetrameric cubane $(Ph_2C{=}NLi{\cdot}pyridine)_4$ (**7**) is depicted in Fig. 14 (*78, 85*).

For reasons just discussed, complexation has led to the basic ring now being a dimeric $(NLi)_2$ one. However, unlike (**6**), these rings can stack, because both the neutral ligands and the imide substituents are flat. This steric compatibility is illustrated in Fig. 15a, a view of (**7**) looking through the face containing atoms Li 1 and Li 2 [*cf.* the through-face

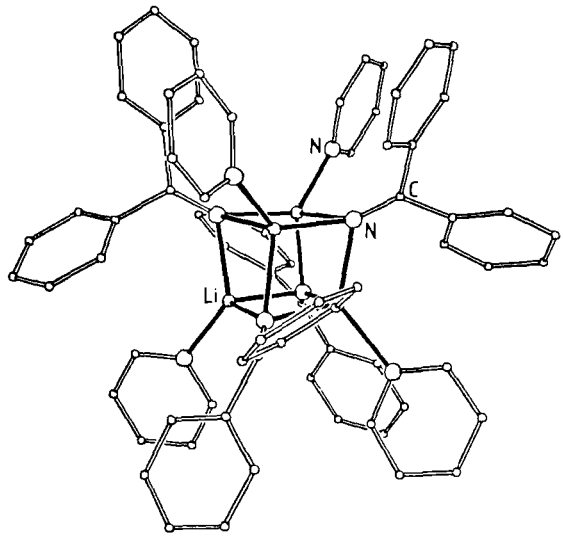

FIG. 14. Molecular structure of the complexed iminolithium tetramer, $(Ph_2C{=}NLi{\cdot}pyridine)_4$ (**7**).

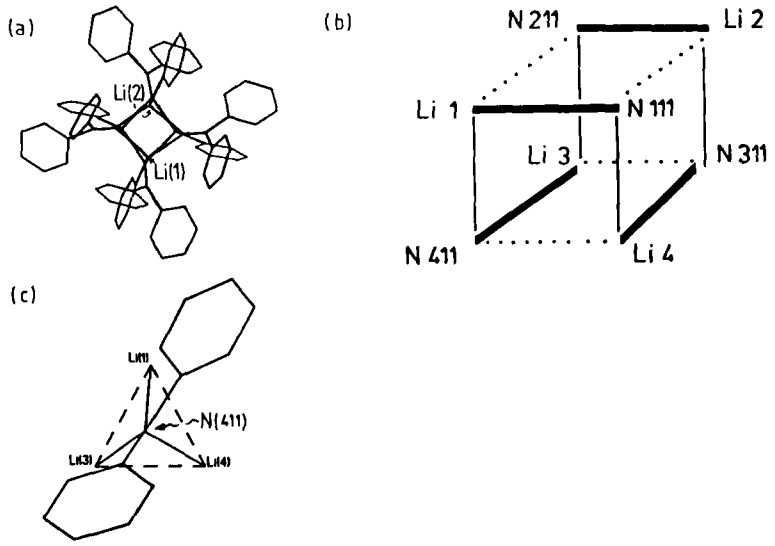

FIG. 15. (a) A view of the $(Ph_2C{=}NLi{\cdot}pyridine)_4$ cubane (**7**), through the face containing Li(1) and Li(2); (b) N—Li bond lengths in $(Ph_2C{=}NLi{\cdot}pyridine)_4$: heavy lines, two center (2.02–2.03 Å, av. 2.03 Å); light lines, between dimers (2.07–2.10 Å, av. 2.08 Å); dotted lines, within dimers (2.15–2.17 Å, av. 2.16 Å); (c) orientation of an imino ligand over one Li_3 face of $(Ph_2C{=}NLi{\cdot}pyridine)_4$.

view for hexamer (**4**) shown in Fig. 6]. The clue to this further association is provided by the (imide)N—Li bond lengths in (**7**). As shown in Fig. 15b, these fall into three distinct sets, *viz.* relatively short (range 2.02–2.03 Å), medium length (2.07–2.10 Å), and long (2.15–2.17 Å). A consistent pattern is seen when one considers the cube as being formed from a top dimer (containing Li 1 and Li 2) stacking upon a lower dimer (containing Li 3 and Li 4) [*cf.* the view of (**7**) in Fig. 15a]. Bonds within a constituent dimer are then alternating short and long ones, with medium-length bonds occurring between dimers. This pattern arises due to the orientation of the $Ph_2C{=}N$ ligands over the Li_3 faces of the tetramer. A typical orientation is shown in Fig. 15c, for imino N 411 bonding to Li3 and Li 4 (within the lower dimer) and to Li 1 (in the top dimer). As illustrated earlier for iminolithium hexamers (Section II,A, especially Fig. 7), the orientation of the $RR'C{=}N^-$ ligand defines the direction of its electrostatic interactions with Li^+ cations. Hence, the bond from N 411 to Li 3 is expected to be relatively short, that to Li 1 rather longer, and that to Li 4 longer still. This is what is observed (Fig. 15b). The changed pattern in going from the hexamers (short and medium-length bonds within rings, long ones between) to this tetramer

(**7**) (short and long bonds within rings, medium ones between) is due to the much greater tilt of RR'C=N ligands over the Li_3 faces in (**7**) (*cf.* Fig. 15c with Fig. 17b). This is caused by the presence of a pyridine molecule on each Li center in (**7**).

The other structurally characterized crystalline complex of $(Ph_2C{=}NLi)_n$, a yellow powder, originated from treatment with HMPA in diethyl ether–toluene. Formulated empirically as ($Ph_2C{=}N$-Li^5_6HMPA), the complex exists in the solid state as the ion pair $[Li(HMPA)_4]^+ \cdot [(Ph_2C{=}N)_6Li_5 \cdot HMPA]^-$ (**8**) (*86*). In the anion of (**8**) (Fig. 16), four uncomplexed Li^+ cations form a tetrahedron (Li—Li mean edge distance, 3.02 Å). The fifth Li^+, which is complexed by an HMPA molecule, caps one face of this tetrahedron, forming much shorter Li—Li contacts (mean distance, 2.60 Å). In the resulting distorted trigonal-bipyramidal anion, three of the imide ligands μ_3 bridge Li_3 faces (those which incorporate the $Li^+ \cdot$HMPA unit) and the other three μ_2 bridge the remaining Li—Li edges. 'Ate complexes (or "triple ions") were first proposed in the 1950s (*87*), but have proved to be rather elusive species (*4*). Apart from (**8**), a crystal structure is available for $[Li(THF)_4]^+ \cdot \{[(Me_3Si)_3C]_2Li\}^-$ (*88*), and the structure of (Ph_4Li-$Na_3 \cdot 3TMEDA$) has recently been interpreted in terms of an 'ate, $[Ph_4Li] \cdot [Na(TMEDA)]_3$ (*89*). Similar triple ions in solution have been

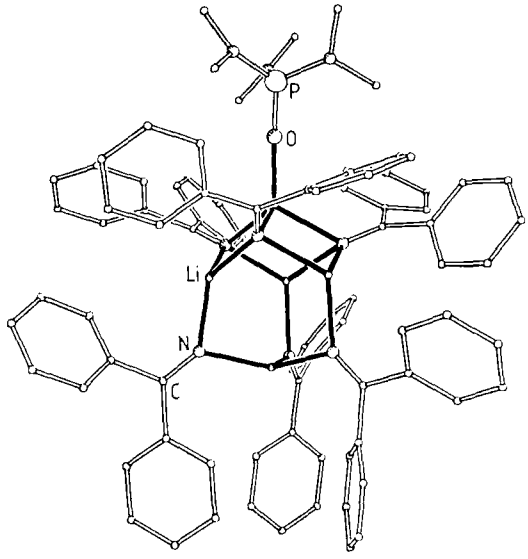

FIG. 16. Structure of the anion of $[Li(HMPA)_4]^+ \cdot [(Ph_2C{=}N)_6Li_5 \cdot HMPA]^-$ (**8**).

detected by NMR spectroscopy, e.g., a combination of ^{6}Li, ^{13}C, and ^{15}N NMR spectra have shown that lithium *N*-isopropylanilide in ether solutions containing HMPA exists partly as $[Li(HMPA)_4]^+ \cdot [(PhPr^iN)_2Li \cdot HMPA]^-$ (*90*). It is not known why (**8**) forms an 'ate structure. However, HMPA and macrocyclic ligands (cryptands, etc.) seem to favor 'ate formation (*4*). It may be pertinent that polar molecules such as these dissolve lithium metal to give $Li(donor)_x^+$ complexed cations and solvated electrons (*91, 92*).

The crystal structure of a mixed-metal imide $[(Me_2N)_2C{=}N]_4LiNa_3 \cdot 3HMPA$ (**9**) (*93*) merits special discussion. Here, complexation leads to formation of a tetrameric pseudocubane structure (Fig. 17) [*cf.* (**7**), Fig. 14]. However, this complex has several unusual features. Although (**9**) was synthesized by reacting two equivalents of $(Me_2N)_2C{=}NH$ with one equivalent each of Bu^nLi and Bu^nNa in an excess (five equivalents) of HMPA, this $LiNa_3$ stoichiometry results, and only the Na^+ ions bear HMPA ligands. The reasons for adoption of an $LiNa_3$ stoichoiometry are not known. However, the large $LiNa_3$ core allows cubane formation even in the presence of bulky HMPA ligands [*cf.* dimeric (**6**)]. Further, it is significant that HMPA ligands are found only on the Na^+ centers. Because of the relatively long Na—O distances

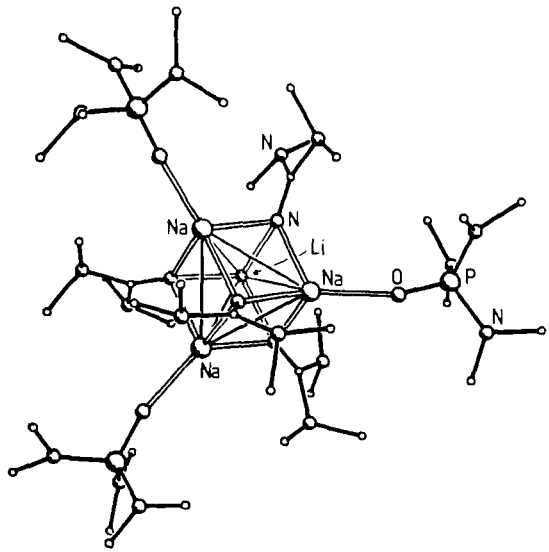

FIG. 17. Molecular structure of the complexed mixed-metal imide $[(Me_2N)_2C{=}N]_4LiNa_3 \cdot 3HMPA$ (**9**).

[mean, 2.25 Å; *cf.* in (**6**), Li—O, 1.86 Å] there is no steric crowding between the Me_2N groups of the HMPA ligands and those of the imide ligands (see Fig. 17). The lack of a ligand on the lithium may be partially compensated by "agostic" Li···H—C interactions (see Section I,B and Fig. 4). Each $Me_2N)_2C{=}N$ ligand bridging the $LiNa_2$ triangular faces of (**9**) has one Me group leaning toward the Li atom, giving Li—C distances of 2.9–3.1 Å and inferred Li—H distances of ~2.5 Å. Unfortunately, the M—N bond lengths observed in this structure do not allow an analysis similar to that performed for the pure N—Li clusters (**1**)–(**4**) and (**7**). The N—Na distances only span the 2.40- to 2.46-Å range and they are distributed randomly within the cluster.

C. Solution Structures of Lithium Imides and Their Complexes

The nature of lithium imides and their complexes in solution has been deduced from cryoscopic measurements in benzene [the relative molecular mass (rmm) values give the degree of association (*n*)] and from high-field ^{7}Li(139.96 MHz) NMR spectroscopic data (*79, 94, 95*). ^{7}Li in conjunction with ^{13}C NMR spectroscopy has been used to study the solution equilibria of C—Li bonded organolithiums, e.g. (*s*- and *t*-butyllithium)$_n$ (*95a*) and (*n*-propyllithium)$_n$ (*96*). However, ^{6}Li-enriched samples often are superior in revealing the nature of the species present in solution *via* observations of ^{6}Li–^{13}C couplings and coupling constants (*97, 98*). ^{6}Li–^{1}H HOESY NMR experiments have also pinpointed the close proximities of Li and H nuclei in several organolithiums (e.g., *51, 51a*). Applications of NMR spectroscopy to the study of organolithiums, with particular emphasis on the recent development of two-dimensional techniques, have been reviewed (*50*).

The solid-state hexamers (**2**)–(**4**) at first appeared to dissolve intact in benzene (*94*). Cryoscopic rmm measurements over a range of concentrations (0.03–0.09 *M*, molarity expressed relative to the empirical formula mass) implied *n* values of 5.9–6.1. Furthermore, their room-temperature ^{7}Li NMR spectra in d_8-toluene each consisted of broad singlets within the narrow chemical shift (δ) range of +0.6 to −0.2 ppm (relative to external phenyllithium in the same solvent). However, variations in temperature and concentration affected the ^{7}Li NMR spectra of (**2**) and, in particular, of (**4**) (*95*). Figure 18a shows these spectra for three d_8-toluene solutions of (**4**) at ~−100°C. The most concentrated solution has a dominant signal at $\delta \sim +0.7$, though five or six other signals (indicated by asterisks) are apparent. On dilution,

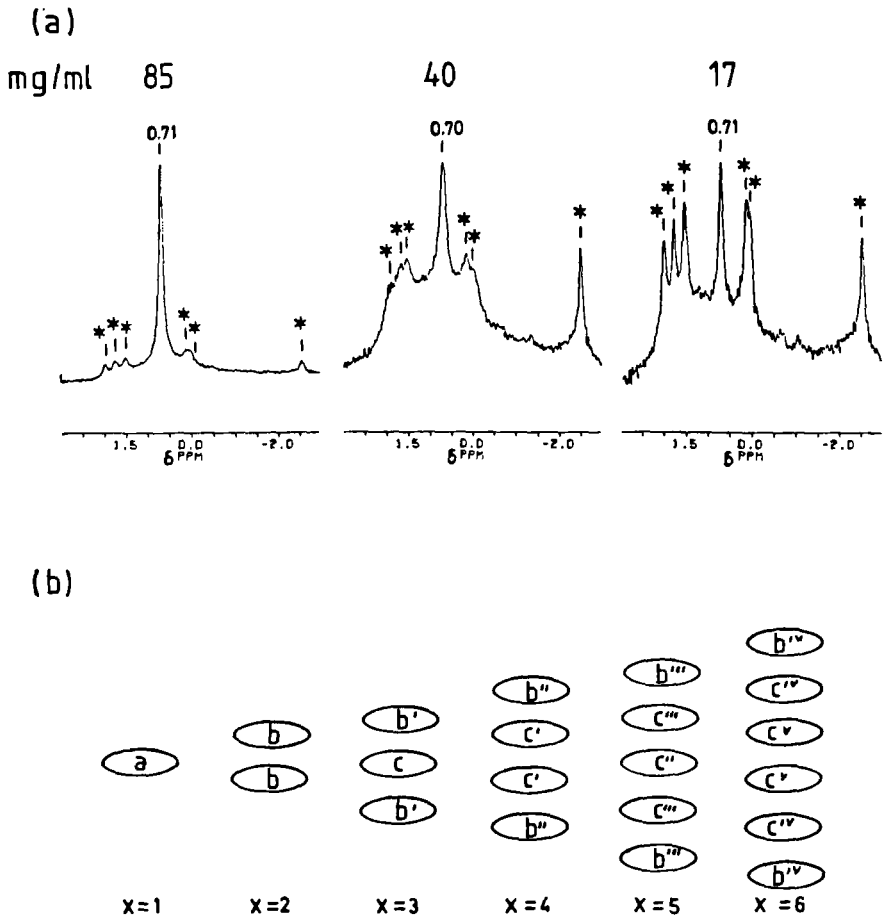

FIG. 18. (a) ^{7}Li NMR spectra (139.96 MHz, −100°C) of three solutions of [Ph(Me$_2$N)C=NLi]$_6$ (4), in d_8-toluene; (b) representation of Li environments in (RR'C=NLi)$_3$ stacks of various extents.

these smaller signals increase in intensity relative to that at δ 0.7. Raising the temperature leads to coalescence; at −60°C, only one resonance is observed. These results may be explained using ring-stacking ideas outlined earlier (Section II,A) and described in full below (Section II,E). Thus, Fig. 18b depicts an iminolithium trimer (RR'C=NLi)$_3$ as an ellipsoid and also shows how the Li environments of type *a* (two coordinate) will vary as trimers (RR'C=NLi)$_{3x}$ stacked to various extents are formed. For example, a hexamer (x = 2) of S_6 symmetry should give only one ^{7}Li signal (type *b*, three-coordinate Li), whereas a non-

amer ($x = 3$) will contain six "outer" Li atoms (with environment b', similar to b) and three equivalent "inner" Li atoms (type c, four coordinate). On this basis, the dominant singlet at δ 0.7 ppm in the ^{7}Li NMR spectrum of the most concentrated solution of (**4**) was assigned to the intact hexamer. The very distinctly separated singlet at $\delta \sim -2.5$ ppm, which increases in relative intensity markedly on dilution, can reasonably be assigned to the trimer (of unique ^{7}Li environment a). The remaining five signals on either side of δ 0.7 ppm must then be due to higher aggregates ($x > 2$). Their formation appears to involve prior dissociation of the hexamer to the trimer, because the growth of these five ^{7}Li signals is accompanied by an increase in the relative intensity of the trimer resonance and a decrease in that of the hexamer signal. Though the precise nature of these higher stacks has not been established, their five ^{7}Li signals fall into two sets. The relative intensities within each set are concentration independent, i.e., two signals at δ +0.12 and 0.04 ppm of ratio 1 : 0.5 and three at δ +1.99, 1.77, and 1.53 ppm of ratio 1 : 1 : 1. These values could correspond to the nonamer $[Me_2N(Ph)C{=}NLi]_9$ (Fig. 18b; $x = 3$, environments $b' \times 2$ and c) and the "octadecamer" ($x = 6$, environments $b^{IV} \times 2$, $c^{IV} \times 2$, and $c^{V} \times 2$]. A nonamer (as well as a hexamer and an octamer) was indicated to be present (by ^{6}Li and ^{13}C NMR data) in hydrocarbon solutions of *n*-propyllithium (*96*).

Much more conclusive results were obtained for solutions of $(Bu^t_2C{=}NLi{\cdot}HMPA)_2$ (**6**) (*79*, *94*), which is a dimer in the solid state. Cryoscopic measurements in benzene gave n values of 1.33 (0.033 *M*) and of 1.12 (0.017 *M*); this implied the existence of a monomer $\rightleftharpoons$ dimer equilibrium with approximate monomer : dimer ratios of 2 : 1 and 6 : 1 for the more concentrated and more dilute solutions, respectively. This inference was supported by the ^{1}H and ^{7}Li room-temperature NMR spectra of (**6**) in benzene-d_6; typical spectra are shown in Fig. 19. Unusually for ^{7}Li NMR spectra recorded at ambient temperature, two signals are observed (Fig. 19a and c). The peak at $\delta \sim +0.4$ ppm is proportionately larger in the dilute (Fig. 19c, 0.05 *M*) than in the concentrated solution (Fig. 19a, 0.25 *M*). This suggests that this δ 0.4-ppm signal is due to the monomer and that the $\delta \sim 0.15$-ppm peak corresponds to a dimer. The ^{1}H NMR spectra provide support (Fig. 19b and d). Apart from the doublet due to HMPA, the two signals at $\delta \sim 1.4$ and 1.2 ppm can be assigned to the Bu^t groups in the dimeric and monomeric species, respectively. Further, both types of spectra agree closely on the relative molar ratios of dimer : monomer in each solution; ~1.45 : 1 in the more concentrated solution (hence a relative integration of ~2.9 : 1, Fig. 19a and b), giving $n \sim 1.6$, and ~0.7 : 1 in the more

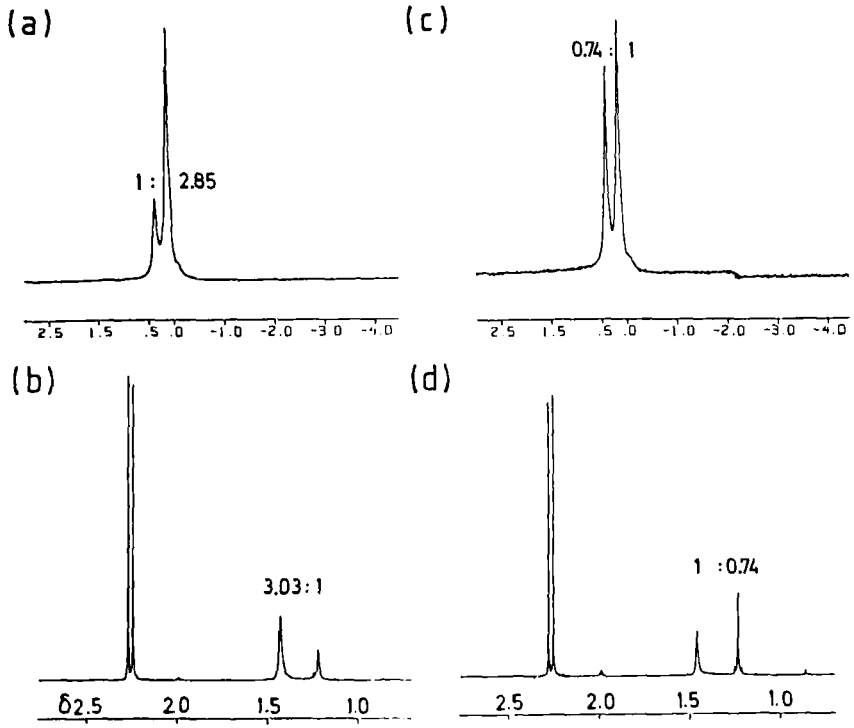

FIG. 19. NMR spectra (25°C, d_8-toluene) of solutions of $(Bu^t_2C{=}NLi{\cdot}HMPA)_2$ (**6**): (a) ^7Li, 0.25 *M*, (b) ^1H, 0.25 *M*, (c) ^7Li, 0.05 *M*, and (d) ^1H, 0.05 *M*.

dilute one, so $n \sim 1.4$. The dimer must be similar to the solid-state structure, whereas the monomer probably has only a single mole of HMPA, $Bu^t_2C{=}NLi{\cdot}HMPA$. If more HMPA were present, ^7Li NMR signals at δ 0.62–0.64 ppm found for solutions of the hexamer $(Bu^t_2C{=}NLi)_6$ (**1**) would be apparent. Remarkably, $Bu^t_2C{=}N$ group and ^7Li atom exchange between the monomer and the dimer of $Bu^t_2C{=}NLi{\cdot}$ HMPA is too slow to be observed on the NMR time scale. This implies stabilization of the monomer, despite its two-coordinate Li. Presumably Li···H—C or Li···NMe_2 (of HMPA) interactions are responsible.

Unlike (**6**), the related dimeric "keteniminate" [Ph(H)C⋯C⋯NLi·TMEDA]$_2$ may dissolve intact (*82*). Earlier rmm measurements on Ph(H)C·CN·Li in THF (at 18.5°C), 1,2-dimethoxyethane, or dimethyl sulfoxide indicated dimers to be present (*99*). However, in THF at −108°C, a monomer is found (*82, 100*). MNDO calculations on model species indicate that the dimer $[Ph(H)C{\cdot}CN{\cdot}Li{\cdot}2NH_3]_2$ (and $2NH_3$) is

only ~5 kcal mol^{-1} more stable than two $Ph(H)C{\cdot}CN{\cdot}Li{\cdot}3NH_3$ monomers. Hence, monomers could be favored, entropically, at low temperatures.

A few solution studies have been carried out on the iminolithium tetramer, $(Ph_2C{=}NLi{\cdot}pyridine)_4$ (**7**) (*94*). Molecular mass measurements in benzene gave n values ranging from ~2.2 (0.07 M) to ~1.4 (0.03 M), implying extensive dissociation of the tetramer. However, the species in benzene must still be ligated by pyridine because $(Ph_2C{=}NLi)_n$ did not precipitate. The ^7Li NMR spectrum of (**7**) in toluene-d_8 at 25°C shows a sharp singlet at δ ~+1.7 ppm and a broader peak at δ ~+1.5 ppm. Because the relative intensity of the latter increases on dilution, from ~1 : 0.25 at 0.40 M to ~ 1 : 1.4 at 0.05 M, it presumably is due to a species with lower association. The correspondence of the n values obtained cryoscopically and those gained by integration of NMR signals (for solutions of identical concentrations) can only be achieved if it is assumed that (**7**) engages in a tetramer $\rightleftharpoons$ monomer equilibrium.

D. Calculations on Iminolithiums and on Lithium Species with Related Structures

MNDO and *ab initio* molecular orbital calculations on organolithium compounds have proved of enormous value in understanding the structures of these species (*2, 36, 37, 101, 102*). They have furnished thermochemical data (rarely available experimentally) such as association, complexation and solvation (*103*), and bond (*103a*) energies. Furthermore, they have both rationalized known solid-state structures and, in many cases and with remarkable accuracy, predicted such structures prior to their solutions by X-ray crystallography. The semiempirical MNDO method (*104–106*), despite having a tendency to overestimate C—Li bonding (*106, 107*), has been particularly successful in giving reliable structural information on lithiated organics, not least because it can deal with relatively large molecules.

Regarding uncomplexed iminolithiums, the structures of $(H_2C{=}NLi)_n$, n= 1, 2, and 3, have been investigated by both MNDO (*108*) and *ab initio* [3-21G basis set (*108*) and 6-31G basis set (*72, 74*)] methods. Figure 20 shows the optimized structures (6-31G) for the two associated species. For the dimer, all the calculations show that the planar D_{2h} form (Fig. 20a) is preferred to a form with the $H_2C{=}N$– ligand plane perpendicular to the $(NLi)_2$ ring plane (Figure 20b). The energy difference calculated by MNDO is quite small, 6.8 kcal mol^{-1} (*108*), though at the 6-31G level (*72, 74*) it is somewhat larger, 17.0 kcal mol^{-1}. As described earlier, the only known example of a solid-state

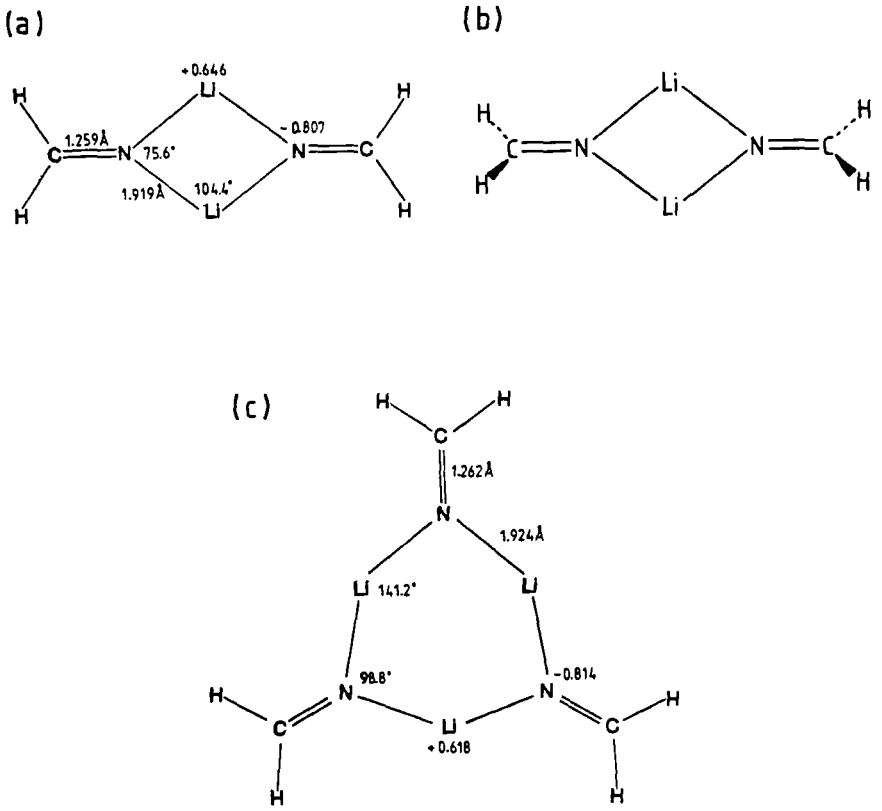

FIG. 20. Optimized structures (6-31G basis set level) of (a) $(H_2C{=}NLi)_2$ dimer, planar, (b) $(H_2C{=}NLi)_2$ dimer, perpendicular, and (c) $(H_2C{=}NLi)_3$ trimer, planar.

iminolithium dimer is $(Bu^t{}_2C{=}NLi{\cdot}HMPA)_2$ (**6**) (*78, 79*), which, for steric reasons, adopts a compromise geometry between planar and perpendicular (see Section II,B, especially Fig. 12). The rather low MNDO energy difference between the two forms may explain the retention of strong N—Li bonding in this structure. Thus, it has been argued (*108*) that in the $H_2C{=}N^-$ anion the two lone pairs on N and the π electrons of the C=N bond can combine to give a quasicylindrical arrangement of electronic charge at N (see Fig. 7). In that case, the Li^+ placements in the dimer are not very critical. What is clear-cut is that dimerization of $H_2C{=}NLi$ is very exothermic. The MNDO dimerization energy (−51.7 kcal mol^{-1}) agrees quite well with the 3-21G/3-21G value (−71.4 kcal mol^{-1}) taking into account the basis set superposition error (*109, 110*) in the quite low-level *ab initio* calculation. At the 6-31G level, this value is −66.0 kcal mol^{-1} (*72, 74*).

For the trimer $(H_2C{=}NLi)_3$ (Fig. 20c), at the 6-31G level the planar form is very strongly preferred (by 91.0 kcal mol^{-1}) to the perpendicular one. This is largely because the latter's six-membered ring is distorted much more from a regular hexagon (*74*). A planar trimeric ring is also preferred to a planar dimer (trimerization energy −119.2 or −39.7 kcal mol^{-1} per $H_2C{=}NLi$ monomer unit, *cf.* for a dimer, −33.0 kcal mol^{-1} per monomer unit). These two preferences, for a trimer over a dimer and for planar forms, lead to the stacking of two or more (trimeric) rings and hence the formation of hexameric or polymeric species (see Section II,B, especially Figs. 6, 9, and 10).

MNDO calculations have also been performed on a model tetrameric lithium imide, $(H_2C{=}NLi)_4$ (*108*). On increasing the association state (n) to four, a planar ring geometry is no longer found. Thus, a tetrahedral cubanelike structure (tetramerization energy, −144.4; −36.1 kcal mol^{-1} per monomer unit) is favored over an eight-membered planar $(NLi)_4$ ring structure. This preference is also found experimentally in the solid-state structures of $(Ph_2C{=}NLi{\cdot}pyridine)_4$ (**7**) and $[(Me_2N)_2C{=}N]_4{\cdot}LiNa_3{\cdot}3HMPA$ (**9**) (see Section II,B, especially Figs. 14 and 17). These dual preferences, for formation of planar dimeric rings and then for their further association [*cf.* for $(H_2C{=}NLi)_2$, the dimerization energy per monomer is only −25.9 kcal mol^{-1}] lead to clustered species. The related tetramers $(LiF)_4$, $(LiOH)_4$ (*111*), and $(MeLi)_4$ (*102*) also favor the tetrahedral arrangement over the planar ring one. These conclusions have been verified experimentally in the case of $(MeLi)_4$, whose solid-state structure is indeed a pseudocubane (*44*). They reflect essentially the dominance of electrostatic interactions in these systems: a cubanelike arrangement gives each Li^+ cation a coordination number of three rather than just two as in a ring structure. In fact, purely electrostatic approaches, using point plus and minus charges in the form of two interpenetrating tetrahedra, can describe these tetrameric clusters quite well (*112–113a; 102*).

Iminolithium hexamers have not so far been examined by MO calculations. Thus there are no *direct* theoretical results pertaining to the structures of the experimentally found hexamers (**1**)–(**4**) [D_{3d}-type clusters viewed as two stacked trimeric rings (*69–72*)] and the mixed-metal hexamer (**5**) [a stack of three dimeric rings (*77*)]. However, MNDO and *ab initio* computations have been carried out on hexamers with smaller anions, e.g. $(LiH)_6$ (*114*), $(LiF)_6$ and $(LiOH)_6$ (*115*), and $(MeLi)_6$ (*102, 116*). In all cases, distorted octahedral (D_{3d}) structures are found to be more stable than hexagonal planar ring (D_{6h}) structures. For example, in the case of $(LiF)_6$, the former structure is favored by 32.1 kcal mol^{-1} (at the HF/6-31G+sp+d level). The merits of further association are also borne out by the ever-increasing binding energies per monomer

unit. For the $(LiF)_n$ systems, these are 32.5 (dimer), 42.0 (trimer), 47.0 (cubic tetramer), and 52.1 (octahedral hexamer) kcal mol^{-1} (*115*). Further, force-field models (*117–121*), which consider only hard-sphere volume exclusion and point-charge electrostatic interactions, have proved capable of predicting the relative dimensions of $(RLi)_6$ hexamers with reasonable accuracy (*113a*).

Calculations on lithium amides, using $(H_2NLi)_n$ models (n = 1–4; 6), are discussed in Section III,B,2.

E. Ring Stacking: General Applications to the Structures of Organolithium Compounds

We have shown in Section II,A how uncomplexed iminolithium hexamers (**1**)–(**4**) can be regarded as double stacks of trimeric rings, and that flat diaryliminolithium ring systems can stack extensively to give polymers (see especially Figs. 5–10). For iminolithium complexes, the constituent ring size is four-membered (Section II,B; see Fig. 13). These rings also can stack, affording tetrameric cubic arrangements such as (**7**) (Figs. 14 and 15) and (**9**) (Fig. 17). Ring stacking takes place because the *exo*-RR′C=N ligands are essentially coplanar with the $(NLi)_{2,3}$ rings, particularly to and including the primary (α) atoms of the R,R′ groups. However, this stereochemistry is by no means unique to imide anions. It occurs widely, as shown in Fig. 21a, for a range of organoli-

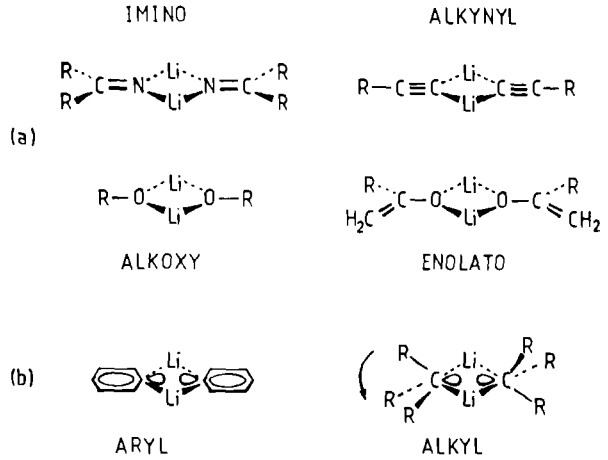

FIG. 21. Organolithium ring systems capable of stacking: (a) imino, alkynyl, alkoxy/aryloxy, and enolato systems; (b) aryl and alkyl systems.

thium ring systems involving alkynyl ($RC{\equiv}C^-$), alkoxy/aryloxy (RO^-), and enolato [$RC(=CH_2)O^-$] anions. Although dimeric rings are shown in Fig. 21a, the same stereochemistry would obviously be found for trimeric or any other size rings. The ring size will depend largely on the bulk of the anion, i.e., the size of the R groups. For alkyl and aryl anions (Fig. 21b), the bonding situation is slightly different. In both, the α-C^- centers have lobes with pseudocylindrical symmetry projecting into the $(CLi)_2$ or $(CLi)_3$ ring. Hence the precise orientation of the ligand as a whole will have little effect on the strength of ring bonding. Thus, aryl ligands can be coplanar with the ring, whereas the substituents of alkyl ones can take up positions that best allow interlocking and stacking.

The stereochemical feature noted above leads to widespread ring stacking in organolithium chemistry. Such structures do not result as a matter of course from a preference of lithium centers for four coordination (though this is often stated to be so). There are many organolithium compounds whose metal centers are only two or three coordinate, and a fair number whose metal centers exceed four coordination (even excluding consideration of Li—Li contacts) (*2*, *3*). Rather, ring-stacking propensities are merely a manifestation of electrostatic principles: a Li^+ cation within any structure will interact, inevitably, with as many anionic centers or polar ligands as possible. Just how many will be present (see Section I) depends on the *steric* features of the anions and ligands. Monoatomic anions, such as Hal^-, allow full three-dimensional association (stacking *and* laddering; Fig. 3c). As just discussed, many organic anions allow only vertical association. This can be extensive when R groups are small or flat (Fig. 3a); bulkier groups limit association to double stacks of trimeric and dimeric rings [hence clustered hexamers (Fig. 3d) and tetramers (Fig. 3e)]. Complexation of such systems, whether by addition of polar ligands ("external" complexation; Section I, Fig. 1) or with internal sites in the organic anion (Fig. 2), usually results in ring dimers. For steric reasons, monodentate ligands allow two such rings to stack to give cubic tetramers. Bidentate ligands, in contrast, result in isolated dimers, or monomers when the R groups in the organic anions are large. Tridentate complexants often favor monomer formation.

Crystal structures illustrating these ring-stacking ideas are given in Table II (aggregated alkyl- and aryllithium species), Table III (alkynyllithium species), Table IV (oxycarbanion–lithium species), and Table V (lithium halides and lithium halide–organolithium mixed species). Figures 1–4 (Section I) have already shown representations of many of the structural types from these tables. For other types, repre-

TABLE II

CRYSTAL STRUCTURES OF ASSOCIATED ALKYL-AND ARYLLITHIUM COMPOUNDS AND COMPLEXES AND RELATED SPECIES

Empirical formula[a]	Formula number[b]	Association state (n)	Figure	Ref.
MeLi	(**10**)	4	3e, 4a	*44*
EtLi	(**11**)	4	3e	*1*
Me_3SiCH_2Li	(**12**)	6	3d	*48*
$c\text{-}C_6H_{11}Li$	(**13**)	6	3d, 4b	*47*
$Me_2\overline{C\cdot Me_2C\cdot CH}\cdot CH_2Li$	(**14**)	6	3d	*75*
Me_3SiLi	(**15**)	6	3d	*73*
$MeLi\cdot\frac{1}{2}TMEDA$	(**16**)	4	1a	*22*
$PhLi\cdot OEt_2$	(**17**)	4	22a	*122*
PhLi·TMEDA	(**18**)	2	1b	*24*
$Me_2N(CH_2)_2CH_2Li$	(**19**)	4	2a	*28, 29*
$2\text{-}Me_2NCH_2\cdot C_6H_4Li$	(**20**)	4	2a	*30*
$MeOCH_2CH_2\cdot(Me)CHLi$	(**21**)	4	2a	*123*
$(Me_2NCH_2)_2CH\cdot(Me)CHLi$	(**22**)	2	2b	*32*
$(2,3,5,6,\text{-}Me_2NCH_2)_4C_6HLi$	(**23**)	2	2b	*33*
$Me_2N(CH_2)_3NMe\cdot\overline{C(CH_2)_4\cdot(=C)}Li$	(**24**)	2	22b	*124*
$8\text{-}Me_2NC_{10}H_6Li\cdot OEt_2$	(**25**)	2	22c	*125*
$(2,6\text{-}MeO)_2C_6H_3Li$	(**26**)	4	22d	126, 127
$(2,6\text{-}Me_2N)_2C_6H_3Li$	(**27**)	3	22e	*133*

[a] With respect to the organolithium component.
[b] See text.

sentations or specific structures are given in Figs. 22–25. Brief comments on the compounds and complexes listed in these tables are now given.

Uncomplexed alkyllithiums [(**10**)–(**14**)] are tetramers or hexamers (Table II). Small alkyl groups (Me, Et) allow dimeric $(CLi)_2$ rings to form. Larger ones, and the large $Si^{\delta-}$ centers of Me_3Si groups in (**15**), dictate trimeric rings. Two such rings can stack, leading to cubic tetramers or pseudooctahedral hexamers. Because each Li atom then becomes only three coordinate, Li···H—C interactions often are prompted (*43–50*). The tetramers (**10**) and (**11**) associate further (hence their insolubility in hydrocarbon solvents) by means of intercube Li···H—C interactions; these were illustrated for (**10**) in Fig. 4a. The hexamers (**12**) and (**13**) have been noted to adopt intramolecular interactions, as detailed for (**13**) in Fig. 4b. Significantly, these examples [(**10**)–(**15**)] do not include an aryllithium. No uncomplexed *oligomeric* aryllithium species are known, presumably because their $(arylLi)_{2,3}$ ring systems

are flat enough to allow more extensive association. For example, $(PhLi)_n$, prepared in a noncomplexing solvent such as toluene, is an amorphous and insoluble material.

"External" complexation by addition of Lewis bases gives three kinds of associated structures. The first is a tetramer [(**16**)] whose individual cubes are linked by a usually bidentate ligand, TMEDA, acting only as a monodentate one; in effect, the $Li\cdots H_3C$ interactions seen in (**10**) have been replaced by these Me_2N coordinations. With a monodentate complexant as such, an isolated cubic tetramer (**17**) results (*122*) (Figure 22a); the Et_2O molecules preclude further linkages. Bidentate ligation, e.g., by TMEDA, results usually in dimeric complexes, e.g. (**18**). Ring stacking is prevented by the ligand's Me_2N groups projecting above and below the $(CLi)_2$ ring plane, giving a pseudotetrahedral Li environment. Complexations by functional groups within the anion result in similar structures to those just noted. A single functionality per anion leads to tetramers (**19**), (**20**), and (**21**) (*123*), while two such functionalities per anion afford dimers (**22**), (**23**), and (**24**); in (**24**) (*124*), both complexing sites of a given anion attach to the same lithium cation (Fig. 22b). The dimer (**25**) (*125*) provides an example of "mixed" coordination, involving both internal (Me_2N) and external (Et_2O) complexants (Fig. 22c). Significantly, all these complexed aggregates are dimers or stacks of two dimers; trimers and their stacks no longer are found. The final two species in Table II [(**26**) and (**27**)] are aryllithium complexes, each with two functional groups per aryl anion, and they provide an interesting contrast. The structure of (**26**) (*126, 127*) substantiated the theoretical prediction of a planar, rather than a tetrahedral, arrangement when two Li atoms are attached to the same C atom (*128–132*). Thus the MeO groups (two per Li) lie in the $(CLi)_2$ ring plane (Fig. 22d). Therefore, association to a tetramer is possible sterically, and each Li becomes five coordinate. For (**27**) (*133*), the larger $(Me_2N)_2C_6H_3^-$ anions cause a trimeric ring to form, and the Me_2N groups project above and below the $(CLi)_3$ ring plane (Fig. 22e), preventing stacking. Complex (**27**) is the only known example of a *complexed* trimer in lithium chemistry.

Alkynyllithium compounds form flat ring systems (Fig. 21) whose vertical association is uninhibited (Fig. 3a): lithiations of alkynes (acetylenes) in nonpolar media produce amorphous materials. When polar ligands (Lewis bases) are added, crystalline complexes can be isolated, their structures depending on the effective denticity of the base and on its molar proportions relative to lithium (Table III). A complexant such as TMHDA, $Me_2N(CH_2)_6NMe_2$, with a long methylene chain, fails to behave in a bidentate manner toward a given Li center; hence complex (**28**) results [*cf.* (**16**)], with the TMHDA linking

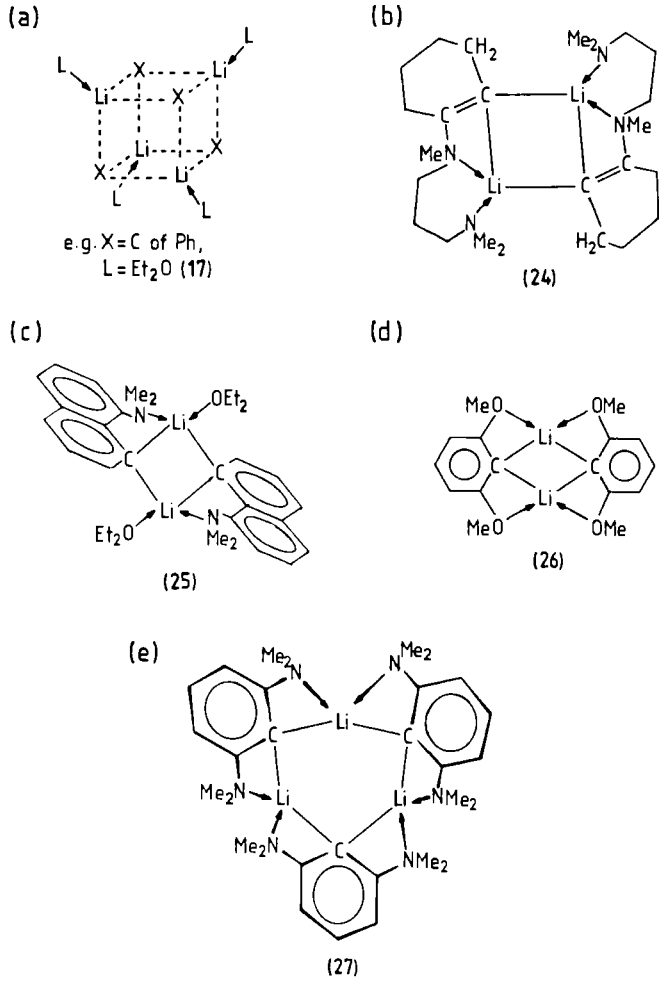

FIG. 22. Structures of selected alkyl- and aryllithium complexes (see also Figs. 1–4 and Table II).

cubic tetramers (Fig. 23a). A monodentate base such as THF allows an isolated cubic arrangement [(**29**)] (*134, 135*) when the base : Li ratio is 1 : 1. In (**30**), the TMPDA ligand, $Me_2N(CH_2)_3NMe_2$, with a short methylene chain, can chelate, and a dimer is formed. The totally new structural option is provided by (**31**) (*134, 135*). This dodecamer exhibits sixfold stacking of $(CLi)_2$ rings, terminated by complexants (Fig. 23b). A structure like this can be regarded as an intercepted polymeric stack

TABLE III

CRYSTAL STRUCTURES OF ALKYNYLLITHIUM COMPLEXES

Empirical formula [a]	Formula number [b]	Association state (n)	Figure	Ref.
PhC≡CLi·½TMHDA	(**28**)	4	1a, 23a	*23*
Bu^{t}C≡CLi·THF	(**29**)	4	22a	*134, 135*
PhC≡CLi·TMPDA	(**30**)	2	1b	*25*
Bu^{t}C≡CLi·⅓THF	(**31**)	12	23b	*134, 135*

[a] With respect to the organolithium component.
[b] See text.

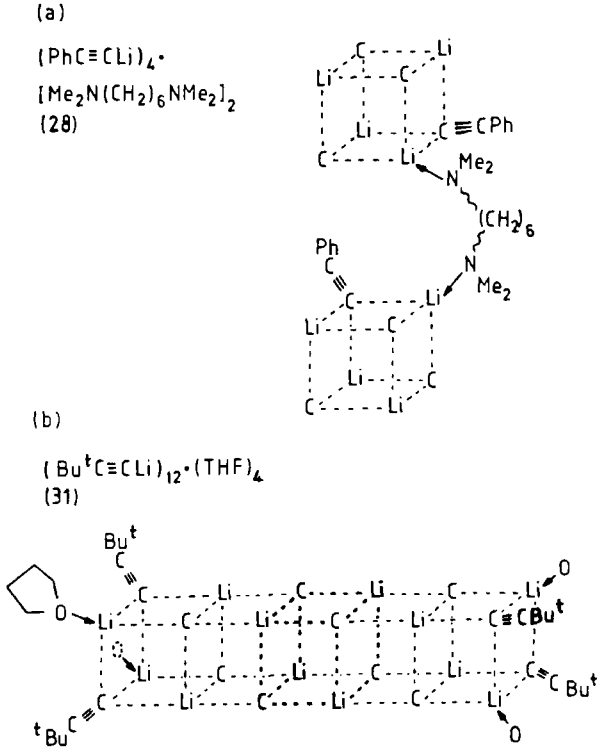

FIG. 23. Structures of selected alkynyllithium complexes.

(Fig. 3a). As in the 1:1 THF:Li analog [(**29**)], each Li center in (**31**) reaches four coordination, though obviously the internal ones do so in a different way. Again significantly, all of complexes (**28**)–(**31**) are dimeric rings or multiples thereof; no trimer rings are present.

The crystal structures of numerous organolithium compounds and complexes with O—Li bonds are now available (*2–5*). Table IV lists a number of these species, as well as two derivatives of heavier alkali metals. As with the C—Li derivatives just discussed (Tables II and III), clustered $(ROLi)_n$ tetramers and hexamers, as well as ring dimers, are prevalent. Note that $(OLi)_{2,3}$ ring systems also are pseudoplanar (Fig. 21a). However, extensive stacking leading to polymers will only occur if the substituents on O are small and if polar ligands are absent. Otherwise, limited (double) stacks or unstacked rings form.

Two lithium enolate hexamers are known [*cf.* (**12**)–(**15**) in Table II]. In (**32**) (*136, 137*), the large Bu^t substituents result in the preference for

TABLE IV

CRYSTAL STRUCTURES OF OXYCARBANION–ALKALI METAL COMPOUNDS AND COMPLEXES WITH O—M BONDS

Empirical formula[a]	Formula number[b]	Association state (n)	Figure	Ref.
Bu^{t}C(=CH_2)OLi	(**32**)	6	3d, 24a	*136, 137*
Et_2N·CH=C(OEt)OLi	(**33**)	6	24b	*138*
Bu^{t}C(=CH_2)OLi·THF	(**34**)	4	22a	*139*
$H_2\overline{C(CH_2)_2CH}=\overline{COLi}$·THF	(**35**)	4	22a	*139*
2-Me_2NCH_2·C_6H_4·C(=CH_2)OLi	(**36**)	4	*cf.* 2a; 24c	*31*
Bu^{t}C(=O)·CH_2·CH(Bu^t)OLi	(**37**)	4	*cf.* 2a	*140*
Bu$^t{}_2$Si(NH_2)OLi	(**38**)	4	*cf.* 2a	*141*
MeO·C(=CHBu^t)OLi·THF	(**39**)	4	22a	*26*
Bu^{t}C(=CH_2)OLi·TMEDA	(**40**)	2	1b	*142*
Bu^{t}O·C(=CMe_2)OLi·TMEDA	(**41**)	2	1b	*26*
Bu^{t}O·C(=CHMe)OLi·TMEDA	(**42**)	2	1b	*26*
MeCH=C(NMe_2)OLi·TMEDA	(**43**)	2	1b	*142*
$H\overline{C}$=CH·$(CH=CH)_2\overline{C}$=C(NMe_2)OLi·2THF	(**44**)	2	*cf.* 1b	*143*
Bu$^t{}_3$COLi·THF	(**45**)	2	24d	*144*
2,6-Bu$^t{}_2$-4-MeC_6H_2OLi·OEt_2	(**46**)	2	24d	*145*
Bu^{t}C(=CH_2)·CH=C(Bu^t)OLi·DMPU[c]	(**47**)	2	24d	*146*
Bu^{t}C(=CH_2)ONa·O=C(Bu^t)Me	(**48**)	4	22a	*137*
Bu^{t}C(=CH_2)OK·THF	(**49**)	6	24e	*137*

[a] With respect to the organometallic component.

[b] See text.

[c] DMPU, $Me\overline{N(CH_2)_3NMe}\cdot\overline{C}$=O.

an $(OLi)_3$ ring. Moreover, only two of these rings can stack (Fig. 24a). Each $=CH_2$ unit appears to π bond to Li; this also deters further stacking. In (**33**), the enolate of ethyl-*N*,*N*-diethylglycinate (*138*), a similar double stack of $(OLi)_3$ trimers is present. The Et_2N groups coordinate to the Li^+ cations in the rings (Fig. 24b). In contrast to other complexed lithium stacks [but note (**49**) below], the constituent rings in (**33**) are trimeric rather than dimeric. This presumably reflects the size and the extent of the enolato substituents. With smaller substituents, and with monocomplexation by "external" polar molecules, cubic tetramers form [(**34**) and (**35**)] (*139*). The presence of a polar group in the oxyanion ligand leads to the same result. Note the tetrameric structures of (**36**) (Fig. 24c), (**37**) (*140*), and (**38**) (*141*), containing Me_2N—Li,

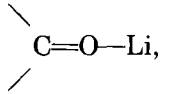

and H_2N—Li coordinations, respectively. In (**39**), a tetramer also results because only the "external" THF ligands, and not the MeO groups, complex to lithium. The dimers (**40**)–(**44**) result from there being two polar groups (as well as the enolato anion) attached to each Li. In (**40**) (*142*) there are no internal complexing sites, and the two polar groups

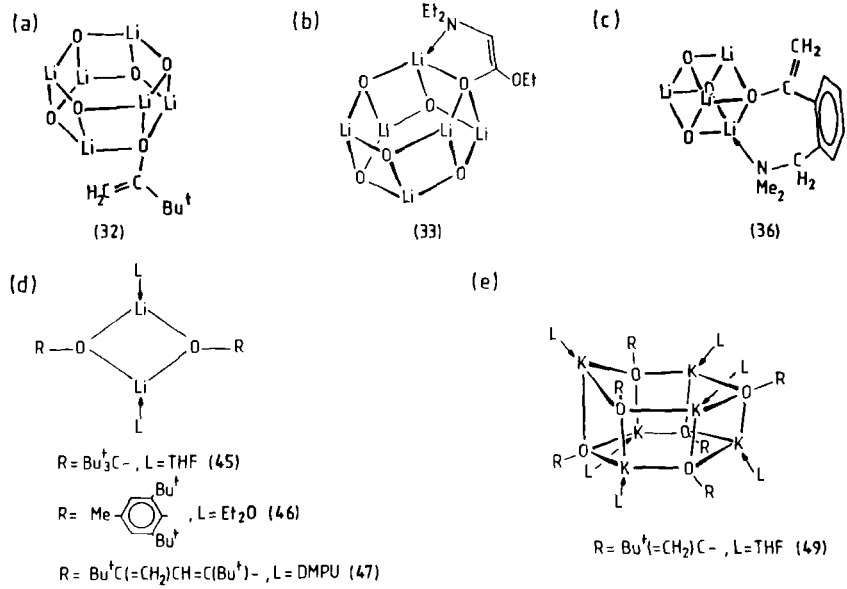

FIG. 24. Structures of selected oxycarbanion–alkali metal compounds and complexes with O—M bonds.

are those of TMEDA (i.e., two Me_2N groups). The same is true for (**41**), (**42**), (**43**) (*142*), and (**44**) (*143*) because their internal and potentially coordinating sites (Bu'O and Me_2N, respectively) are not capable, for steric reasons, of attaching to lithium. Complexes (**45**) (*144*), (**46**) (*145*), and (**47**) (*146*) all are dimers (Fig. 24d) despite having only one added monodentate ligand per Li center, and no additional internal ligand sites. The particularly bulky R groups attached to the O^- centers extend above and below each $(OLi)_2$ ring. This precludes stacking [*cf.* (**34**) and (**35**)]. The final two examples in Table IV illustrate what happens due to the switching from lithium to heavier alkali metals (*137*). The behavior of the sodium enolate (**48**) mirrors that of similar lithium derivatives. Complexation of each Na^+ cation by a single monodentate base leads to dimeric $(ONa)_2$ rings, two of which stack. The larger potassium cations favor formation of trimeric $(OK)_3$ rings; double stacking then gives hexamer (**49**) (Fig. 24e). It is interesting that the larger cations dictate the ring size here, but not the extent of stacking.

Finally we turn to lithium halides and their coaggregates with organolithiums (Table V). By themselves, lithium halides can form dimeric rings that are perfectly set up to both stack and to ladder. This is so for both electrostatic and steric reasons: the Hal^- anions have high electron densities and there are no substituents *exo* the ring. Three-dimensional infinite ionic lattices (Fig. 3c) result. Addition of polar molecules might break down these systems, at least partially. Note the major complexed structural types described earlier for N—Li, C—Li, and O—Li bonded derivatives: ring dimers and double stacks (cubic tetramers) of such dimers. For example, $(LiBr)_\infty$ provides the dimer (**50**) (*146*) (Fig. 25a) with acetone. The rings can neither stack, because the acetone molecules (two per lithium center) project above and below the $(LiBr)_2$ ring plane, nor can they ladder, because these complexants use

TABLE V

CRYSTAL STRUCTURES OF LITHIUM HALIDE AND MIXED LITHIUM HALIDE–ORGANOLITHIUM COMPLEXES

Structural formula[a]	Formula number[a]	Figure	Ref.
$[LiBr{\cdot}(O{=}CMe_2)_2]_2$	(**50**)	25a; *cf.* 2b	*146*
$(LiCl{\cdot}HMPA)_4$	(**51**)	25b; *cf.* 22a	*85, 147, 148*
$(\underline{PhLi{\cdot}OEt_2})_3{\cdot}LiBr$	(**52**)	25c; *cf.* 22a	*122*
$(\overline{CH_2CH_2CHLi}{\cdot}OEt_2)_2{\cdot}(LiBr{\cdot}OEt_2)_2$	(**53**)	*cf.* 25b, c; 22a	*149*

[a] See text.

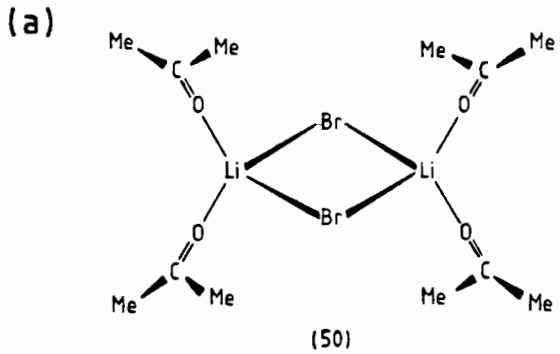

(50)

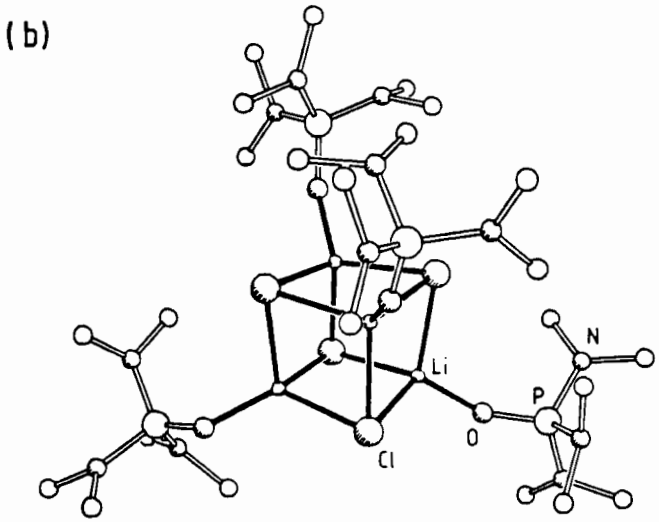

(51)

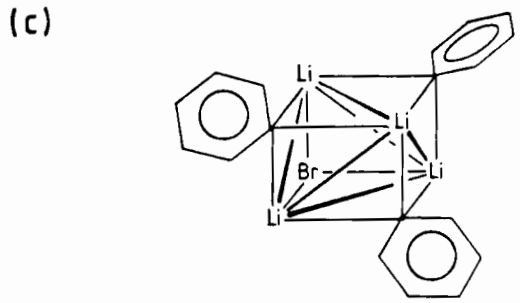

(52)

FIG. 25. Structures of selected lithium halide and lithium halide–organolithium complexes.

up lateral space as well. The presence of just one monodentate base per Li center will allow two such rings to stack, as in (**51**) (Fig. 25b). Many anhydrous salts [$(LiHal)_\infty$] cannot be dissolved directly in the polar solvents, but small $(LiHal)_n$ units can be captured using *in situ* methods, e.g., by reactions, in the presence of complexants, of organolithium reagents in hydrocarbon solvents with organic or metal halides (*85*), or of solid ammonium halides suspended in toluene with Bu^nLi, with solid LiH, or with metallic Li (*147, 148*). Two tetrameric mixed aggregates also have been structurally characterized, (**52**) (*122*) and (**53**) (*149*). These species are relevant to the well-known and distinct differences in reactivity between "pure" organolithium (RLi) reagents and those containing lithium halides (by virtue of their preparation from RHal plus two equivalents of Li metal). Deliberate addition of lithium halides to solutions of lithium amides (see Section III) and of lithium enolates is also known to lead to the formation of mixed aggregates (*4*). In (**52**), which can be regarded as a stack of $(CLi)_2$ and Li(C,Br)Li rings (Fig. 25c), the unique Li^+ cation attached to three Ph^- anions is not fully ligated. The other lithium centers, each bonded to two Ph^- and a Br^- anion, have more open coordination sites. Complex (**53**) has a structure similar to (**52**), although every Li^+ is bonded to at least one Br^-.

III. "Simple" Lithium Amides (Amidolithiums) and Their Complexes; Ring Laddering

A. Introduction

The products obtained by lithiating amines RR'NH, usually by employing commercially available organolithium reagents, e.g., MeLi and Bu^nLi, are commonly referred to as lithium amides. Unfortunately, the "amide" designation refers to two distinctly different classes of molecules: (1) those containing RR'N·C(=O)·R" groups and (2) salts of ammonia or of amines, $RR'N^-M^+$. A "lithiated amide" would be, e.g., RCONHLi, whereas a "lithium amide" would be RR'NLi. This rather schizophrenic nomenclature is widely used, and has been employed in this present review. The "simple" in the title of this section should also be explained. We restrict ourselves here to describing the products of lithiating monoamines RR'NH whose R,R' groups contain no additional functionalities that involve themselves with N-attached Li centers in the resulting structures. Such functionalities, inherent in RR'NH precursors, can be of several types, e.g. (1) further N centers

when R or R′ is pyridyl (C_5H_4N), when an —NMe_2 side-arm is present, or when the precursor is a di- or triamine, (2) O centers provided by —OMe side-arms or by O atoms of aza crowns, (3) S centers, as in the lithiation of mercaptoamines, and (4) potentially coordinating π systems, when heterocyclic amines (e.g., pyrrole, carbazole, and indole) are lithiated. Studies on such functionalized lithium amides are in general quite recent. To date, they have involved mainly the elucidation of solid-state structures, with rather less emphasis on calculational and solution investigations. We will discuss such species in a follow-up review.

Section II of this review concentrated on iminolithium species and showed that their ring-stacking propensities are widespread in organolithium chemistry (see especially Section II,E). These structural preferences occur because substituents attached to most $(NLi)_n$, $(CLi)_n$, or $(OLi)_n$ rings (n = 2, 3) usually also lie in the same plane. This allows vertical association ("stacking"). Rings also are basic building blocks for lithium amides, but there is a crucial stereochemical difference. Because of the near-tetrahedral geometries at the amide N centers in these $(RR'NLi)_n$ systems, the R and R′ groups project above and below

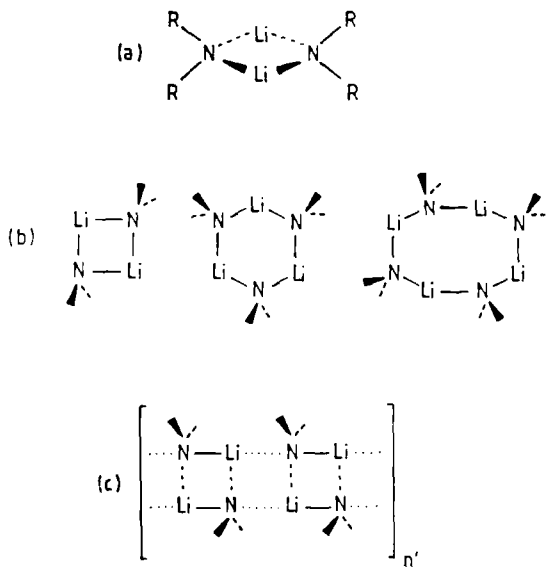

FIG. 26. Structural types for uncomplexed lithium amides $(RR'NLi)_n$: (a) dimeric ring (n = 2), showing the projection of R,R′ groups above and below the ring plane; (b) rings with n = 2, 3, and 4; (c) further association of rings into ladders.

the $(NLi)_n$ ring plane (Figure 26a), shown for $n = 2$). Therefore stacking is prevented. Several $(RR'NLi)_n$ rings ($n = 2, 3, 4$) have been observed (Fig. 26b). However, further association of such rings may occur *laterally,* by so-called ring laddering (*20, 21, 150*) (Fig. 26c).

We describe first the structures found for uncomplexed lithium amides (i.e., those not containing added neutral Lewis bases such as THF, HMPA, or TMEDA) by X-ray crystallography, by molecular orbital calculations, and by solution methods (Section III,B). In Section III,C, the structures of lithium amide complexes are discussed similarly.

B. Uncomplexed Lithium Amides

1. Solid-State Structures

As described above, ring oligomers or ladders are structural options for uncomplexed lithium amides $(RR'NLi)_n$. Isolated rings occur when the R and R′ groups are bulky and occupy much of the lateral space around the ring. Such sterically hindered lithium amides are widely used in organic syntheses as strong bases (see Section I,A). Significantly, they can be both prepared and used in nonpolar solvents. Notable examples include those with R = R′ = Pr^i, Me_3Si, *c*-hexyl; R=Ph, R′=Bu^t,*t*-amyl, *l*-adamantyl; R=Bu^t, R′=*t*-octyl; R=Pr^i, R′=*c*-hexyl; and RR′N=$Me_2\overline{C(CH_2)_3CMe_2N}$ (*4, 6–8, 11, 13, 151–155*). Although most of these compounds can be expected to form rings, only five solid-state structures are available (Table VI). The ring size (Fig. 26b) depends on the size of the R and R′ groups. The large tetramethylpiperidinato anion leads to the formation of $[Me_2\overline{C(CH_2)_3CMe_2N}Li]_4$ (**54**) (*19*), the only simple ring tetramer known in organolithium chemistry. The N—Li—N arrangements in the ring are almost linear. When R,R′ groups are less sterically demanding, trimeric rings are formed: $[(PhCH_2)_2NLi]_3$ (**55**) (*20, 76*), $[(Me_3Si)_2NLi]_3$ (**56**) (*17, 18*), and $[(Me_3Ge)_2NLi]_3$ (**57**) (*156*). The two-coordinate nature of the Li^+ cations in (**55**) (Fig. 27a) allows (or prompts) additional Li···H—C interactions (*43–49*). The $PhCH_2$ groups pivot toward the Li^+ cations (Fig. 27b) and quite short Li—H_2C, Li—*α*—C, and Li—*o*—CH contacts result (shortest distance to C, 2.60 Å; to H, 2.32 Å). The $[(c\text{-hexyl})_2NLi]_n$ amide has been isolated as a colorless crystalline material (melting point 209–211°C), but twinning has so far prevented solution of the structure (*157*). An unsolvated $(AsLi)_3$ ring trimer $\{[(Me_3Si)_2CH]_2AsLi\}_3$ has also been reported (*158*). However, in contrast to the $(NLi)_3$ species (**55**)–(**57**), the ring is not planar and deviates from threefold symmetry. One of the

TABLE VI

STRUCTURES AND KEY PARAMETERS FOUND FOR UNCOMPLEXED LITHIUM AMIDES

Structural formula[a]	Formula number[b]	Range of N–Li distances (Å)[c]	Range of NLiN angles (°)[c]	Figure	Ref.
$[Me_2\overline{C(CH_2)_3CMe_2NLi}]_4$	(**54**)	(2.00)	(169)	26b	*19*
$[(PhCH_2)_2NLi]_3$	(**55**)	1.91–2.04	141–147	26b; 27	*20,76*
		(1.95)	(144)		
$[(Me_3Si)_2NLi]_3$	(**56**)	1.98–2.02	144–151	26b	*17,18*
		(2.00)	(147)		
$[(Me_3Si)_2NLi]_2$[d]		(1.99)	(100)	26b	*80*
$[(Me_3Ge]_2NLi]_3$	(**57**)	1.88–1.99	142–157	26b	*156*
		(1.92)	(149)		
$[H_2\overline{C(CH_2)_5NLi}]_6$	(**58**)	1.99–2.00 (2.00)	—	28	*164*
		2.06–2.12 (2.09)	—		

[a] By X-ray crystallography unless otherwise stated.
[b] See text.
[c] Mean value in parentheses.
[d] By electron diffraction in the gas phase.

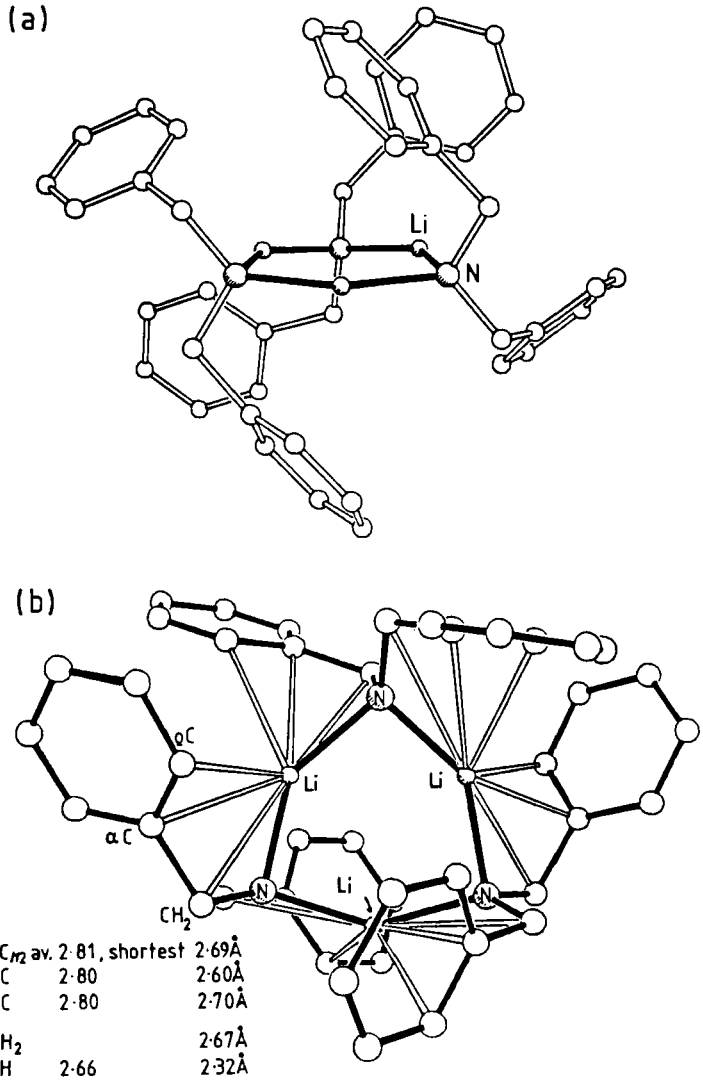

FIG. 27. (a) Molecular structure of $[(PhCH_2)_2NLi]_3$ (**55**); (b) Li···H_2C, ···αC, and ···*o*-CH interactions in (**55**).

Li—As—Li angles is significantly smaller [98(1)°] than the other two [103(1)/104(1)°].

Isolated uncomplexed lithium amide dimers are not known in the solid state. However, electron diffraction shows (**56**) to be dimeric in the gas phase (*80*). The major change in structural parameters with ring

size occurs for the NLiN angles. Comparisons can be made with the phosphidolithium compound $\{[(Me_3Si)_2CH]_2PLi\}_2$, a dimer even in the solid state (*159*). Presumably the larger P atom (hence longer P—Li bonds versus N—Li bonds) allows adequate separation of the R and R′ groups and so removes any steric necessity to adopt a larger ring.

Heavier alkali metal analogs of (**55**) and (**56**) are noteworthy. Dibenzylamidosodium $[(PhCH_2)_2NNa]_n$ has been prepared as red crystals (*160*). A structure is not yet available, but its low melting point (98–101°C) and reasonable solubility in hydrocarbons suggest an oligomeric ring structure. The sodium and potassium analogs of (**56**) also are known, $[(Me_3Si)_2NNa]_\infty$ (*161*) and $[(Me_3Si)_2NK\cdot toluene]_2$ (*162*), respectively. The former is a polymer with N—Na—N—Na zig-zag chains (angles at Na, ~150°). For the latter, the larger size of K versus Li allows dimer formation despite the decreased NKN ring angle (94°).

Lithium amides with relatively small or flat R and R′ groups will give ladder structures (Figure 26c). Further association occurs laterally by joining N—Li ring edges [*cf.* $(NLi)_{2,3}$ ring faces in the case of stacks]. The internal Li centers become three coordinate. In many cases the lithiation of amines in nonpolar solvents results in the formation of amorphous materials, insoluble in such solvents and having high melting points, e.g., R=Ph, R′=Ph, naphthyl, $PhCH_2$, and Me, all with melting points >250°C (*20, 163*) and $RR'N{=}H_2\overline{C(CH_2)_3N}$ (pyrrolidide) (*21, 150*). All of these lithium amides presumably form very long ladders. Only one oligomeric lithium amide ladder is known so far. Lithiation of hexamethyleneimine in hexane/toluene produces the crystalline and hydrocarbon-soluble compound $[H_2\overline{C(CH_2)_5NLi}]_n$, (**58**) (*164*), a hexamer ($n = 6$) in the solid state (Fig. 28a). This is the first structurally characterized uncomplexed lithium amide with $n > 4$ and the first structure that is not a simple planar $(NLi)_n$ ring. Other views of (**58**) make clear that it could be regarded as a stack of two six-membered $(NLi)_3$ rings (Figure 28b) or as a cyclized ladder of six N–Li rungs/three $(NLi)_2$ rings (Fig. 28c).

In this regard, one can predict the N—Li bond length pattern expected for a cyclized ladder (Fig. 29). The shortest N—Li bond length is expected in uncomplexed RR′NLi monomers, e.g., in the gas phase or in calculational studies. Longer, but still short, N—Li bonds are expected in isolated rings because each $RR'N^-$ ligand presents two lobes, each containing a pair of electrons, for bonding to two Li^+ centers [*cf.* the N—Li bond lengths for (**54**)–(**57**), Table VI]. However, when such rings associate, the electron density on the amide ligands must interact with three Li^+ centers, and this requires an electronic reorientation. Hence, one expects alternating shorter and longer N—Li bonds for the ladder edges, and longer bonds also for the N—Li ladder rungs.

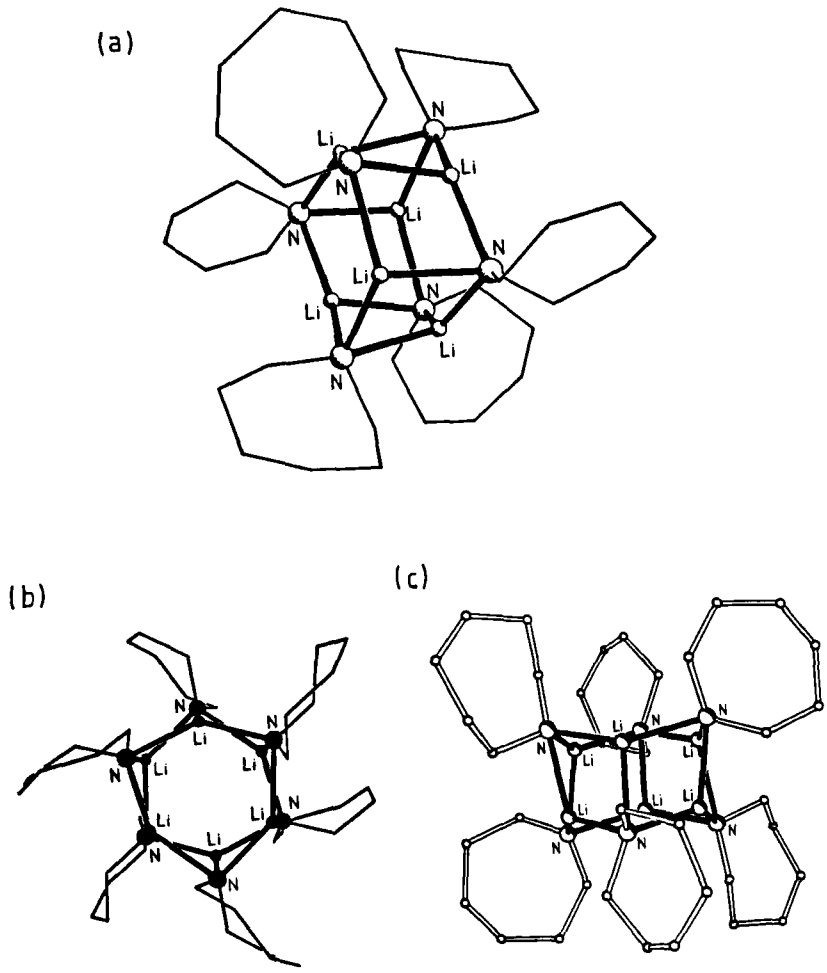

FIG. 28. (a) Molecular structure of $[H_2\overline{C(CH_2)_5NLi}]_6$ (**58**); (b) view of (**58**) as two stacked trimeric rings; (c) view of (**58**) as a cyclized ladder of three dimeric rings/six N—Li rungs.

This is observed for (**58**), whose N—Li bond lengths fall into two very distinct sets (Table VI). In fact, the general pattern is one of alternating shorter (1.99–2.00 Å, mean 2.00 Å) and longer (2.07–2.12 Å, mean 2.10 Å) bonds within the six-membered rings (Fig. 28b), and medium distances (2.06–2.09 Å, mean 2.07 Å) between the rings. This is different from the pattern found for iminolithium hexamers (**1**)–(**4**), whose structures were interpreted in terms of two stacked trimeric rings. There, alternating shorter and medium-length bonds are found within each

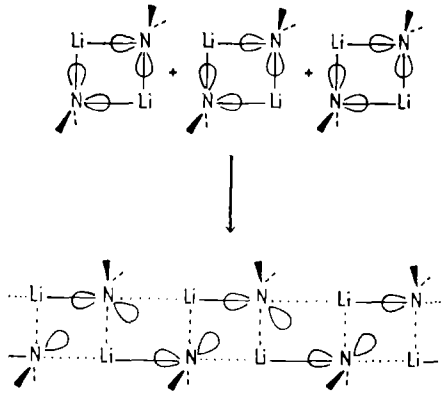

FIG. 29. Representation of the association of $(NLi)_2$ rings into a ladder structure, and of the bond length pattern expected.

ring and longer bonds are found between the rings (Section II,A; Table I). Hence (**58**) is better regarded as a cyclized ladder (Fig. 28c). We will return to this point when the MO optimized structures of $(H_2NLi)_6$ are discussed (Section III,B,2).

2. *Calculational Studies*

Ab initio and MNDO calculations have been performed on uncomplexed $(H_2NLi)_n$ models. Structures with $n = 1$ (*103*), with $n = 2$ and 3 (*108, 165–168*), with $n = 4$ (*21, 108, 111, 150, 168*), and with $n = 6$ (*115, 169*) have been optimized at various theoretical levels. For the oligomers with $n = 2$ and 3, the geometries are in excellent agreement with the experimental X-ray and electron diffraction data (Section III,B,1; Table VI). All calculations show the $(NLi)_n$ rings with H atoms perpendicular to the ring plane (Fig. 30a and c) to be preferred to the forms with all atoms in the same plane (Fig. 30b and d).

The relative energies of the two forms of each ring are given in Table VII. The electronic reason for these preferences is clear. The amido N^- electron density is tetrahedral-like and interactions with two lithium centers in the same plane as H_2N^- are much less effective (see Section III,A and Fig. 26a). Contast this with the directionality of the imide N^- (sp^2) electron density, which dictates the formation of ring systems with substituent atoms in the same plane. For example, planar $(H_2C{=}NLi)_2$ is preferred to the perpendicular form by 17.0 kcal mol^{-1} [6-31G (*72, 74*)] or by 6.8 kcal mol^{-1} [MNDO (*108*)] (Section II,D; Fig. 20).

The association energies for the favored perpendicular forms of

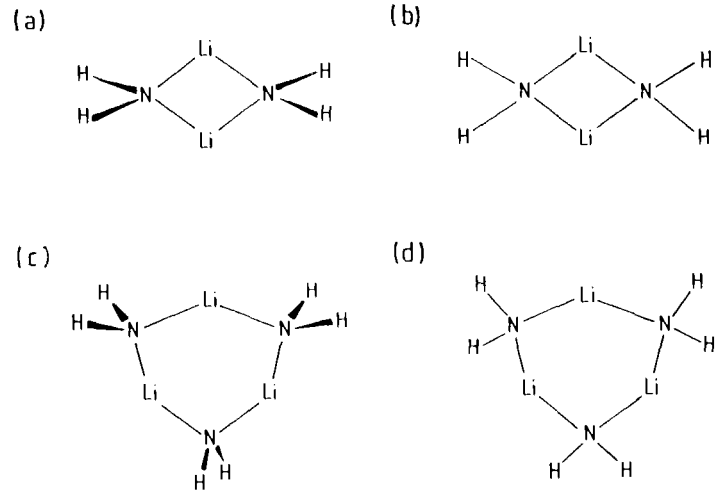

FIG. 30. Perpendicular and planar forms of $(H_2NLi)_2$ and $(H_2NLi)_3$ rings.

$(H_2NLi)_2$ and $(H_2NLi)_3$ (Table VIII) show that a trimer is preferred over a dimer. This is most simply ascribed to the more favorable Li—N—Li angles in the larger ring (Table IX) and to the reduction in repulsive interactions (see below). Though these calculations neglect the bulk of the substituent groups and crystal packing effects, no crystalline $(RR'NLi)_2$ dimers are known experimentally (Table VI), only trimers (**55**), (**56**), and (**57**) and a tetramer (**54**). The calculated N—Li bond lengths (Table IX) are similar for the dimer and the trimer. However, the expansion in ring size is manifested particularly by the large increase in the angle at lithium (approaching 40°), as the Li—N—Li

TABLE VII

RELATIVE ENERGIES OF PERPENDICULAR AND PLANAR FORMS OF $(H_2NLi)_2$ AND $(H_2NLi)_3$

	Perpendicular D_{nh} (kcal mol^{-1})	Planar D_{nh} (kcal mol^{-1})	Theoretical level	Figure	Ref.
$(H_2NLi)_2$	0.0	21.9	6-31 + G*/6-31G*//6-31G*[a]	30a and b	*165*
	0.0	22.0	MNDO[b]		*108,165*
$(H_2NLi)_3$	0.0	42.6	3-21 + G/3-21G//3-21G[a]	30c and d	*165*
	0.0	45.4	MNDO		*165*

[a] The diffuse orbitals were omitted from Li in these calculations.
[b] Minimum neglect of differential overlap.

TABLE VIII

ASSOCIATION ENERGIES OF PERPENDICULAR FORMS OF $(H_2NLi)_2$ AND $(H_2NLi)_3$

	Association energy (kcal mol^{-1} per monomer unit)	Theoretical level	Ref.
$(H_2NLi)_2$	−32.6	6-31 + G*/6-31G*//6-31G*[a]	*165*
	−31.4	MNDO[b]	*108, 165*
	−35.9	MP2/6-31G*//3-21G	*166a*
	−36.8	6-31G//6-31G	*167*
$(H_2NLi)_3$	−41.3	3-21 + G/3-21G//3-21G[a]	*165*
	−38.0	MNDO	*165*
	−44.6	6-31G//6-31G	*167*

[a] Diffuse functions on N, but not on Li.
[b] MNDO, Minimum neglect of differential overlap.

angle, is less variable. 6-31G* calculations on $H_2NLi_2^+$ show that the geometry with the Li—N—Li angle being ~130° is the lowest point in energy. The energy rises similarly on deviation above or below this ideal Li—N—Li angle (*168*). Also, as the Li—Li and N—N distances are increased on ring expansion, the reduction in these repulsive interactions favors the trimer. These $(H_2NLi)_n$ species are obviously highly ionic. A natural population analysis (*38*) indicates lithium charges of +0.9 for monomeric, planar H_2NLi (*170*). The ionic nature of N—Li bonds, and X—Li bonds in general, is also exemplified by the calculated dimerization energies of lithium compounds with first-row substituents. The association energies correlate well with the electronegativity of the substituent, e.g., they become more negative with increasing electronegativity (*166*).

For the tetramer $(H_2NLi)_4$, three structures have been examined.

TABLE IX

SELECTED BOND PARAMETERS FOR PERPENDICULAR FORMS OF $(H_2NLi)_2$ AND $(H_2NLi)_3$

	Distance (Å)			Angle (°)		Theoretical level	Ref.
	N—Li	Li—Li	N—N	LiNLi	NLiN		
$(H_2NLi)_2$	1.943	2.314	3.122	73.1	106.9	6-31G*	*165*
	1.931	—	—	72.3	107.7	6-31G	*167*
$(H_2NLi)_3$	1.906	2.781	3.649	93.7	146.3	3-21G	*165*
	1.95	2.94	3.69	98	142	6-31G	*165*
	1.928	—	—	94.5	145.5	6-31G	*167*

These are depicted in Fig. 31a showing a planar eight-membered ring, with NH_2 groups perpendicular to the ring plane, in Fig. 31b showing a ladder formed by lateral association of two dimeric rings, and in Fig. 31c showing a tetrahedral form, which can be viewed as two stacked dimeric rings. All studies find the large ring structure to be more stable than the stack. The energy difference depends on the calculational method used (Table X). Low-level (3-21G) *ab initio* calculations on $(H_2NLi)_n$ species result in energies that are far too negative due to the basis set superposition error (BSSE) (*171, 172*). It is now well established that diffuse as well as polarization functions are necessary to eliminate BSSE and hence to provide a more nearly complete description of first-row molecules with lone pairs (*173–176*). One study (*21*) found the ladder structure to be a local minimum, intermediate in

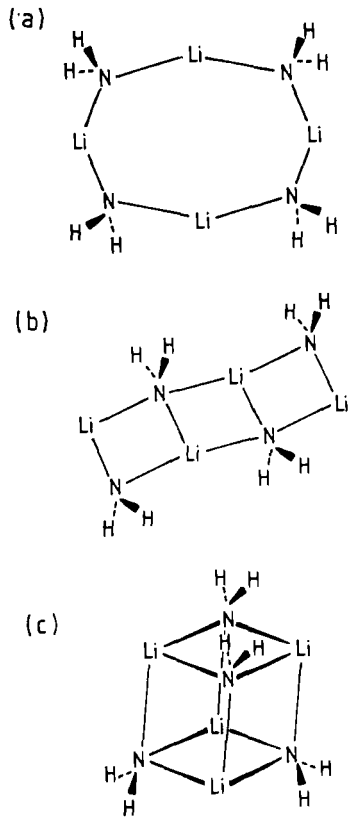

FIG. 31. (a) Ring (D_{4h}), (b) ladder (C_{2h}), and (c) stack (D_{2d}) forms of $(H_2NLi)_4$.

TABLE X

RELATIVE ENERGIES AND ASSOCIATION ENERGIES FOR OPTIMIZED STRUCTURES OF $(H_2NLi)_4$[a]

Relative energies			Association energy for ring form (kcal mol^{-1})	Theoretical level	Ref.
Ring (D_{4h})	Ladder (C_{2h})	Stack (D_{2d})			
0.0	—	8.9	−41.8	HF/6-31G + sp + d	*111*
0.0	—	11.5	−52.9	3-21G	*111*
0.0	—	28.4	−40.0	MNDO[b]	*108*
0.0	7.4	11.4	—	6-31G	*21,150*

[a] See Fig. 31.
[b] Minimum neglect of differential overlap.

energy between the ring and the stack. The association energies found for the tetrameric ring are large, comparable to those noted earlier for a trimer (Table VIII).

The above results are significant for several reasons. Calculations on most other lithium-containing tetramers favor stacked, tetrahedral forms, e.g. $(LiF)_4$, $(LiOH)_4$ (*111*), and $(MeLi)_4$ (*101, 102*). Why then is a ring preferred to a stack for $(H_2NLi)_4$? One possible answer emphasizes the importance of lone-pair orientation effects (*111*). The two lone-pair lobes on H_2N^- are unable to interact with the three Li^+ centers on a tetrahedral face as effectively as with the two centers of a dimer. Compare this with the situation for F^- and HO^-, which have four or three lone pairs, respectively. Moreover, H_3C^- (with only one lone-pair lobe) also has effective conical (threefold) symmetry. However, $RR'C{=}N^-$ (with two lobes, the same as H_2N^-) manages to bond to three Li^+ ions, and forms stacks. This is due to the contribution from the C=N π bond, which again results in effective conical symmetry. Another argument can be based on stereochemistry. Consider the approach and subsequent stacking of two $(RLi)_2$ rings, with R=F, OH, or NH_2 (Fig. 32). Only in the case of $R{=}NH_2$ (Fig. 32c) are there substituents *between* the two $(RLi)_2$ rings. The NH_2 groups cannot twist much in order to allow closer approach of the two rings. If they did, the N—Li bonding *within* each ring would be weakened (Fig. 30a and b). These points are quantified when one examines bond lengths within the optimized ring and stack structures of $(H_2NLi)_4$ (Table XI). The N—Li bonds are considerably shorter in the ring, and the interdimer N—Li contacts in the stack are particularly long. However, though there are only eight N—Li electrostatic interactions in the ring, stack formation generates 12 such contacts, albeit rather longer ones. The summation of

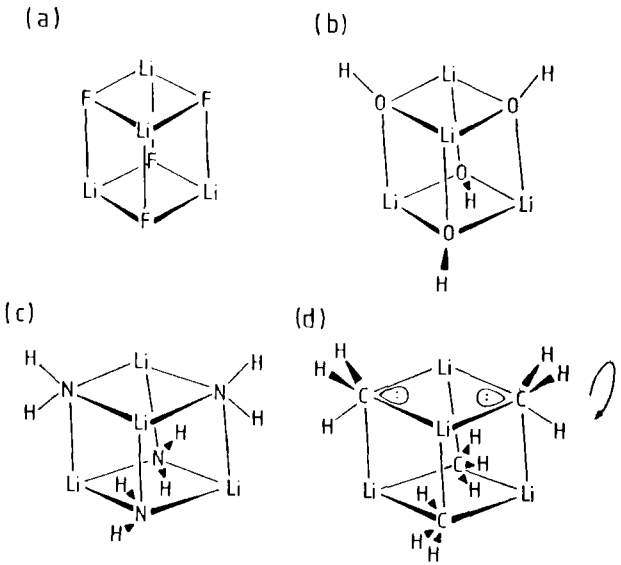

FIG. 32. Representations of the stacking of two $(RLi)_2$ rings: (a) R=F, (b) R=OH, (c) R=H_2N, and (d) R=CH_3.

TABLE XI

SELECTED BOND PARAMETERS FOR OPTIMIZED STRUCTURES OF $(H_2NLi)_4$

	Figure	Distance (Å) N—Li	Distance (Å) Li···Li	NLiN angle (°)	Theoretical level	Ref.
$(H_2NLi)_4$ ring	31a	1.906	3.003[a]	166.0	3-21G	*111*
		1.927	3.058[a]	165.0	6-31G	*21, 150*
$(H_2NLi)_4$ ladder	31b	1.882–2.115 (mean 2.008 for 10 bonds)	2.431/2.444/ 3.780[b] (mean 2.855)	—	6-31G	*21,150*
$(H_2NLi)_4$ stack	31c	1.962/2.027[c] 2.013/2.042[c] (mean 2.023 for 12 bonds)	2.239/2.426[d] 2.343/2.528[d] (mean 2.405)	— —	3-21G 6-31G	*111* *21,150*

[a] Two closest contacts per Li.
[b] Across an outer ring/across the inner ring/going along the ladder, respectively.
[c] Within dimeric rings/between them, respectively.
[d] Between Li atoms in different rings/within each ring, respectively.

N—Li bond energies could perhaps be similar for both forms. But repulsions also are important. Eight-membered ring formation allows $Li^{\delta+}$ (and $N^{\delta-}$) centers to be widely spaced. In contrast, Li—Li distances in the stack are much shorter, both within each ring (now only four-membered) and, especially, between rings (Table XI).

These theoretical results help explain why the only known lithium amide tetramer is a ring [(**54**), Table VI], and also why pseudocubane tetramers, so prevalent elsewhere in organolithium chemistry [Section II,B; (**7**) and (**9**); Section II,E; Tables II–V], are unknown for lithium amides. If two $(H_2NLi)_2$ rings prefer not to stack (as shown by the MO calculations), it is unlikely that two "real" $(RR'NLi)_2$ rings, i.e., with more bulky R and R′ substituents, will do so, especially if the lithiums are coordinated further.

The ladder structure of $(H_2NLi)_4$ (Fig. 31b) is intermediate in energy between an eight-membered ring and a stacked arrangement (Table X). Though RR′NLi aggregation avoids three-dimensional stacking, lateral (ladder) association (see Section III,C) may be a viable alternative to the formation of open rings. The close relationship between the two forms is obvious: if the two central N—Li rungs of the ladder are broken, an eight-membered ring will form (Fig. 31a). The bond distances for the ladder (Table XI) are intermediate. The N—Li bonds in the ladder are, on average, longer than those in the ring, but shorter than those in the stack. Antibonding contacts are more important (shorter Li—Li and N—N distances) than those in the ring, but are less important than those in the stack.

Related MO calculations on $(LiH)_4$ tetramers are relevant (*114*). As in $(H_2NLi)_4$, an eight-membered ring was found to be the lowest energy form. Higher in energy were a stack of two dimers (a tetrahedral structure, termed a "ring dimer," relative energy +3.7 kcal mol^{-1}) and then a ladder structure (termed a "fence," +11.0 kcal mol^{-1}). The reversal of stack–ladder preference versus $(H_2NLi)_4$ is understandable. There are no substituents in $(LiH)_2$ rings [*cf.* Fig. 32a, for $(LiF)_2$ rings], so their vertical approach is not discouraged.

Ab initio calculations have also been carried out on hexamers $(RLi)_6$ with R=H (*114*), Me (*102, 116*), F, OH, and NH_2 (*115, 169*). For these highly associated species, rings become disfavored. For example, $(LiH)_6$ prefers a stack of two trimers (relative energy 0.0 kcal mol^{-1}) versus the preference of a ring for $(LiH)_4$ (*114*). Next in energy comes a stack of three dimers (termed a "fence dimer," relative energy +3.5 kcal mol^{-1}), followed by a twelve-membered ring (+7.7 kcal mol^{-1}), and then a ladder (+19.5 kcal mol^{-1}). Specifically for $(H_2NLi)_6$ (*115*), it is not surprising that a stack of two puckered trimers (Fig. 33a) is favored by

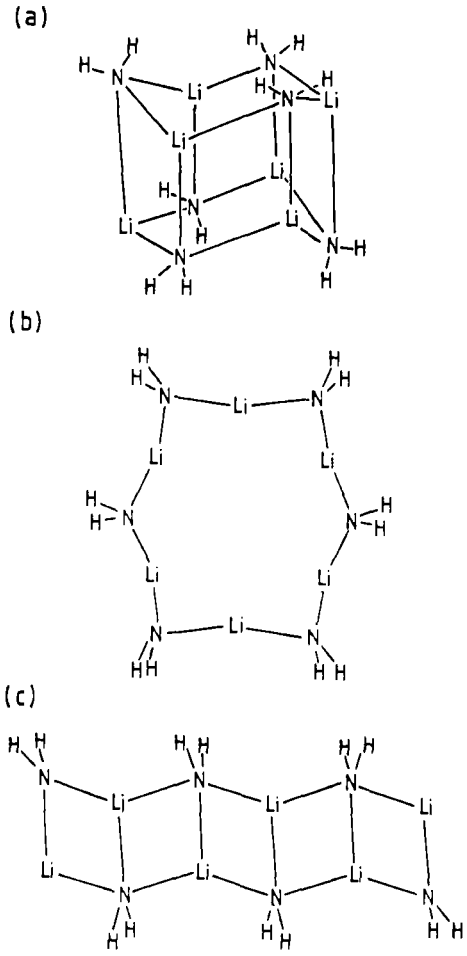

FIG. 33. (a) Stack, (b) ring, and (c) ladder forms of $(H_2NLi)_6$.

20.2 kcal mol^{-1} (6-31G basis set augmented by a set of diffuse sp functions and a set of six d-type functions on N) over a large ring structure (Fig. 33b). The "star" shape shown in Fig. 33b (inverted lithiums) results from the preference of the Li—N—Li angle for lower values. Comparisons were drawn between the stacked $(H_2NLi)_6$ structure and those of the iminolithium hexamers $(RR'C{=}NLi)_6$ (**1**)–(**4**) (see Section II,A). In $(H_2NLi)_6$, just *two* types of N—Li bonds are found, of lengths 1.989 Å within constituent rings and 2.055 Å between the rings. The fact that *three* types of N—Li bond lengths are found in the

experimental iminolithium hexamers (see especially Fig. 8 and Table I) was attributed to crystal packing effects (*115*). This was refuted (*177*). The stereochemical propensities of $RR'N^-$ and $RR'C{=}N^-$ ligands are different. The former favors ring formation or, if this is unattainable, laddering; the latter ligand favors stacking. The $(H_2NLi)_6$ ladder (Fig. 33c) is intermediate in energy between the stack and the ring, i.e., the stack is still preferred by 15 kcal mol^{-1} (*169*). The apparent preference of $(H_2NLi)_6$ for a stack over a ladder may be reversed in experimental systems $(RR'NLi)_6$, where R ≠ H. As has been pointed out (*164*), the structure of the only known amidolithium hexamer, $[H_2\overline{C(CH_2)_5}\overline{N}Li]_6$ (**58**), which displays three sets of N—Li bond lengths, is better viewed as a cyclized ladder than as a stack (see Section III,B,1, Table VI, and Figs. 28 and 29).

3. *Structures in Solution*

Very few studies on *uncomplexed* lithium amides have been carried out in solution, e.g., in hydrocarbon solvents. Only five oligomeric, ligand-free compounds of this type have been characterized structurally [(**54**)–(**58**); Table VI; Section III,B,1]. Studies carried out on solutions in polar solvents would, in effect, involve complexes. For example, the unsolvated crystalline trimers (**55**) and (**56**) both form dimeric etherate complexes (*19*, *20*, *76*, *81*). Solution studies of complexed lithium amides will be described in Section III,C,3.

The solid-state trimer $[(PhCH_2)_2NLi]_3$ (**55**) dissolves in arene solvents to give pink solutions (*20*, *76*). Cryoscopic measurements of benzene solutions gave association state values (n) of 2.87–2.66 (0.033–0.025 M concentrations, respectively). ^{7}Li NMR spectra of relatively concentrated solutions at 20°C only show a single resonance (e.g., at −0.66 ppm for a 0.17 M solution). However, two singlets were observed in more dilute solutions (e.g., $\delta \neq -0.71$ and δ −2.91 ppm, ratio ~10 : 1, for a 0.06 M solution). Because n is <3, and two well-separated ^{7}Li NMR resonances are observable, an equilibrium between the trimer and a dimer or a monomer must be present. The electronic spectra of (**55**) gave more information. In benzene solution, absorption occurs in the visible region at λ_{max} 525–530 nm. The absorptivity of this band increased on dilution, e.g., for 5.3×10^{-3} and 5.3×10^{-4} M solutions, a = 100 and 300 M^{-1} cm^{-1}, respectively. Hence, the pink color of solutions of (**55**) seems due to the lower association species (dimer or monomer) present. In fact, configuration interaction MO calculations (*178*) predicted that only a monomer, $(PhCH_2)_2NLi$, should give a visible region HOMO–LUMO transition, at 545 nm. The calculated λ_{max} values are 255 and 320 nm

for the trimer and dimer, respectively. As already noted, in the crystal structure of (**55**) the benzyl groups bend in toward the two-coordinate Li centers of the trimeric ring (see Fig. 27b). It was concluded that in solution the trimer is in equilibrium with a monomer, and that the latter (containing one-coordinate Li) has much increased Li···benzyl interactions. These interactions allow a charge transfer mechanism to operate, producing the solution color observed.

The only other relevant study concerns the uncomplexed hexamer, $[H_2\overbrace{C(CH_2)_5}\overbrace{N}Li]_6$ (**58**). This dissolves in arene solvents apparently to give even higher aggregates (*164*). In benzene, cryoscopic measurements gave association state (n) values of 5.4 ± 0.2 to 10.1 ± 0.5 (0.06–0.14 *M* solutions, respectively). The ^{7}Li NMR spectra of d_8-toluene solutions of (**58**) at −90°C are concentration dependent. Relatively dilute solutions give two sharp singlets [0.19 *M*, δ −0.50, −1.63 ppm (ratio 1:1); 0.25 *M*, δ −0.49, −1.61 ppm (ratio 2:1)]. At higher concentrations, only the higher field resonance occurs (e.g., at 0.61 *M*, δ −0.48 ppm). Clearly, at least two species are present in solution: presumably one is the hexamer (^{7}Li signal at ~δ −1.6 ppm) and the second is an aggregate with $n > 6$ (^{7}Li signal at ~δ −0.5 ppm).

C. Complexed Lithium Amides [$(RR'NLi{\cdot}xL)_n$]

1. Solid-State Structures

We showed earlier that the basic structural units of uncomplexed lithium amides are rings, $(RR'NLi)_n$, with $n = 2, 3, 4$ (Section III, A; Fig. 26). Only rarely, when R,R′ groups are particularly large, can such rings be isolated [Table VI; (**54**)–(**57**)]. More usually, these small rings associate further, laterally, joining N—Li ring edges to give ladders. Although one exception is known [(**58**); Fig. 28], such laddering appears generally to be extensive and gives amorphous, hydrocarbon-insoluble materials. Therefore most lithium amide reagents are generated in polar solvents (L), e.g., Et_2O, THF, HMPA, DMPU, and TMEDA (*6, 7, 11–13, 179*). This results in complexes of type $(RR'NLi{\cdot}xL)_n$. The polar Lewis base molecules (L) coordinate to the Li centers and limit the degree of association sterically; in particular, extensive laddering is prevented and crystalline, hydrocarbon-soluble materials can be isolated. For example, whereas lithiation of Ph_2NH in hexane or toluene results in the precipitation of a white powder [$(Ph_2NLi)_\infty$, melting point 326°C], the same reaction in Et_2O or Et_2O/toluene media affords colorless crystals of $(Ph_2NLi{\cdot}OEt_2)_2$ (melting point 50°C). These are very soluble (~2 g ml^{-1}) in toluene or benzene (*157*). Furthermore, the

lithium amide reagents made in the presence of these complexants (commonly termed "additives") are much more reactive in subsequent metalations. It has long been assumed that this enhancement is kinetic in origin, reflecting the low association states of the complexes produced (*179–182*).

The major structural types found for lithium amide complexes in the solid state are illustrated in Fig. 34. These comprise ladders of limited extent when the L : Li ratio is less than 1 : 1 (Fig. 34a), dimeric $(NLi)_2$ rings, when this ratio is 1 : 1 and, usually, when the complexants are monodentate (Fig. 34b), and monomers, both contact-ion pairs (CIPs) and solvent-separated ion pairs (SSIPs) (Fig. 34c). Monomers occur always when there are two or more monodentate complexants per Li. This also is usual with bidentate ligands, and is always found when the ligands have higher denticity.

Lithiation of pyrrolidine, $H_2\overline{C(CH_2)_3NH}$, in hexane produces a white insoluble powder, $[H_2\overline{C(CH_2)_3N}Li]_n$ (*21, 150*). This is assumed to have an extensive ladder structure (Section III,A; Fig. 26c); compare the cyclized-ladder structure of crystalline $[H_2\overline{C(CH_2)_5N}Li]_6$ (*164*). However, if lithiation is carried out in the presence of the ligands PMDETA or TMEDA, crystalline complexes are isolated: $\{[H_2\overline{C(CH_2)_3N}Li]_3 \cdot PMDETA\}_2$ (**59**) (*21, 150*) and $\{[H_2\overline{C(CH_2)_3N}Li]_2 \cdot TMEDA\}_2$ (**60**)

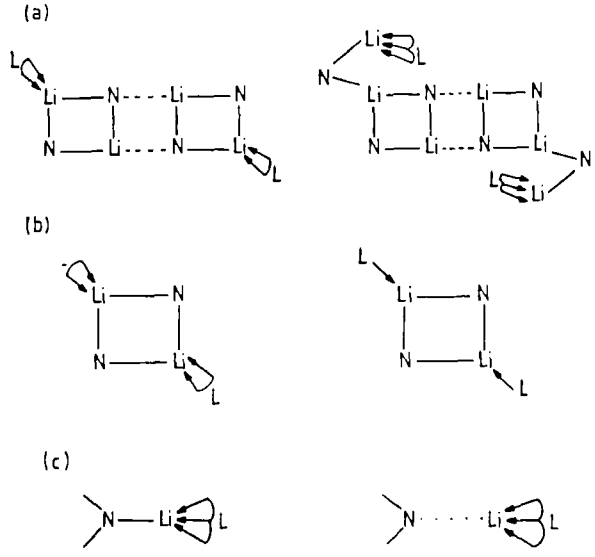

FIG. 34. Structural types for complexed lithium amides $(RR'NLi \cdot xL)_n$, L = a Lewis base: (a) ladders with n = 2 and 3; (b) dimeric rings; (c) monomers (CIPs and SSIPs).

(*150*). The molecular structures are shown in Fig. 35 (see also Fig. 34a). Both are limited-length ladders and only their terminal Li centers are complexed. These provide indirect evidence that association of $(RR'NLi)_n$ rings to give polymers occurs by continuous laddering. Indeed, structures (**59**) and (**60**) may be formed *via* interception of longer ladders [note the structure of (**31**), an intercepted stack, in Fig. 23b]. The structures of both (**59**) and (**60**) contain central ladders made up of two attached $(NLi)_2$ rings or, alternatively, four N—Li rungs. The internal ring of each ladder, N(1)Li(1)·N(1′)Li(1′) in each case, is planar. The N atoms of the outer rungs, N(2) and N(2′), lie near this inner ring plane, but the terminal Li atoms, Li(2) and Li(2′), deviate considerably from this common plane [by ±0.71 Å for (**59**), and by ±1.01 Å for

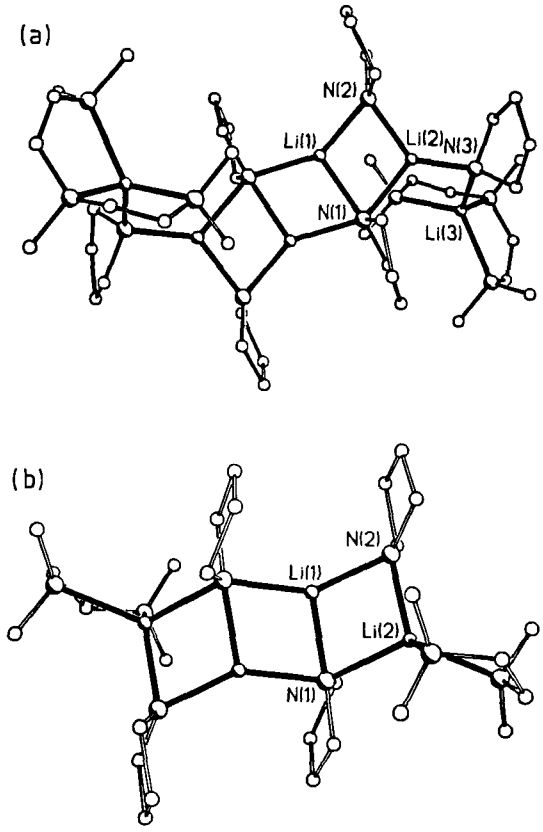

FIG. 35. Molecular structures of (a) $\{[H_2\overline{C(CH_2)_3NLi}]_3 \cdot PMDETA\}_2$ (**59**) and (b) $\{[H_2\overline{C(CH_2)_3NLi}]_2 \cdot TMEDA\}_2$ (**60**).

(**60**)]. In (**60**), these end-Li atoms are each complexed by a TMEDA molecule. For (**59**), there are two N—Li(PMDETA) units attached to these end-Li atoms. Thus, interception (by ligation) of the continuous ladder envisaged for $[H_2\overline{C(CH_2)_3NLi}]_\infty$ leads to its partial disconnection.

The N—Li bond lengths and ring internal angles for (**59**) and (**60**) are given in Fig. 36. These will be analyzed in detail below along with the results of MO calculations on $(H_2NLi)_4 \cdot (H_2O)_n$ complexes (n = 2 and 4) (Section III,C,2). We note here that the expected N—Li bond length pattern is found (see Section III,B,1; Fig. 29) when two or more $(NLi)_2$ rings join to give a ladder. Alternating relatively short and long bonds occur along the uncomplexed ladder edges [1.95 and 2.03 Å for (**59**), 1.96 and 2.03 Å for (**60**)], and relatively long bonds are also found for the inner rungs [2.05 Å for (**59**), 2.04 Å for (**60**)].

Lateral association is not restricted to lithium amides. Lithium phosphide rings $(RR'PLi)_n$ will have a stereochemistry similar to $(RR'NLi)_n$ rings. The R,R′ groups perpendicular to the $(PLi)_n$ ring plane will preclude stacking, but facilitate laddering. The presence of a deficiency of Lewis base (less than one per Li) already precludes the formation of

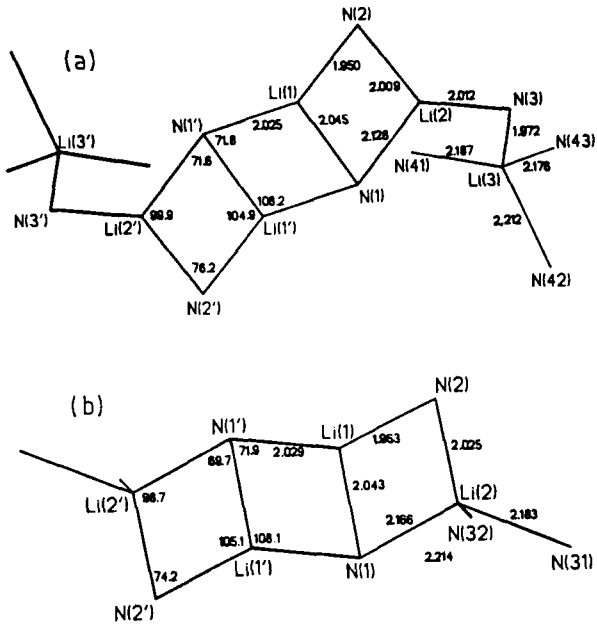

FIG. 36. Key bond lengths and angles in the structures of (a) (**59**) and (b) (**60**).

continuous ladders. Hence, the crystalline complexes $[(Me_3Si)_2PLi]_4 \cdot 2THF$ (*183*) and $(Bu^t{}_2PLi)_4 \cdot 2THF$ (*184*) have been isolated and structurally characterized. Each has a limited ladder structure with four PLi rungs. Because the complexants (one per terminal Li atom) are monodentate, the P_4Li_4 frameworks are essentially planar.

When the Lewis base (L):Li ratio is 1:1 or greater, ladder-type structures no longer persist (see Section III,C,2). Dimeric rings or monomers (C.I.P.s or S.S.I.P.s) are formed instead (Fig. 34b and c). Structural details for the known solid-state dimers (**61**)–(**68**) are shown in Table XII (*185–188*). Excluding (**68**) for the time being, all contain one monodentate oxyligand (Et_2O, HMPA, or THF) per Li center. The $(NLi)_2$ rings are planar and rhomboidal, with angles at Li of 102–106°. The relatively short Li—Li cross-ring contacts (~2.4–2.5 Å) are due to the acute angles (74–78°) at the μ_2-amido N^- centers, but have little or no metal–metal bonding significance.

The Li centers in these rings are only three coordinate. What limits further association? Two views of $[(PhCH_2)_2NLi \cdot OEt_2]_2$ (**61**) provide an answer. Figure 37a shows very clearly the perpendicular projection of R,R′ groups (here, $PhCH_2$) relative to the $(NLi)_2$ ring plane. Such rings cannot stack. Figure 37b, a side-on view of the $(NLi)_2$ ring, demonstrates equally clearly how a single monodentate ligand per Li atom occupies the lateral space around such a ring. Laddering is precluded as well. This contrasts with most other $(RLi \cdot L)_2$ systems, e.g., with R = imino, alkyl, aryl, alkynyl, and enolato; L is a monodentate

TABLE XII

DIMERIC LITHIUM AMIDE COMPLEXES: KEY STRUCTURAL PARAMETERS (X-RAY DIFFRACTION DATA)

Complex	Formula number[a]	Distance (Å)			N—Li—N ring angle (°)	Ref
		N—Li	Li—O	Li—Li		
$[(PhCH_2)_2NLi \cdot OEt_2]_2$	(**61**)	1.98–1.99	2.01	2.45	104.0	*20, 7*
$[(PhCH_2)_2NLi \cdot HMPA]_2$	(**62**)	2.00–2.01	1.85	2.51	102.7	*20, 7*
$[(Me_3Si)_2NLi \cdot OEt_2]_2$	(**63**)	2.06	1.94	—	104.9	*19, 8*
$[(Me_3Si)_2NLi \cdot THF]_2$	(**64**)	2.03	1.88	2.43	106.3	*185*
$[2,4,6\text{-}Bu^t{}_3C_6H_2 \cdot N(H)Li \cdot OEt_2]_2$	(**65**)	1.99–2.04	1.91	—	102.2	*186*
$[Mes_2B \cdot N(H)Li \cdot OEt_2]_2$	(**66**)	2.01–2.02	1.96	—	105.1	*187*
$[1,8\text{-}C_{10}H_6NH \cdot SiMe_2 \cdot NLi \cdot OEt_2]_2$	(**67**)	2.00–2.03	1.94	2.43	106	*188*
$[Ph \cdot N(Me)Li \cdot TMEDA]_2$	(**68**)	2.08	—[b]	2.74	97.6	*163*

[a] See text.

[b] Li—N (of TMEDA) distances, 2.30 Å.

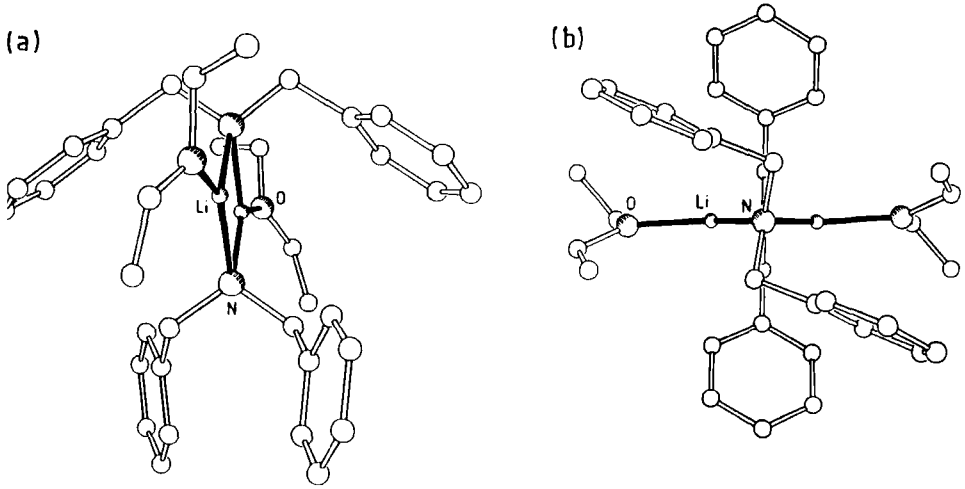

FIG. 37. Molecular structure of $[(PhCH_2)_2NLi{\cdot}OEt_2]_2$ (**61**): (a) view showing the perpendicular projection of $PhCH_2$ groups relative to the $(NLi)_2$ ring; (b) view showing the lateral extension of Et_2O ligands.

base, where stacking is not precluded, and cubic tetramers result (see Section II,B, Figs. 14 and 17, Section II,E, and Tables II–V).

Why are complexes (**61**)–(**68**) *dimers?* The same question was posed earlier regarding iminolithium species (Section II,B;Fig. 13). For the lithium amide complexes, the structures of (**61**), (**62**), (**63**), and (**64**) are particularly relevant here because the uncomplexed analogs, $[(PhCH_2)_2NLi]_3$ (**55**) and $[(Me_3Si)_2NLi]_3$ (**56**) (Section III,B,1; Table VI], are both trimers. As shown in Fig. 38a, the wide angle at Li in such trimers (~145°) leaves only a narrow coordination arc for an incoming complexant. In contrast, in a $(RR'NLi)_2$ dimer the ring angle at Li is expected to be ~100° (Fig. 38b): such is found for $[(Me_3Si)_2NLi]_2$ in the gas phase (Table VI). This leaves much more space for accommodation of an additional ligand. We will address this question in a more quantitative way in Section III,C,2.

Further comparison of the structures of (**61**) and (**62**) (Table XII) with that of (**55**) (Table VI) and of (**63**) and (**64**) with that of (**56**) shows that complexation of the Li centers (making them three coordinate) lengthens the N—Li distances slightly. Judging from Li—O bond lengths, HMPA and THF seem to be rather stronger complexants than Et_2O. A final point worth noting is that the unsymmetrically substituted lithium amides ($R \neq R'$), i.e., (**65**)–(**68**), all crystallize in the *transoid* form. This is illustrated for (**68**) in Fig. 39. This particular structure is the

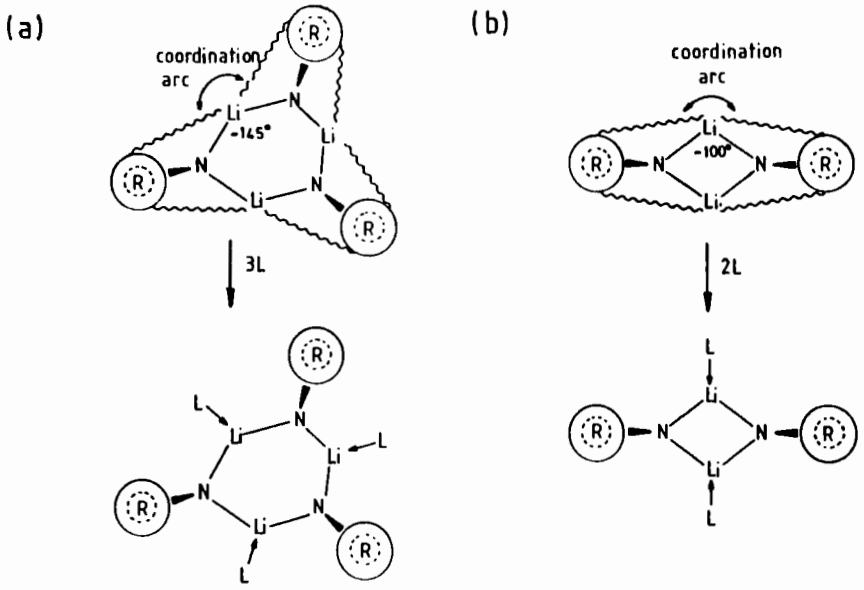

FIG. 38. Coordination arcs available for attachment of Lewis base molecules (a) to a trimeric lithium amide ring and (b) to a dimeric lithium amide ring.

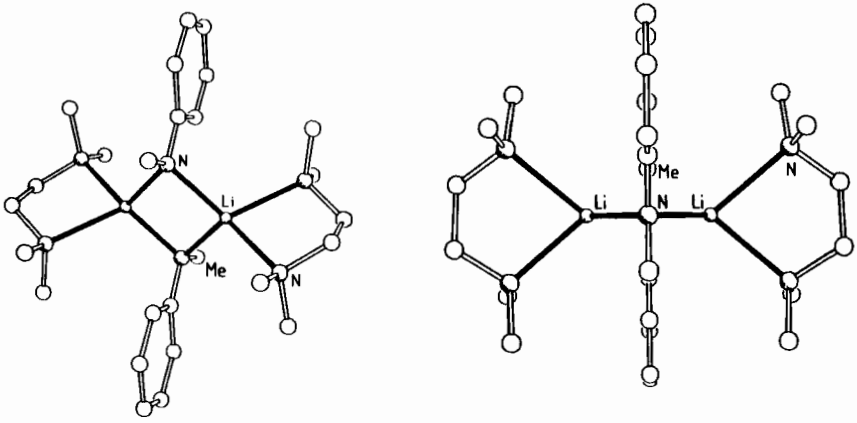

FIG. 39. Molecular structure of [PhN(Me)Li·TMEDA]$_2$ (**68**).

only one containing bidentate ligands. Each Li is four coordinate, leading to longer (amide)N—Li bonds and a smaller angle at Li.

Table XIII (*189–199*) gives details of solid-state lithium amide monomeric complexes (**69**)–(**87**). These include just three [(**79**), (**80**), and (**87**)] solvent-separated ion pairs. The remainder are contact-ion pairs, each with an (amido)N—Li bond. Association to dimers or higher oligomers is prevented sterically. The size of the R and/or R′ group in the $RR'N^-$ anions can lead to monomers even when Li^+ is complexed only by a single bidentate (e.g., TMEDA) or by two monodentate (e.g., THF or Et_2O) ligands. In such cases [(**69**), (**71**), (**72**), (**75**)–(**78**), and (**81**)–(**83**)], the lithium centers are only three coordinate. Electronic factors in the anion [notably, B⋯N multiple bonding in (**75**)–(**78**)] also may reduce the charge density at N, and lower the ability to bridge two

TABLE XIII

MONOMERIC LITHIUM AMIDE COMPLEXES: KEY STRUCTURAL PARAMETERS (X-RAY DIFFRACTION DATA)

Complex	Formula number[a]	N—Li distance (Å)	Ligand–Li distances (Å)	Ref.
Ph(naphthyl)NLi·TMEDA	(**69**)	1.97	2.12, 2.13	*163*
Ph(naphthyl)NLi·PMDETA	(**70**)	2.00	2.18, 2.21, 2.22	*163*
2,4,6-$Bu^t_3C_6H_2$(H)NLi·TMEDA	(**71**)	1.90	2.14, 2.16	*80*
2,4,6-$Bu^t_3C_6H_2$[Si(CHMe$_2$)$_2$Cl]NLi·2THF	(**72**)	1.99	—	*189*
$C_{12}H_8$SNLi·3THF	(**73**)	1.98	—	*190*
$C_{12}H_8$ONLi·3THF	(**74**)	2.03	—	*190*
$Mes_2B(Ph)NLi·2Et_2O$	(**75**)	1.94	av. 1.93	*191*
$Mes_2B(Mes)NLi·2Et_2O$	(**76**)	1.94	av. 1.95	*192*
$Bu^t_2BN(Bu^t)Li·TMEDA$	(**77**)	1.97	2.17, 2.24	*193*
$MeBN(Bu^t)BMe_2N(Bu^t)Li·TMEDA$	(**78**)	2.00	2.13, 2.20	*193*
$[Mes_2BNBMes_2]^-·[Li·3Et_2O]^+$	(**79**)	—	1.88, 1.90, 1.91	*187*
$[Mes_2BNSiPh_3]^-·[Li(12\text{-crown-}4)_2]^+$	(**80**)	—	—	*194*
$(Me_3Si)_2NLi·TMEDA$	(**81**)	1.79	2.12, 2.16	*195*
$(Ph_3Si)_2NLi·2THF$	(**82**)	2.00	1.95	*196*
$(Ph_2MeSi)_2NLi·2THF$	(**83**)	1.95	1.91	*196*
$(Me_3Si)_2NLi·(12\text{-crown-}4)$	(**84**)	1.97	2.09, 2.11, 2.33, 2.39	*194, 197*
$Ph_2NLi·(12\text{-crown-}4)$	(**85**)	2.01	2.11, 2.16 2.23, 2.24	*194, 198*
$(Ph_2MeSi)_2NLi·(12\text{-crown-}4)$	(**86**)	2.06	2.17, 2.23	*196*
$[(Ph_3Si)_2N]^-·[Li(12\text{-crown-}4)_2]^+·THF$	(**87**)	—	—	*194, 196, 199*

[a] See text.

Li^+ centers. Attachment of three monodentate ligands [THF; (**73**) and (**74**)], a tridentate one [PMDETA; (**70**)], or a single 12-crown-4 [(**84**)–(**86**)] to Li^+ also results in monomers. The bulk of these donors prevents association, even irrespective of the size of the amido R,R′ groups. Of course, Li^+ is four or five coordinate. These features are seen in the structure of (**70**) (Fig. 40); although the amido R,R′ groups (Ph, naphthyl) are two dimensional, the PMDETA ligand prohibits any further association of the monomer.

A further structural feature, namely "agostic" Li···H or Li···HC interactions (see Section I,B), occurs in several of these monomers. In the lithiated phenothiazin and phenoxazin complexes [(**73**) and (**74**), respectively], the annelated benzene rings are tilted, resulting in short Li^+—*o*-H distances. In (**73**) the four-coordinate Li^+ cation is placed unsymmetrically between the *ortho* hydrogens (Li—*o*-H, 2.54 and 2.82 Å), but in (**74**) the Li—*o*-H distances are identical (2.76 Å). More typically, such interactions are apparent when the metal centers are coordinatively unsaturated, i.e., when the steric bulk of the R,R′ amido groups and/or the bidentate neutral ligand (or two monodentate ones) prevents association. Note the short intramolecular Li—H(N) distance of 2.08 Å in (**71**) and the contacts with both aryl and *t*-butyl groups in (**72**) (Li—C, 2.47 and 2.75 Å, respectively). More unusual *inter*molecular interactions are found in the structure of (**69**) (Fig. 41a). In the monomer, the aryl groups adopt very different orientations, naphthyl being roughly perpendicular to the N—Li bond axis, but phenyl running alongside this axis. This arrangement allows these monomers to associate in "slipped" vertical pairs; each unit is displaced opposite to the other (Fig. 41b). Each Li^+ interacts with one *ortho*- and one *meta*-

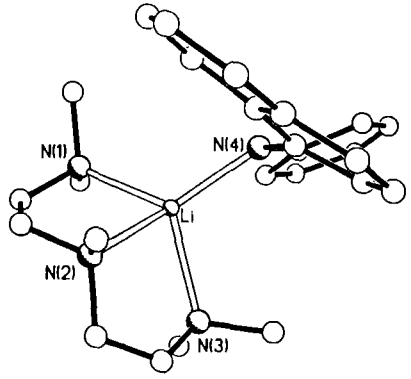

FIG. 40. Molecular structure of the monomer Ph(naphthyl)NLi·PMDETA (**70**).

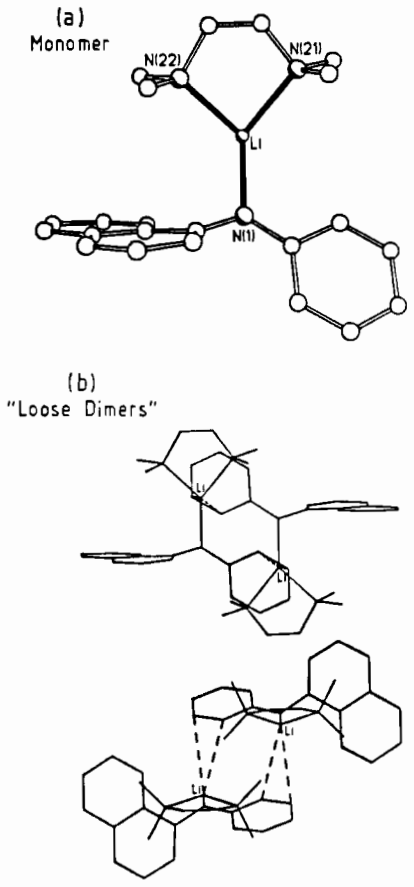

FIG. 41. Molecular structure of Ph(naphthyl)NLi·TMEDA (**69**): (a) the monomeric unit; (b) loose association of these monomers into dimers, via Li···HC interactions.

CH unit of the neighboring phenyl group (Li—C′, 3.12 and 3.15 Å, respectively) giving "loose dimers."

2. *Calculational Studies*

Section III,B,2 described how results from *ab initio* and MNDO calculations can explain many of the structural features found in the solid state for uncomplexed lithium amides $(RR'NLi)_n$. In particular, they explain (1) why rings formed experimentally, with $n = 2, 3$, and 4, have R,R′ groups perpendicular to the $(NLi)_n$ ring plane; (2) why a trimer ($n = 3$) is favored over a dimer ($n = 2$); and (3) why the only known

tetramer ($n = 4$) is a ring, rather than a tetrahedral "stack" of two dimers. Here we discuss the results of calculations on complexed lithium amides. These also rationalize the experimentally found structures (Section III,C,1) of such species.

One marked structural feature is that the six-membered rings preferred for $(RR'NLi)_n$ species [e.g. (**55**) and (**56**) in Table VI, Section III,B,1] become four-membered rings on complexation with monodentate Lewis bases (base: Li ratio, 1 : 1) [e.g. (**61**)–(**67**) in Table XII, Section III,C,1]. A qualitative explanation for this diminution in ring size suggests that the dimer offers a wider coordination arc for attachment of the base (Fig. 38, Section III,C,1). However, more quantitative reasons have emerged from an *ab initio* study (6-31G basis set) on the model systems $(H_2NLi{\cdot}H_2O)_n$, with $n = 1$, 2, and 3 (*20*). The optimized geometries for these complexes are shown in Fig. 42. Comparing the structures of $H_2NLi{\cdot}OMe_2$ and $H_2NLi{\cdot}H_2O$ confirms that H_2O is a reasonable model (electronically) for the usual O ligands. In each of the aquo species, the H_2O molecule adopts a perpendicular (staggered) orientation to the plane of the H_2N groups; in the all-planar (eclipsed) conformations, the energies of the monomer, dimer, and trimer are higher (by 1.0, 5.8, and 10.4 kcal mol^{-1}, respectively). Expectedly, the N—Li bond lengths are longer than those in the uncomplexed analogs [(*165, 167*); see Table IX, Section III,B,2]; the largest increase (~0.05 Å) is for the trimer and this can be attributed to more pronounced steric effects at Li as the $\widehat{OLiN}$ angle decreases with increased association. The Li—O bond lengths increase from monomer, through dimer, to trimer so that stabilization by solvation becomes less important. Thus, the calculated total hydration energies (−26.4, −38.0, and −40.7 kcal mol^{-1} for $n = 1$, 2, and 3, respectively), when expressed in terms of each additional H_2O attachment, become −26.4, −19.0, and −13.6 kcal mol^{-1}, respectively. The calculated association energies for $H_2NLi{\cdot}H_2O$ to $(H_2NLi{\cdot}H_2O)_n$ are −58.6 and −95.4 kcal mol^{-1} for $n = 2$ and $n = 3$, respectively. These values are much less than the association energies of the uncomplexed species (for $n = 2$, −73.7 kcal mol^{-1} and for $n = 3$, −133.9 kcal mol^{-1}; see also Table VIII, Section III,B,2).

The experimental preference for solvated dimers over solvated trimers (but the reverse for uncomplexed systems) can best be explained by considering association energies as sums of two components (Fig. 43). The first is the energy needed to reorganize the monomeric units, H_2NLi or $H_2NLi{\cdot}H_2O$, into the required geometry for the dimer or trimer, i.e., lengthening of the N—Li bond, and bending the H_2N group toward this bond. The second is the energy gained by association of these reorganized monomers to $(H_2NLi)_n$ or $(H_2NLi{\cdot}H_2O)_n$, $n = 2$ or 3. For the uncomplexed species (Fig. 43a), the reorganization energies are

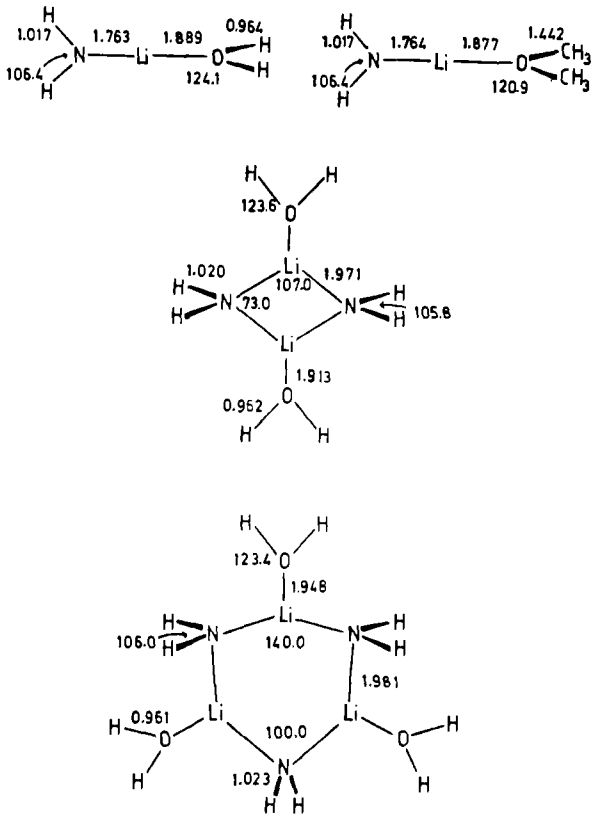

FIG. 42. Optimized structures (6-31G basis set) of $(H_2NLi{\cdot}H_2O)_n$ complexes, with $n = 1$, 2, and 3; the structure of $H_2NLi{\cdot}OMe_2$ is included for comparison with $H_2NLi{\cdot}H_2O$.

small, particularly that for the trimer. The dominant term is the association energy of the reorganized H_2NLi unit, and this is more favorable for the trimer. Thus, both components make the trimer $(H_2NLi)_3$ the preferred association product. In comparison, both reorganization energies are larger for $H_2NLi{\cdot}H_2O$ (Fig. 43b), but these energies are now considerably greater for the trimer than for the dimer. In the trimer, the H_2O ligand is moved from a linear OLiN arrangement to an angle of 110°. In the dimer, the ligand is only moved to 126.5° (Fig. 42). Though the total association energies show that $H_2NLi{\cdot}H_2O$ still prefers to form a trimer rather than a dimer (by 2.5 kcal mol^{-1} per unit), this preference is reduced (*cf.* 7.8 kcal mol^{-1} per unit for the uncomplexed H_2NLi species). With the much bulkier complexants used in practice (notably, Et_2O, THF, and HMPA), the reorganization term may become

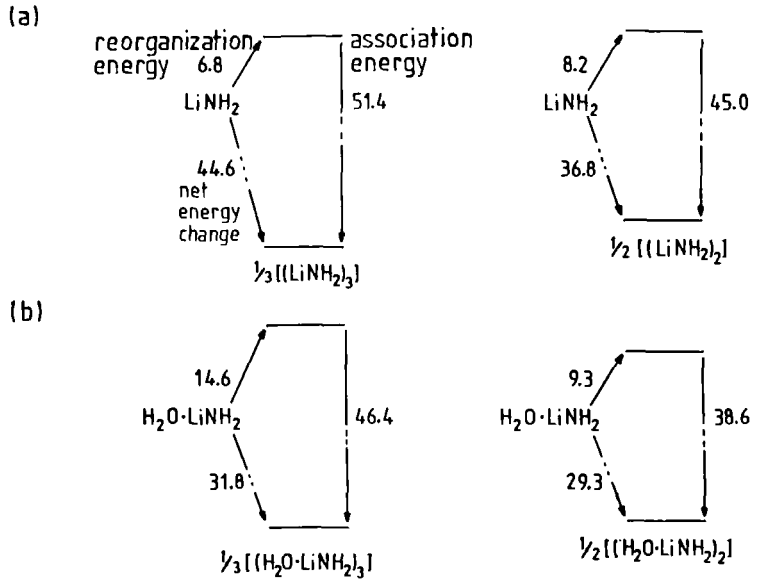

FIG. 43. Calculated energy profiles (6-31G basis set, energies in kcal mol^{-1}) for formation of (a) $(H_2NLi)_n$, $n = 2$ or 3, and (b) $(H_2NLi{\cdot}H_2O)_n$, $n = 2$ or 3.

dominant, so that association to a dimer would be expected, in line with experimental findings.

A further notable structural feature of complexed lithium amides is the isolation of ladder structures when ligands are attached to only *some* of the Li centers, i.e., when the base : Li ratio is <1 : 1 [(**59**) and (**60**) in Fig. 35, Section III,C,1]. Individual ring structures are not observed, even though experiment and calculation both show that dimeric rings are strongly favored when *each* Li is complexed. These structural preferences have been probed by *ab initio* calculations on $(H_2NLi)_4$, at the 6-31G and STO-3G (a smaller basis set) levels, and on $(H_2NLi)_4{\cdot}2H_2O$ and $(H_2NLi{\cdot}H_2O)_4$ (STO-3G level only) (*21*). The computations on $(H_2NLi)_4$ at 6-31G (see Fig. 31 and Tables X and XI, Section III,B,2) show that a ring is preferred, followed by a ladder (+7.4 kcal mol^{-1}), and then by a stack of two dimers (+11.4 kcal mol^{-1}). These preferences are reflected by the N—Li bond lengths, which are shortest in the ring and longest in the stack, whereas the N—N and Li—Li repulsive contacts are longest in the ring and shortest in the stack. In each instance, the ladder structure displays intermediate distances. To calibrate the results on the aquo complexes, $(H_2NLi)_4$ was reexamined at STO-3G (excluding the stacked structure). The ring also

was found to be preferred to the ladder, and by a larger energy difference, 10.9 kcal mol^{-1}. For both, the STO-3G bond lengths and angles agree quite well (maximum changes of 0.08 Å and 3°, respectively) with those found at the 6-31G level.

For $(H_2NLi)_4 \cdot 2H_2O$, the optimized structure with the water ligands bound only to the outer Li atoms of the ladder is more stable (by 7.2 kcal mol^{-1}) than the ring structure with H_2O coordinated to the opposite Li atoms (Fig. 44). The large H_2O complexation energies (−85.2 and −67.1 kcal mol^{-1}, respectively) of both complexes are exaggerated by STO-3G, but the difference between them (18.1 kcal mol^{-1}) reverses the ring-over-ladder preference found for uncomplexed $(H_2NLi)_4$. This energy difference is reflected in changes in geometry at the coordination sites of the $(H_2NLi)_4$ ladder and ring structures. Thus, the NLiN angles at the outer rungs of the ladder change little (112.1–108.2°) upon coordination by H_2O, whereas in the ring model the angles at Li compress much more (162.4–138.4°) to accommodate these additional ligands. Significantly, attempts to optimize a ladder structure with H_2O attached to the inner Li atoms failed: the inner N—Li bonds of the ladder are cleaved on optimization and the ring geometry results.

Three possible structures of $(H_2NLi \cdot H_2O)_4$ were optimized (Fig. 45): a ring and a ladder, both with each Li complexed by H_2O, and a ladder with only the end-Li centers complexed. The last is the most stable structure, 17.1 kcal mol^{-1} lower in energy than the ring. Compared to

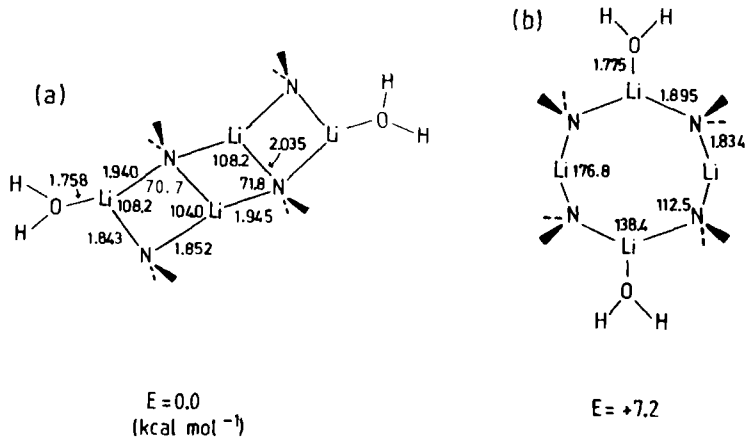

FIG. 44. Optimized geometries and relative energies (STO-3G basis set, energies in kcal mol^{-1}) of $(H_2NLi)_4 \cdot 2H_2O$ complexes: (a) a ladder, with H_2O on the outer Li atoms only; (b) a ring, with H_2O ligands on diagonally opposite Li atoms.

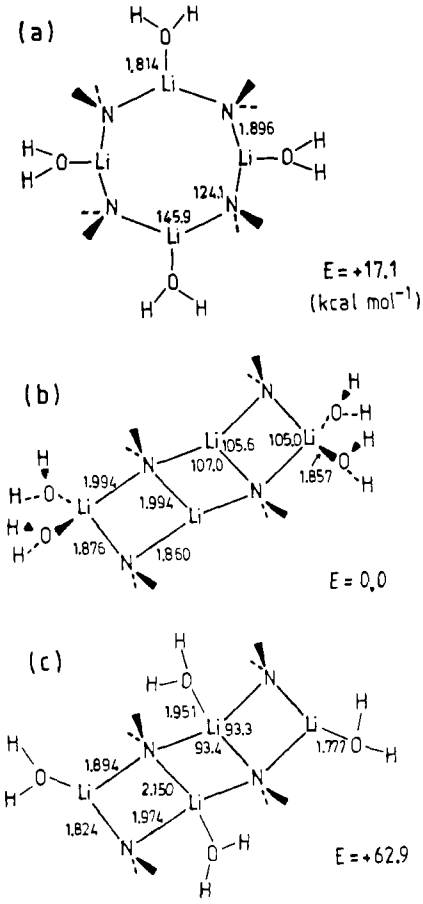

FIG. 45. Optimized geometries and relative energies (STO-3G, kcal mol^{-1}) of $(H_2NLi \cdot H_2O)_4$ complexes: (a) a ring, with each Li complexed by H_2O; (b) a ladder, with H_2O on the outer Li atoms only; (c) a ladder, with H_2O on each Li atom.

the $(H_2NLi)_4 \cdot 2H_2O$ species, further complexation increases the preference for a ladder over a ring. This arises because addition of four H_2O molecules to the ends of a ladder results in a gain in stability of 142.9 kcal mol^{-1} (*cf.* 114.9 kcal mol^{-1} for their addition to a ring). This reflects the extent of reorganization in each case: the outer $N\hat{L}iN$ angles of the ladder are reduced only by 7.1° on bis(solvation) (112.1–105.0°) whereas the $N\hat{L}iN$ angles in the ring change much more (by 16.5 to 145.9°). The third structure, a ladder with H_2O on each Li, is 62.9 kcal mol^{-1} less stable than the solely end-solvated ladder. This reflects the

crowded nature of the geometry about the inner Li atoms if H_2O molecules are attached here. Such steric hindrance leads to long (inner) Li—O bonds, 1.951 Å [*cf.* (outer) Li—O bond lengths of 1.777 Å, and Li—O bond lengths in the end-complexed ladder and in the ring, 1.857 and 1.814 Å, respectively].

These calculational results concur extremely well with the experimental findings. Lithium amide complexes are dimeric rings (or monomers) if the complexant : Li ratio is 1 : 1 or greater, and if every Li bears (at least) one complexant. However, there is a switch of structural preference from ring to ladder if a base is not coordinated to each Li. In such cases, only the end-Li centers of the ladder are complexed, even though a 1 : 1 complexant : Li ratio may be present under the experimental conditions.

3. *Structures in Solution*

The structures of lithium amide complexes $(RR'NLi{\cdot}xL)_n$ in solution have been probed by colligative measurements (notably, cryoscopy and vapor-pressure barometry) and by combinations of ^6Li, ^7Li, ^{13}C, and ^{15}N NMR spectroscopy. In several cases, attempts have been made to correlate the results from the two kinds of experiments. When hydrocarbon solvents (notably, benzene, toluene, and their deuterated versions) are used, the preisolated complex is dissolved. With coordinating solvents (notably, Et_2O and THF), the "parent" amide $(RR'NLi)_n$ is dissolved and the complexes are formed in solution. These studies give information on the nature of the lithium amide reagents under the conditions in which they are employed. Solid-state structures are a guide. As shown in Section III,C,1, lithium amide complexes can be limited ladders (only two examples known), or, more commonly, dimers or monomers in the crystal. Similarly, dimers ($n = 2$) and monomers ($n = 1$) for $(RR'NLi{\cdot}xL)_n$ complexes dominate in solution. There are, however, three important caveats: (1) the degree of solvation or complexation (x) of these species can vary, *e.g.*, dimers can have a total of two, three, or four complexants ($x = 1$, 1.5, or 2) and monomers can have two, three, or four complexants; (2) there are frequently equilibria between dimeric solvates, between monomeric solvates, and between dimers and monomers (of various kinds); (3) all the variations described in (1) and (2) are solvent dependent, and for a particular solvent usually are temperature and concentration dependent.

These are the essential features. Hence, this section is not intended to be comprehensive but rather provides key references and gives illustrative examples. The section is organized in the same order as in Section

III,C,1, which discussed solid-state structures of lithium amide complexes.

The two limited-ladder structures known in the solid state, $\{[H_2\overline{C(CH_2)_3NLi}]_3 \cdot PMDETA\}_2$ (**59**) and $\{[H_2\overline{C(CH_2)_3NLi}]_2 \cdot TMEDA\}_2$ (**60**), behave very differently in solution (*21*). Complex (**60**) appears to retain its integrity ($n = 2$) on dissolution in hydrocarbon solvents. Cryoscopic relative molecular mass (crmm) measurements in benzene give fairly constant association state values (n) of 2.02 ± 0.06 and 2.10 ± 0.06 for solutions of 3.4×10^{-2} and 9.0×10^{-2} mol dm^{-3} concentrations, respectively. In addition, the ^{7}Li NMR spectra of d_8-toluene solutions of (**60**) at −95°C all reveal essentially just two signals of equal integral (*e.g.*, Fig. 46a and inset) corresponding to the two kinds of Li environment (ladder-end and inner) expected for intact dimeric (**60**) (see Fig. 35b). The natural-abundance ^{6}Li NMR spectra show these two 1 : 1 signals more clearly (e.g., Fig. 46b), because the low-quadrupole moment of ^{6}Li(*cf.* ^{7}Li) affords much sharper resonances. In contrast, complex (**59**) exhibits very complicated solution behavior. Cryoscopic rmm measurements on benzene solutions give n values of 1.77 ± 0.12 to 6.51 ± 0.31 (*cf.* $n = 2$ in the solid state) for concentrations 2.0×10^{-2} to 6.5×10^{-2} mol dm^{-3}, respectively. However, at yet higher concentrations, crmm, and hence n, values fall, e.g., $n = 5.26 \pm 0.32$ at 8.0×10^{-2} mol dm^{-3}. Such results have been interpreted (*21*) in terms of PMDETA ligands amending their role from tridentate within each ladder to bidentate or even monodentate. Resultingly "free" Me_2N and/or MeN groups might then complex to Li centers in other ladders, so joining ladders together and giving n values of 4, 6, . . . etc. These two processes should show different concentration dependence (ligand amendment being encouraged at low concentrations but association of resulting coordinatively unsaturated ladders being favored at high concentrations), and support for this interpretation has come from variable-concentration ^{7}Li NMR spectra of d_8-toluene solutions of (**59**) at −95°C. At very high concentrations (double that of solutions examined by cryoscopy), essentially three signals of equal integral are observed (Fig. 46c and inset). These correspond to the three Li environments of the intact dimeric ladder (see Fig. 35a); at this high concentration, ligand amendment is suppressed. Twofold dilution results in a more complicated ^{7}Li NMR spectrum (Fig. 46d); the three signals (asterisks) attributed to dimeric (**59**) are still apparent, but there are several other distinct resonances and probably many more beneath these broad peaks. Further dilution (to 6.0×10^{-2} mol dm^{-3}) gives one broad, ill-defined resonance. Crucially, though, for even more dilute solutions, the spectra begin to simplify again and the distinct

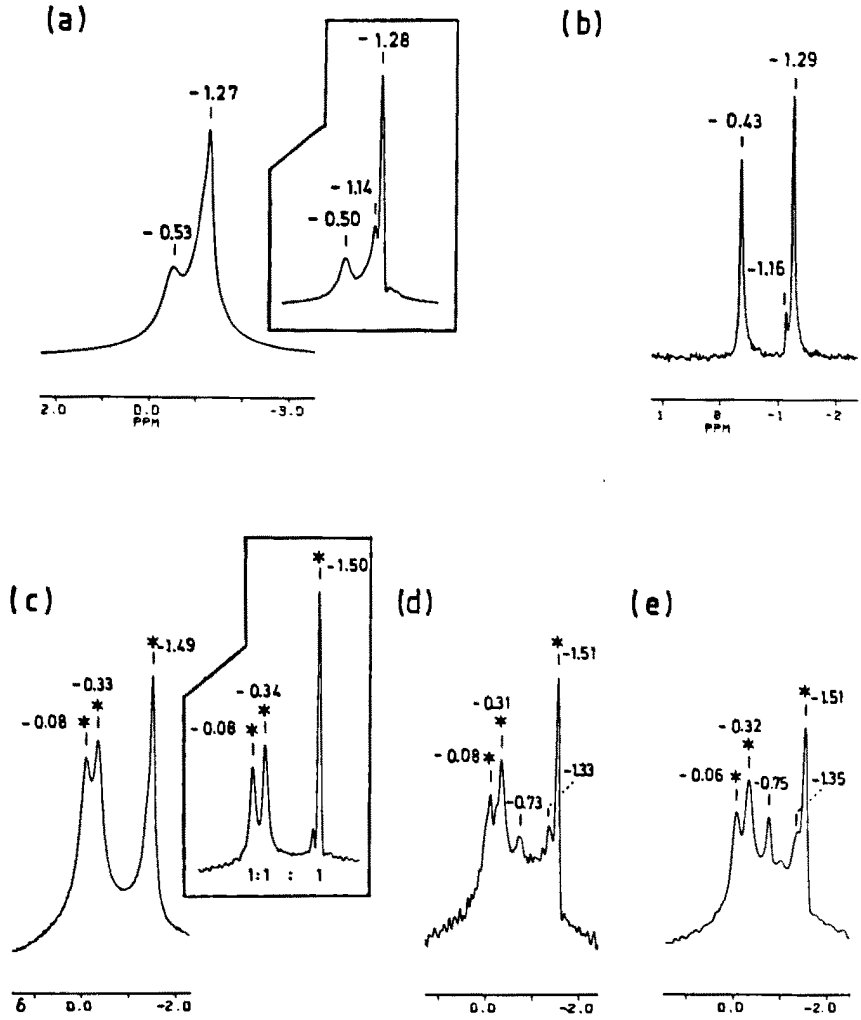

FIG. 46. (a) ^{7}Li NMR spectrum (139.96 MHz) of (**60**), 2.5×10^{-1} mol dm^{-3} in d_8-toluene at −95°C; inset, resolution-enhanced spectrum; (b) ^{6}Li NMR spectrum (52.99 MHz) of (**60**), 6.7×10^{-1} mol dm^{-3} in d_8-toluene at −95°C; (c, d, and e) ^{7}Li NMR spectra (139.96 MHz) of (**59**) in d_8-toluene at −95°C: (c) 1.8×10^{-1} mol dm^{-3}; inset, resolution-enhanced spectrum; (d) 9.0×10^{-2} mol dm^{-3}, resolution-enhanced spectrum; (e) 4.0×10^{-2} mol dm^{-3}, resolution-enhanced spectrum.

signals due to dimeric (**59**) reemerge (e.g., Fig. 46e); at these low concentrations, partial PMDETA amendment can occur, but only limited association of the resulting ladders is possible.

A similar strategy of linking variable-concentration rmm results to variable-concentration ^{7}Li NMR spectroscopic results has been used to ascertain the solution equilibria of amidolithium complexes having at least one complexant per Li (*cf.* the aforementioned ladder species, having a deficiency of complexant). For example, $[(PhCH_2)_2NLi{\cdot}OEt_2]_2$ (**61**), a dimer in the solid state (see Section III,C,1) affords cryoscopic n values of 1.20–1.07 (3.1×10^{-2} to 1.8×10^{-2} mol dm^{-3} concentrations in benzene, respectively) (*20, 94*). The ^{7}Li NMR spectra of benzene solutions of (**61**) exhibit only two resonances, at the same positions as those found in the spectra of the uncomplexed amide $[(PhCH_2)_2NLi]_3$ (**55**). Amide (**55**) was shown earlier (Section III,B,3) to engage in a trimer $\rightleftharpoons$ monomer equilibrium. Hence, these results prove that on dissolution (**61**) totally loses Et_2O (hence n values <2), the uncomplexed dimers so produced then rearranging to trimers and monomers. In a similar study, linking variable-concentration and -temperature ^{1}H and ^{7}Li NMR spectroscopic results to those from isopiestic and cryoscopic rmm values, $[(Me_3Si)_2NLi]_n$ (**56**), like (**55**), a trimer in the solid state, was proposed to exist as a dimer $\rightleftharpoons$ tetramer equilibrium in hydrocarbons. In THF, however, an equilibrium between a complexed dimer and a complexed monomer, both of uncertain degrees of solvation, was indicated (*200*). The experimental solution data for a complex of lithium dicyclohexylamide is even more illustrative. The parent species $(c\text{-hexyl}_2NLi)_n$ is known, but crystal twinning has so far prevented a solid-state structure determination (n probably equals 3 or 4; see Section III,B,1). This lithium amide is used widely in organic syntheses as a bulky reagent of somewhat greater basicity than the more familiar LDA, $(Pr^i{}_2NLi)_n$ (e.g., *6–8*). However, reported reactions of this reagent are carried out in complexing solvents, e.g., Et_2O and THF; in fact, this species is rather insoluble in hydrocarbons (*94, 157*). Thus the reagent is *not* $(c\text{-hexyl}_2NLi)_n$, but a complex of it. One such complex, $(c\text{-hexyl}_2NLi{\cdot}HMPA)_n$, has been isolated from lithiation of $c\text{-hexyl}_2NH$ in hexane containing HMPA (*94*). Although its solid-state structure is as yet unknown (but probably $n = 2$), crmm measurements on benzene solutions give n values of 1.60–1.15 for 4.0×10^{-2} to 2.0×10^{-2} mol dm^{-3} concentrations, respectively. The 25°C ^{7}Li NMR spectra of benzene solutions of various concentrations (Fig. 47) each consist of two signals, neither of which can be due to $(c\text{-hexyl}_2NLi)_n$ species (not ruled out by crmm results) because this uncomplexed lithium amide affords one broad ^{7}Li signal at δ +0.75 ppm. Hence these results point to

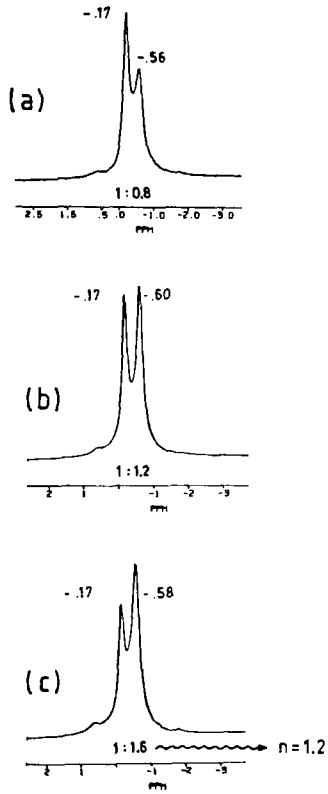

FIG. 47. ^{7}Li NMR spectrum (139.96 MHz) of (*c*-hexyl$_2$NLi·HMPA)$_n$ in d_6-benzene at 25°C: (a) 2.0×10^{-1} mol dm^{-3}; (b) 1.0×10^{-1} mol dm^{-3}; (c) 2.0×10^{-2} mol dm^{-3}.

a (remarkably slow) monomer $\rightleftharpoons$ dimer solution equilibrium. The low-frequency resonance ($\sim\delta$ −0.6) becomes more pronounced on dilution, and so can be assigned to the monomeric complex, *c*-hexyl$_2$NLi·HMPA; the higher frequency signal must be due to an aggregate, almost certainly a dimer, (*c*-hexyl$_2$NLi·HMPA)$_2$. Assuming a dimer (as pointed out earlier, there are no known solid-state complexed trimers), there is fair agreement between n values measured by cryoscopy and n values implied by consideration of ^{7}Li signal integration ratios; for example, for the most dilute solution looked at both by spectroscopy (Fig. 47c) and by cryoscopy, n is calculated at 1.20 and 1.15, respectively. Clearly, studies such as these can pinpoint the actual species present, at various concentrations and temperatures, in solutions of lithium amide reagents; such information is crucial to the proper understanding of how

these reagents operate in their regio- and stereospecific reactions with organics.

Several important studies have employed the somewhat different strategy of preparing a lithium amide complex $(RR'NLi \cdot xL)_n$ *in situ* in a complexing solvent (e.g., Et_2O and THF), and then identifying solution species present by $^{6,7}Li$, ^{13}C, and ^{15}N NMR spectroscopies (singly or in conjunction) with or without rmm measurements. With very few exceptions, species found are dimers or monomers (or both), although the degree of solvation (x) can vary considerably. These typical structures are illustrated in Fig. 48, structures (**I**)–(**VI**). A series of Li salts of aromatic secondary amines, including those with R = Ph, R = Me, Pr^i, Bu^n, Bu^t, and RR'N = indolide, $\overbrace{C_6H_4 \cdot (CH_2)_2}\overbrace{N}$, were studied in Et_2O and THF solutions, chiefly by ^{13}C NMR spectroscopy (*201*). In THF at 17°C, lithium indolide appears to be mainly dimeric; vapor pressure barometric measurements give n values of 1.8–1.9 for 0.09–0.49 mol dm^{-3} concentrations. In the ^{13}C NMR spectra, chemical shifts are con-

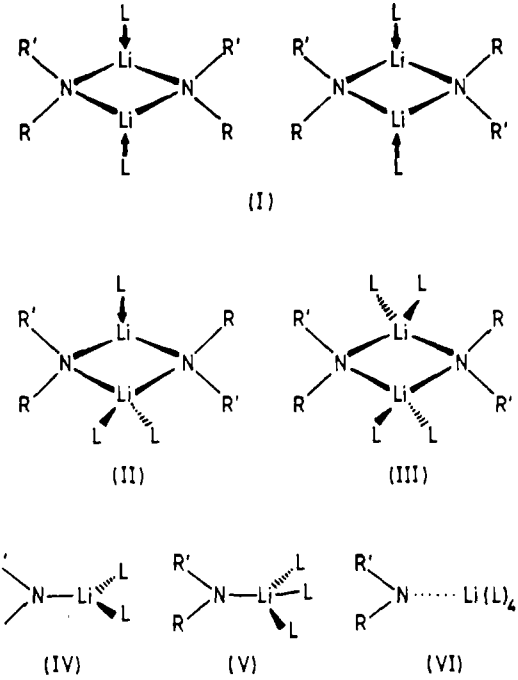

FIG. 48. Principal structures identified for lithium amides $(RR'NLi)_n$, in coordinating solvents L: (I) dimers with one molecule of L per Li (*cis/trans* or *E/Z* isomers); (II) a trisolvated dimer; (III) a tetrasolvated dimer; (IV)–(VI) monomers with two or three (contact-ion pairs) or four (solvent-separated ion pairs) L molecules per Li.

stant from −100 to 40°C, but then become temperature (but not concentration) dependent. The shift of C(4) ("para" to N) in particular decreases, implying decreased charge density at C(4) and increased localization of negative charge on N. Such results were interpreted in terms of a tetrasolvated dimer [Fig. 48, structure (**III**)] prevailing at very low temperatures, but a bisolvated dimer [(**I**)] being present at higher temperatures. In Et_2O solutions, only dimer (**I**) could be observed, although at −120°C it was possible to detect its *E* and *Z* isomers. Similar analysis of ^{13}C chemical shifts showed that $(PhMeNLi)_n$, $(PhPr^iNLi)_n$, and $(PhBu^nNLi)_n$ also exist in THF as dimers of types (**I**) and (**III**) together with a trisolvated monomer [Fig. 48, structure (**V**)]. In contrast, $(PhBu^tNLi)_n$ in THF is a monomer alone, (**V**) or the bisolvated species (**IV**), depending on temperature. All four lithium N-substituted anilides exist in Et_2O solutions only as the bisolvated dimer, (**I**). In the case of $(PhMeNLi{\cdot}Et_2O)_2$, the presence of a dimer was confirmed by observation of a ^{15}N pentuplet resonance at −100°C for a solution of the $^6Li,^{15}N$ isotopomer (J = 3.8 Hz), i.e., each N atom is attached to two Li atoms. Similarly, a ^{15}N triplet resonance (J = 7.5 Hz) was found at −80°C in the spectrum of $^6Li,^{15}N$-enriched $(PhPr^iNLi)_n$ in THF, in agreement with the presence of a monomer [probably (**V**)]. In a related study (*90*), $^{6,7}Li$, ^{13}C, and ^{15}N NMR spectroscopies were all employed to show that addition of HMPA (two to four equivalents) to an ether solution of $(PhPr^iNLi)_n$ converts the dimer [of type (**I**)] into a mixture of monomer $PhPr^iNLi{\cdot}(THF)_{3-n}(HMPA)_n$ and the triple-ion salt, $[(PhPr^iN)_2Li{\cdot}(HMPA)_n]^-{\cdot}Li(HMPA)_4^+$ [*cf.* the 'ate complex (**8**); see Section II,B].

Many of the above results on lithium arylamides have been backed up by determinations of ^7Li quadrupole splitting constants (QSCs) from ^7Li and ^{13}C spin-lattice relaxation data (*202*). The QSCs (in kHz) are remarkably sensitive to the degree of aggregation (n) and, especially, to the degree of solvation (x). For example, lithium indolide in Et_2O is believed to exist as a bisolvated dimer [Fig. 48, structure (**I**)] and the ^7Li QSC at 30°C is 317 ± 6 kHz, whereas in THF the tetrasolvated dimer (**III**) dominates (QSC at −80°C, 151 ± 5 kHz). Similarly, $(PhPr^iNLi)_n$ has been shown to exist as the trisolvated monomer (**V**) in THF at −80°C (QSC, 211 kHz) though it converts to the tetrasolvated dimer (**III**) (typical QSC ~ 155) and then to the bisolvated dimer (**I**) (typical QSC ~ 315 kHz) as the temperature increases. These empirical correlations between QSC values and solution structures have also been applied to lithium phenolates in solvents such in Et_2O, THF, pyridine, Me_3N, and dioxolane; as discussed in Section II,E, unlike lithium amides, rings of type $(ROLi{\cdot}xL)_n$ (n = 2 or 3) have the potential to stack once, so that tetramers and hexamers are also observed (*202–204*).

A final approach to unraveling lithium amide solution structures has been to employ ^{6}Li–^{15}N double labeling; ^{6}Li ($I = 1$) and ^{15}N ($I = \frac{1}{2}$) NMR resonance patterns reveal the number of N—Li connectivities, and this, particularly in conjunction with rmm measurements, often allows complete structural assignment. For example, in a study of lithiated cyclohexanone phenylimine $[(Ph(1\text{-}c\text{-}hexenyl)NLi)]_n$ in hydrocarbon (benzene or toluene)/THF solutions (*205*), cryoscopic measurements at 0°C implied the presence of a bisolvated dimer [Fig. 48, structure (**I**)] at low THF concentrations. The ^{6}Li NMR spectrum at −94°C of the doubly labeled amide in d_8-toluene containing THF (two equivalents per Li) showed two triplets (J = 3.3 Hz), and the ^{15}N NMR spectrum of the same solution consisted of two pentuplets (average J = 3.5 Hz). Thus, a cyclic structure is confirmed, with N—Li—N and Li—N—Li units; almost certainly the structure is the bisolvated dimer (**I**), existing in solution as the two (*cis* and *trans*) stereoisomers. At higher THF concentrations, the ^{6}Li NMR spectrum contains a doublet (J = 6.3 Hz) and the ^{15}N spectrum contains a triplet (J = 6.1 Hz), consistent with the presence of a monomeric, contact-ion pair species, probably trisolvated [Fig. 48, structure (**V**)]. Similar experiments have indicated that $[Pr^{i}(c\text{-}hexyl)NLi]_n$ in d_8-toluene/THF solutions exists as a mix of *cis* and *trans* stereoisomeric dimers, probably having one THF per Li [Fig. 48, structure (**I**)] (*206*). The N—Li—N and Li—N—Li connectivities proved by ^{6}Li and ^{15}N coupling patterns do not, of course, rule out higher oligomers; however, lower symmetry trimers and tetramers should exhibit increased spectral complexity (not observed), plus there are no known examples of solid-state complexed lithium amide oligomers higher than dimers (see Section III,C,1). The assignment of bisolvation is less clear-cut; the vast majority of complexed lithium amide dimers have one O complexant per Li (Table XII), although there is one example of a related trisolvated lithium dienamide dimer [Fig. 48, structure (**II**)] (*207*).

Recent studies have begun to explore the consequences of complexed lithium amide solution structures for reaction mechanisms and rates. Double-labeling (^{6}Li and ^{15}N) NMR experiments, allied to colligative measurements, show that lithium diphenylamide in THF/hydrocarbon solutions exists as a cyclic oligomer at low THF concentrations, probably a bi- or trisolvated dimer [Fig. 48, structure (**I**) or (**II**), respectively] (*208*). At intermediate THF concentration, ^{13}C NMR spectroscopy detects a second species, a monomer of uncertain solvation [(**IV**), (**V**), or (**VI**)]. In the presence of LiBr, a 1:1 adduct is formed at low THF concentrations, and NMR and cryoscopic measurements show this to be a trisolvated mixed dimer, $Ph_2NLi{\cdot}LiBr{\cdot}3THF$ [*cf.* (**52**) and (**53**) in Table V, Section II,E]; at higher THF concentrations this mixed dimer

dissociates to the monomeric lithium amide and free LiBr. Rate studies of the N-alkylation of Ph_2NLi with Bu^nBr in THF/hydrocarbon solutions imply that all the above three species are involved in the reaction mechanism, i.e., the dimer, the mixed dimer (formed after a considerable induction period), and, at intermediate THF concentrations, the monomer (*209*). The significance of which species are present in THF/hydrocarbon solutions of LDA, $(Pr^i_2NLi)_n$, regarding this reagent's reaction with an *N,N*-dimethylhydrazone, have also been examined (*210*). Earlier colligative measurements (*211*) had indicated that LDA in THF exists in a solvated dimer $\rightleftharpoons$ monomer equilibrium. However, ^6Li and ^7Li NMR experiments in this most recent study could detect only an oligomer, probably a bisolvated dimer [Fig. 48, structure (**I**)], over a wide range of concentrations. Rate measurements on the lithiation of 2-methylcyclohexanone *N,N*-dimethylhydrazone, $MeCH(CH_2)_4C{=}N{\cdot}NMe_2$, using this LDA reagent suggest that the hydrazone itself acts as a further complexant toward this dimer, producing the monomer $Pr^i_2NLi{\cdot}THF{\cdot}$hydrazone. This kinetically active monomer than undergoes rate-determining proton transfer. These results spotlight a very important point. Reactions between organolithium reagents and organic substrates in general are represented conventionally in terms of nucleophilic attack by the organolithium residue (R^-, R_2N^-, etc.; the "carbanion") on the organic. It may well be that the opposite is true: that many organics act first as Lewis bases/nucleophiles toward the organolithium reagent, i.e., Li^+, not C^- or N^-, is the effective reactive and controlling center in these reagents.

IV. Conclusions

As is implied by the title of this review, the goal has been not only to describe and explain the known structures of organonitrogen–lithium compounds, but also to emphasize some key points about organolithium chemistry in general. The factual evidence and the arguments have been presented in the text, and we do not repeat these here. Rather, we give a checklist of the major conclusions we have reached. These conclusions (or, arguably, generalities) are presented in the following discussion.

A. Definitions and Nomenclature

We believe that the term "organolithium" can now in effect be taken to mean a lithiated derivative of *any* organic molecule. The stricture that a C—Li bond must be present is inappropriate and unwieldy. It

seems best to link the term to the type of compound that has been lithiated: thus, suitable species with O—Li bonds (derived from alcohols, methyl ketones, esters, sulfones, etc.) and ones with N—Li bonds (derived from imines, amines, etc.) qualify. Claiming such species under the umbrella of "coordination chemistry," just because they contain no C—Li bonds, is somewhat grandiose: there *are* no "noncoordination" compounds. For the purist who insists on the presence of a C—Li bond to justify the epithet "organolithium," then "lithiated organic" seems a suitable compromise description.

B. Bonding

Organolithium compounds do not have any appreciable, or even significant, covalent character as regards the bonds to lithium. The central E—Li bonds (E = C, or N, or O, etc.) are essentially *ionic* ones. Many of the properties of these compounds might well be reminiscent of those of covalently bound discrete molecules, e.g., they are frequently crystalline materials, with low melting points and with good solubilities in weakly polar organic solvents. However, such properties are attributable to the *structures* of these compounds, which are often ones of limited association and dimensionality. It is these restricted aggregations, and the fact that the peripheries of the aggregates consist of organic groups, that lead to these properties. Accordingly, organolithiums are best termed "supramolecules" or "ionic molecules."

The short Li—Li distances (often much shorter than those in the metal and in the Li_2 molecule) found in the structures of many organolithium compounds do not imply that *lithium–lithium bonding* is of thermodynamic importance in these species. Close approach of Li centers is usually dictated by the need for acute angles at bridging atoms (E), e.g., of $(ELi)_n$ rings (n = 2 and 3 especially). Thus, the distances represent the optimization of maximized E—Li bridge bonding and minimized $Li^{\delta+}$—$Li^{\delta+}$ repulsions.

There is much evidence that low-coordinate lithium centers found within certain organolithiums $(RLi)_n$ (e.g., two-coordinate centers in rings with n = 2 or 3) will interact with C—H bonds within the R groups. Such "*agostic*" interactions can be intra- or intermolecular.

C. Implications for Organic Reaction Mechanisms

It is a gross and unjustified simplification to consider an organolithium as a monomer "RLi" or as a "*carbanion*" R^-. Most organolithiums are associated, $(RLi)_n$ (commonly, n = 2, 3, 4, 6, or ∞). Fre-

quently, because many lithiations are carried out in polar solvents, they are complexed $(RLi \cdot xL)_n$, with L being a polar neutral ligand (Lewis base). For many such complexes, association persists (often n = 2 or 4). Monomers *are* known, but they are usually contact-ion pairs. Free carbanions are nebulous: even for supposedly solvent-separated ion pairs, $R^- \cdots Li^+(L)_x$, there is often a retained interaction between the ions. These points have implications for the mechanisms of the reactions of these organolithium reagents. It is not logical to ignore the lithium and to represent such reactions as proceeding *via* nucleophilic R^- attack on an electrophilic center of an added substrate. Indeed, all calculational investigations to date imply that it is the "nucleophilic" (coordinating) center of the substrate that first interacts with the Li^+ center of the intact organolithium $(RLi)_n$.

Experimental mechanistic studies of such reactions are in their early days. However, it is clear that proper understanding will rely on the prior isolation of the organolithium reagent, rather than on its production, then use, *in situ*. Thereafter, the reagent needs to be identified (e.g., RLi or $RLi \cdot xL$?) and characterized structurally, in the solid by X-ray diffraction and, perhaps more importantly, in solutions (by colligative molecular mass measurements and multinuclear NMR spectroscopic studies) in which it will be used.

D. Structures of Uncomplexed Organolithiums

The basic structural building block of any organolithium is an ion pair, R^-L^+. In the absence of a complexing agent, these will associate, first to give *rings*, $(RLi)_n$, with n = 2 or 3, or, less commonly, 4. The coordination numbers of the cations are raised thereby to two. Further association of these rings might (and usually does) occur. Whether this happens, and to what extent, depends only on the *steric* constraints imposed by the groups R. These associations, to rings and then possibly beyond rings, are a consequence of the *electrostatic nature* of the bonding. They are nothing to do with the supposed preference of lithium to reach four coordination, thereby (supposedly) using to the full its four valence orbitals: many (indeed, probably most) uncomplexed organolithiums have Li^+ centers in two or (particularly) three coordination. The R^- anions are *groups* (*cf.* point-charge anions such as Cl^-, which allow mutual six coordination of cations and anions). Such groups fall into two categories.

1. *For the majority of organolithiums,* RLi {e.g., R = aryl, R = alkoxy and aryloxy (R'O—), R = enolato [R'(=CH_2)CO—], R = im-

ino($R_2'C{=}N{-}$)}, the initially formed $(RLi)_n$ ring systems are quite flat. The central $(ELi)_n$ ring (E = C or O or N) is itself planar, and the substituents on E, up to and including the α atom of R', lie in this same plane. Hence such rings can and do associate vertically, a process termed *stacking*. If the R' groups are themselves small and/or especially flat (e.g., Me and/or Ph) this stacking can be extensive; amorphous materials result. If the R' groups are bulkier, double stacking of $(RLi)_n$ rings (n = 2 or 3) is the norm: hence, most crystalline (by inference, oligomeric) uncomplexed organolithiums are tetrahedral tetramers or pseudooctahedral hexamers.

2. *Lithium amides* [R = amido ($R_2'N{-}$)] are the exception. The $(R_2'NLi)_n$ rings (n = 2, 3, or 4) cannot stack because the R' groups project above and below the $(NLi)_n$ ring plane: the N^- center has a tetrahedral disposition of two R' groups and two lone pairs. Further association of such rings must be lateral, joining N—Li ring edges in a process termed *laddering*. If R' groups are small and/or tied together, such laddering is usually extensive, giving amorphous materials. The only generally found alternative is that, with large or floppy R' groups, the rings themselves (n = 2, 3, or 4) are isolated.

E. Structures of Complexed Organolithiums

Complexation of $(RLi)_n$ rings (n = 2, 3, or 4) by added Lewis base molecules (L) or by base functions within R (e.g., NMe_2 or OMe groups) introduces a further steric constraint on their association. In addition, any ring forthcoming after complexation will be a dimeric one, i.e., $(RLi{\cdot}xL)_2$ complexes are produced, even if n = 3 or 4 for the parent $(RLi)_n$. Such dimers might stack (except when R = $R_2'N{-}$), but now they can do so only once. Hence, many complexed tetrahedral tetramers are known. If even such limited (twofold) stacking is precluded sterically, the dimers themselves are found. Dimers are also common for complexed lithium amides: stacking is excluded anyway (see Section IV,D,2) but now so too is laddering, because the base molecules occupy the lateral space around the ring. In the limit, of course, complexation can prevent R^-Li^+ ion pairs from associating even only as far as a single ring. Monomers result, $R^-Li^+{\cdot}xL$. If the R^- group is large, x can equal two (two monodentate ligands or a single bidentate one). More usually, x equals three or more (e.g., tridentate bases or crowns).

The above comments pertain to complexes in which each lithium center is ligated by at least one base function. Where there is a deficiency of the ligand L (less than one per Li), then these ligands are found only on the end-Li centers of aggregates. Such aggregates can be viewed as "intercepted" stacks or ladders.

The identities and structures of complexed organolithiums are of particular importance. These are the species that will be present in solutions of $(RLi)_n$ in polar solvents and most reactions of organolithiums are carried out using such solutions.

ACKNOWLEDGMENTS

Many colleagues have provided us with reprints of their published work and/or with information prior to publication; we thank in particular Professors Gernot Boche (Marburg), David B. Collum (Cornell), Michael F. Lappert (Sussex), Philip P. Power (Davis, California), Dieter Seebach (ETH, Zurich), Erwin Weiss (Hamburg), and Paul G. Williard (Brown University). Thanks are due also to the many of our co-workers and collaborators who, through their efforts and ideas, have contributed greatly to the understanding of the structures of organonitrogen–lithium species. Regarding the United Kingdom, we mention particularly Drs. David R. Armstrong (Strathclyde), Donald Barr (Cambridge), William Clegg (Newcastle), Robert E. Mulvey (Strathclyde), and David Reed (Edinburgh), Professor Kenneth Wade (Durham), and Dr. Dominic S. Wright (Cambridge); in Erlangen, we mention especially Drs. Walter Bauer, Matthias Bremer, and Timothy Clark.

The research in this area in Cambridge (and earlier in Strathclyde) has been supported by the U.K. Science and Engineering Research Council and by the Associated Octel Company Ltd. Organo-alkali metal research in Erlangen is supported by the Deutscheforschungsgemeinschaft, the Fonds der Chemischen Industrie, Stiftung Volkswagenwerk, and the Convex Computer Corporation. Such financial input is essential, and it is appreciated.

Finally, we acknowledge with gratitude the provision of a Ciba–Geigy "Award for Collaboration in Europe." These funds allowed two-way visits to be made, during which this review was planned and partially written.

REFERENCES

1. Dietrich, H., *Acta Crystallogr.* **16,** 681 (1963). The structure of $(EtLi)_4$ was later refined at low temperature: *J. Organomet. Chem.* **205,** 291 (1981).
2. Setzer, W., and Schleyer, P.v.R., *Adv. Organomet. Chem.* **24,** 353 (1985).
3. Schade, C., and Schleyer, P.v.R *Adv. Organomet. Chem.* **27,** 169 (1987). This review gives an extensive bibliography.
4. Seebach, D., *Angew. Chem.* **100,** 1685 (1988). *Angew, Chem., Int. Ed. Engl.* **27,** 1624 (1988).
4a. Boche, G., *Angew. Chem.* **101,** 286 (1989); *Angew. Chem., Int. Ed. Engl.* **28,** 277 (1989).
5. Williard, P. G., *In* "Comprehensive Organic Synthesis," Pergamon, Oxford (in press).
6. Fieser, M., "Reagents for Organic Synthesis," Vol. 15. Wiley (Interscience), New York, 1990. Vol. 15 and earlier volumes give specific uses of lithium amides arranged according to individual N—Li compounds.
7. Stowell, J. C., "Carbanions in Organic Synthesis." Wiley (Interscience), New York, 1979.

8. Wakefield, B. J., "The Chemistry of Organolithium Compounds." Pergamon, Oxford, 1974.
9. Barr, D., Berrisford, D. J., Jones, R. V. H., Slawin, A. M. Z., Snaith, R., Stoddart, J. F., and Williams, D. J., *Angew. Chem.* **101,** 1048 (1989); *Angew Chem., Int. Ed. Engl.* **28,** 1044 (1989).
10. Heathcock, C. H., *in* "Asymmetric Synthesis" (J. D. Morrison, ed.), Vol. 3B. Academic Press, New York, 1984.
11. Gill, G. B., and Whiting, D. A., *Aldrichim. Acta* **19,** 31 (1986).
12. Wardell, J. L., *in* "The Chemistry of the Metal-Carbon Bond" (F. R. Hartley, ed.), Vol. 4. Wiley, Chichester, 1987.
13. Brandsma, L., and Verkruijsse, H. D., "Preparative Polar Organometallic Chemistry," Vol. 1. Springer, Berlin, 1987.
14. King, R. B., and Eisch, J. J., eds., "Organometallic Syntheses," Vol. 3, pp. 352–406. Elsevier, Amsterdam, 1986.
15. Shriver, D. F., and Drezdzon, M. A., "The Manipulation of Air-Sensitive Compounds," 2nd ed. Wiley, New York, 1986.
16. Lappert, M. F., Power, P. P., Sanger, A. R., and Srivastava, R. C., "Metal and Metalloid Amides." Wiley, New York, 1980.
17. Rogers, R. D., Atwood, J. L., and Grüning, R., *J. Organomet. Chem.* **157,** 229 (1978).
18. Mootz, D., Zinnius, A., and Böttcher, B., *Angew. Chem.* **81,** 398 (1969); *Angew Chem., Int. Ed. Engl.* **8,** 378 (1969).
19. Lappert, M. F., Slade, M. J., Singh, A., Atwood, J. L., Rogers, R. D., and Shakir, R., *J. Am. Chem. Soc.* **105,** 302 (1983).
20. Armstrong, D. R., Mulvey, R. E., Walker, G. T., Barr, D., and Snaith, R., *J. Chem. Soc., Dalton Trans.* p. 617 (1988).
21. Armstrong, D. R., Barr, D., Clegg, W., Hodgson, S. M., Mulvey, R. E., Reed, D., Snaith, R., and Wright, D. S., *J. Am. Chem. Soc.* **111,** 4719 (1989).
22. Köster, H., Thoennes, D., and Weiss, E., *J. Organomet. Chem.* **160,** 1 (1978).
23. Schubert, B., and Weiss, E., *Angew. Chem.* **95,** 499 (1983); *Angew. Chem., Int. Ed. Engl.* **22,** 496 (1983).
24. Thoennes, D., and Weiss, E., *Chem. Ber.* **111,** 3157 (1978).
25. Schubert, B., and Weiss, E., *Chem. Ber.* **116,** 3212 (1983).
26. Seebach, D., Amstutz, R., Laube, T., Schweizer, W. B., and Dunitz, J. D., *J. Am. Chem. Soc.* **107,** 5403 (1985).
27. Schümann, U., Kopf, J., and Weiss, E., *Angew. Chem.* **97,** 222 (1985); *Angew. Chem., Int. Ed. Engl.* **24,** 215 (1985).
28. Klumpp, G. W., Vos, M., de Kanter, F. J. J., Slob, C., Krabbendam, H., and Spek, A. L., *J. Am. Chem. Soc.* **107,** 8292 (1985).
29. Lee, K.-S., Williard, P. G., and Suggs, J. W., *J. Organomet. Chem.* **299,** 311 (1986).
30. Jastrzebski, J. T. B. H., van Koten, G., Konijn, M., and Stam, C. H., *J. Am. Chem. Soc.* **104,** 5490 (1982).
31. Jastrzebski, J. T. B. H., van Koten, G., Christophersen, M. N., and Stam, C. H., *J. Organomet. Chem.* **292,** 319 (1985).
32. Moene, W., Vos, M., de Kanter, F. J. J., and Klumpp, G. W., *J. Am. Chem. Soc.* **111,** 3463 (1989).
33. van der Zeijden, A. A. H., and van Koten, G., *Recl. Trav. Chim. Pays-Bas* **107,** 431 (1988).
34. Klumpp, G. W., *Recl. Trav. Chim. Pays-Bas* **105,** 1 (1986).
34a. Snieckus, V., *Chem. Rev.* **90,** 879 (1990).
35. Wehmann, E., Jastrzebski, J. T. B. H., Ernsting, J.-M., Grove, D. M., and van Koten, G., *J. Organomet. Chem.* **353,** 145 (1988).

36. Schleyer, P.v.R., *Pure Appl. Chem.* **55,** 355 (1983); **56,** 151 (1984).
37. Streitwieser, A., *Acc. Chem. Res.* **17,** 353 (1984).
38. Reed, A. E., Weinstock, R. B., and Weinhold, F., *J. Chem. Phys.* **83,** 735 (1985).
39. Oliver, J. P., *Adv. Organomet. Chem.* **15,** 235 (1977).
40. O'Neill, M. E., and Wade, K., *in* "Comprehensive Organometallic Chemistry" (G. Wilkinson, F. G. A. Stone, and E. W. Abel, eds.), Vol. 1, p. 1. Pergamon, Oxford, 1982.
41. Wardell, J. L., *in* "Comprehensive Organometallic Chemistry" (G. Wilkinson, F. G. A. Stone, and E. W. Abel, eds.), Vol. 1, p. 43. Pergamon, Oxford, 1982.
42. Kaufmann, E., Schleyer, P.v.R., Houk, K. N., and Wu, Y.-D., *J. Am. Chem. Soc.* **107,** 5560 (1985).
43. Coates, G. E., Green, M. L. H., and Wade, K., "Organometallic Compounds: The Main Group Elements," 3rd ed., Vol. 1, pp. 35–38. Methuen, London, 1967.
44. Weiss, E., and Lucken, E. A. C., *J. Organomet. Chem.* **2,** 197 (1964); Weiss, E., and Hencken, G., *ibid.* **21,** 265 (1970).
45. Brockhart, M., and Green, M. L. H., *J. Organomet. Chem.* **250,** 395 (1983).
46. Rhine, W., Stucky, G. D., and Patterson, S. W., *J. Am. Chem. Soc.* **97,** 6401 (1975).
47. Zerger, R., Rhine, W., and Stucky, G. D., *J. Am. Chem. Soc.* **96,** 6048 (1974).
48. Tecle, B., Rahman, A. F. M. M., and Oliver, J. P., *J. Organomet. Chem.* **317,** 267 (1986).
49. Barr, D., Snaith, R., Mulvey, R. E., and Perkins, P. G., *Polyhedron* **7,** 2119 (1988).
50. Günther, H., Moskau, D., Bast, P., and Schmalz, D., *Angew. Chem.* **99,** 1242 (1987); *Angew. Chem., Int. Ed. Engl.* **26,** 1212 (1987).
51. Bauer, W., Clark, T., and Schleyer, P. v.R., *J. Am. Chem. Soc.* **109,** 970 (1987).
51a. Hoffmann, D., Bauer, W., and Schleyer, P. v.R., *J. Chem. Soc., Chem. Commun.* p. 208 (1990).
52. Ritchie, J. P., and Bachrach, S. M., *J. Am. Chem. Soc.* **109,** 5909 (1987).
53. Günther, H., Moskau, D., Dujardin, R., and Maercker, A., *Tetrahedron Lett.* **27,** 2251 (1986).
54. Hall, B., Farmer, J. B., Shearer, H. M. M., Sowerby, J. D., and Wade, K., *J. Chem. Soc., Dalton Trans.* p. 102 (1979).
55. Collier, M. R., Lappert, M. F., Snaith, R., and Wade, K., *J. Chem. Soc. D* p. 370 (1972).
56. Jennings, J. R., Snaith, R., Mahmoud, M. M., Wallwork, S. C., Bryan, S. J., Halfpenny, J., Petch, E. A., and Wade, K., *J. Organomet. Chem.* **249,** C1 (1983).
57. Snaith, R., Summerford, C., Wade, K., and Wyatt, B. K., *J. Chem. Soc. A* p. 2635 (1970).
58. Bryan, S. J., Clegg, W., Snaith, R., Wade, K., and Wong, E. H., *J. Chem. Soc., Chem. Commun.* p. 1223 (1987).
59. Farmer, J. B., Snaith, R., and Wade, K., *J. Chem. Soc. D* p. 1501 (1972).
60. Hall, B., Keable, J., Snaith, R., and Wade, K., *J. Chem. Soc., Dalton Trans.* p. 986 (1978).
61. Kilner, M., and Pinkney, J. N., *J. Chem. Soc. A* p. 2887 (1971).
62. Kilner, M., and Midcalf, C., *J. Chem. Soc., Dalton Trans.* p. 1620 (1974).
63. Chan, L.-H., and Rochow, E. G., *J. Organomet. Chem.* **9,** 231 (1967).
64. Anderson, H. J., Wang, N.-C., and Jwili, E. T. P., *Can. J. Chem.* **49,** 2315 (1971).
65. Pickard, P. L., and Talbot, T. L., *J. Org. Chem.* **26,** 4886 (1961).
66. Pattison, I., Wade, K., and Wyatt, B. K., *J. Chem. Soc. A* p. 837 (1968).
67. Samuel, B., Snaith, R., Summerford, C., and Wade, K., *J. Chem. Soc. A* p. 2019 (1970).
68. Sanger, A. R., *Inorg. Nucl. Chem. Lett.* **9,** 351 (1973).

69. Shearer, H. M. M., Wade, K., and Whitehead, G. *J. Chem. Soc., Chem. Commun.* p. 943 (1979).
70. Clegg, W., Snaith, R., Shearer, H. M. M., Wade, K., and Whitehead, G., *J. Chem. Soc., Dalton Trans.* p. 1309 (1983).
71. Barr, D., Clegg, W., Mulvey, R. E., Snaith, R., and Wade, K., *J. Chem. Soc., Chem. Commun.* p. 295 (1986).
72. Armstrong, D. R., Barr, D., Snaith, R., Clegg, W., Mulvey, R. E., Wade, K., and Reed, D., *J. Chem. Soc., Dalton Trans.* p. 1071 (1987).
73. Ilsley, W. H., Schaaf, T. F., Glick, M. D., and Oliver, J. P., *J. Am. Chem. Soc.* **102,** 3769 (1980).
74. Armstrong, D. R., and Walker, G. T., *J. Mol. Struct. (Theochem.)* **137,** 235 (1986).
75. Maercker, A., Bsata, M., Buchmeier, W., and Engelen, B., *Chem. Ber.* **117,** 2547 (1984).
76. Barr, D., Clegg, W., Mulvey, R. E., and Snaith, R., *J. Chem. Soc., Chem. Commun.* pp. 285, 287 (1984).
77. Barr, D., Clegg, W., Mulvey, R. E., and Snaith, R., *J. Chem. Soc., Chem. Commun.* p. 57 (1989).
78. Barr, D., Snaith, R., Clegg, W., Mulvey, R. E., and Wade, K., *J. Chem. Soc., Dalton Trans.* p. 2141 (1987).
79. Barr, D., Clegg, W., Mulvey, R. E., Reed, D., and Snaith, R., *Angew. Chem.* **97,** 322 (1985); *Angew. Chem., Int. Ed. Engl.* **24,** 328 (1985).
80. Fjeldberg, T., Hitchcock, P. B., Lappert, M. F., and Thorne, A. J., *J. Chem. Soc., Chem. Commun.* p. 822 (1984).
81. Engelhardt, L. M., May, A. S., Raston, C. L., and White, A. H., *J. Chem. Soc., Dalton Trans.* p. 1671 (1983).
82. Boche, G., Marsch, M., and Harms, K., *Angew. Chem.* **98,** 373 (1986); *Angew. Chem., Int. Ed. Engl.* **25,** 373 (1986).
83. Boche, G., Harms, K., and Marsch, M., *J. Am. Chem. Soc.* **110,** 6925 (1988).
84. Zarges, W., Marsch, M., Harms, K., and Boche, G., *Chem. Ber.* **122,** 1307 (1989).
85. Barr, D., Clegg, W., Mulvey, R. E., and Snaith, R., *J. Chem. Soc., Chem. Commun.* p. 79 (1984).
86. Barr, D., Clegg, W., Mulvey, R. E., and Snaith, R., *J. Chem. Soc., Chem. Commun.* p. 226 (1984).
87. Wittig, G., *Angew. Chem.* **70,** 65 (1958).
88. Eaborn, C., Hitchcock, P. B., Smith, J. D., and Sullivan, A. C., *J. Chem. Soc., Chem. Commun.* p. 827 (1983).
89. Schümann, U., and Weiss, E., *Angew. Chem.* **100,** 573 (1988); *Angew. Chem., Int. Ed. Engl.* **27,** 584 (1988).
90. Jackman, L. M., Scarmoutzos, L. M., and Porter, W., *J. Am. Chem. Soc.* **109,** 6524 (1987).
91. Dye, J. L., *Prog. Inorg. Chem.* **32,** 327 (1984).
92. Edmonds, R. N., Holton, D. M., and Edwards, P. P., *J. Chem. Soc., Dalton Trans.* p. 323 (1986).
93. Clegg, W., Mulvey, R. E., Snaith, R., Toogood, G. E., and Wade, K., *J. Chem. Soc., Chem. Commun.* p. 1740 (1986).
94. Reed, D., Barr, D., Mulvey, R. E., and Snaith, R., *J. Chem. Soc., Dalton Trans.* p. 557 (1986).
95. Barr, D., Snaith, R., Mulvey, R. E., Wade, K., and Reed, D., *Magn. Reson. Chem.* **24,** 713 (1986).
95a. Bauer, W., Winchester, W. R., and Schleyer, P. v. R., *Organometallics* **6,** 2371 (1987).

96. Fraenkel, G., Fraenkel, A. M., Geckle, M. J., and Schloss, F., *J. Am. Chem. Soc.* **101,** 4745 (1979).

97. Fraenkel, G., Henrichs, M., Hewitt, J. M., Su, B. M., and Geckle, M. J., *J. Am. Chem. Soc.* **102,** 3345 (1980).

98. Fraenkel, G., Henrichs, M., Hewitt, J. M., and Su, B. M., *J. Am. Chem. Soc.* **106,** 255 (1984).

99. Das, R., and Wilkie, C. A., *J. Am. Chem. Soc.* **94,** 4555 (1972).

100. Bauer, W., and Seebach, D., *Helv. Chim. Acta* **67,** 1972 (1984).

101. Armstrong, D. R., and Perkins, P. G., *Coord. Chem. Rev.* **38,** 139 (1981).

102. Kaufmann, E., Raghavachari, K., Reed, A. E., and Schleyer, P.v.R., *Organometallics* **7,** 1597 (1988).

103. Kaufmann, E., Gose, J., and Schleyer, P. v.R., *Organometallics* **8,** 2577 (1989).

103a. Würthwein, E.-U., Sen, K. D., Pople, J. A., and Schleyer, P. v.R., *Inorg. Chem.* **23,** 496 (1983).

104. Dewar, M. J. S., and Thiel, W., *J. Am. Chem. Soc.* **99,** 4899 (1977).

105. Clark, T., Rohde, C., and Schleyer, P. v.R., *Organometallics* **2,** 1344 (1983).

106. Thiel, W., and Clark, T., submitted for publication.

107. Glaser, R., and Streitwieser, A., *J. Mol. Struct.* **163,** 19 (1988).

108. Kaneti, J., Schleyer, P. v.R., Clark, T., Kos, A. J., Spitznagel, G. W., Andrade, J. G., and Moffat, J. B., *J. Am. Chem. Soc.* **108,** 1481 (1986).

109. Bachrach, S. M., and Streitwieser, A., *J. Am. Chem. Soc.* **106,** 2283, 5818 (1984).

110. Waterman, K. C., and Streitwieser, A., *J. Am. Chem. Soc.* **106,** 3138 (1984).

111. Sapse, A.-M., Raghavachari, K., Schleyer, P. v.R., and Kaufmann, E., *J. Am. Chem. Soc.* **107,** 6483 (1985).

112. Streitwieser, A., *J. Organomet. Chem.* **156,** 1 (1978).

113. Bushby, R. J., and Steel, H. L., *J. Organomet. Chem.* **336,** C25 (1987).

113a. Bushby, R. J., and Steel, H. L., *J. Chem. Soc., Perkin Trans. 2* p. 1143 (1990).

114. Kato, H., Hirao, K., and Akagi, K., *Inorg. Chem.* **20,** 3659 (1981).

115. Raghavachari, K., Sapse, A.-M., and Jain, D. C., *Inorg. Chem.* **26,** 2585 (1987).

116. Graham, G., Richtsmeier, S., and Dixon, D. A., *J. Am. Chem. Soc.* **102,** 5759 (1980).

117. Snow, M. R., *J. Am. Chem. Soc.* **92,** 3610 (1970).

118. Cremashi, P., Gamba, A., and Simonetta, M., *Theor. Chim. Acta* **40,** 303 (1975).

119. Wipff, G., Weiner, D., and Kollmann, P., *J. Am. Chem. Soc.* **104,** 3245 (1982).

120. Bushby, R. J., and Tytko, M. P., *J. Organomet. Chem.* **270,** 265 (1984).

121. Wipff, G., and Kollmann, P., *Nouv. J. Chem.* **9,** 457 (1985).

122. Hope, H., and Power, P. P., *J. Am. Chem. Soc.* **105,** 5320, (1983).

123. Spek, A. L., Duisenberg, A. J. M., Klumpp, G. W., and Geurink, P. J. A., *Acta Crystallogr., Sect. C* **C40,** 372 (1984).

124. Polt, R. L., Stork, G., Carpenter, G. B., and Williard, P. G., *J. Am. Chem. Soc.* **106,** 4276 (1984).

125. Jastrzebski, J. T. B. H., van Koten, G., Goubitz, K., Arlen, C., and Pfeffer, M., *J. Organomet. Chem.* **246,** C75 (1983).

126. Harder, S., Boersma, J., Brandsma, L., van Heteren, A., Kanters, J. A., Bauer, W., and Schleyer, P. v.R., *J. Am. Chem. Soc.* **110,** 7802 (1988).

127. Dietrich, H., Mahdi, W., and Storck, W., *J. Organomet. Chem.* **349,** 1 (1988).

128. Collins, J. B., Dill, J. D., Jemmis, E. D., Apeloig, Y., Schleyer, P. v.R., Seeger, R., and Pople, J. A., *J. Am. Chem. Soc.* **98,** 5419 (1976).

129. Nillsen, E. W., and Skancke, A., *J. Organomet. Chem.* **116,** 251 (1976).

130. Laidig, W. D., and Schäfer, H. F., *J. Am. Chem. Soc.* **100,** 5972 (1978).

131. Bachrach, S. M., and Streitwieser, A., *J. Am. Chem. Soc.* **106,** 5818 (1984).

132. Maercker, A., and Theis, M., *Top. Curr. Chem.* **138,** 1 (1987).

133. Harder, S., Boersma, J., Brandsma, L., Kanters, J. A., Bauer, W., and Schleyer, P.v.R., unpublished work.
134. Geissler, M., Schümann, U., and Weiss, E., *Proc. Int. Conf. Organomet. Chem. 12th*, Vienna, *1985* Abstracts, p. 12 (1985).
135. Geissler, M., Kopf, J., Schubert, B., Weiss, E., Neugebauer, W., and Schleyer, P.v.R., *Angew. Chem.* **99,** 569 (1987); *Angew. Chem., Int. Ed. Engl.* **26,** 587 (1987).
136. Williard, P. G., and Carpenter, G. B., *J. Am. Chem. Soc.* **107,** 3345 (1985).
137. Williard, P. G., and Carpenter, G. B., *J. Am. Chem. Soc.* **108,** 462 (1986).
138. Jastrzebski, J. T. B. H., van Koten, G., and van der Mieroop, W. F., *Helv. Chim. Acta* **142,** 169 (1988).
139. Amstutz, R., Schweizer, W. B., Seebach, D., and Dunitz, J. D., *Inorg. Chim. Acta* **64,** 2617 (1981).
140. Williard, P. G., and Salvino, J. M., *Tetrahedron Lett.* **26,** 3931 (1985).
141. Graalmann, O., Klingebiel, U., Clegg, W., Haase, M., and Sheldrick, G. M., *Angew. Chem.* **96,** 904 (1984); *Angew. Chem., Int. Ed. Engl.* **23,** 891 (1984).
142. Laube, T., Dunitz, J. D., and Seebach, D., *Helv. Chim. Acta* **68,** 1373 (1985).
143. Bauer, W., Laube, T., and Seebach, D., *Chem. Ber.* **118,** 764 (1985).
144. Hvoslef, J., Hope, H., Murray, B. D., and Power, P. P., *J. Chem. Soc., Chem. Commun.* p. 1438 (1983).
145. Çetinkaya, B., Gümrükçü, I., Lappert, M. F., Atwood, J. L., and Shakir, R., *J. Am. Chem. Soc.* **102,** 2086 (1980).
146. Amstutz, R., Dunitz, J. D., Laube, T., Schweizer, W. B., and Seebach, D., *Chem. Ber.* **119,** 434 (1986).
147. Barr, D., Snaith, R., Wright, D. S., Mulvey, R. E., and Wade, K., *J. Am. Chem. Soc.* **109,** 7891 (1987).
148. Barr, D., Doyle, M. J., Mulvey, R. E., Raithby, P. R., Reed, D., Snaith, R., and Wright, D. S., *J. Chem. Soc., Chem. Commun.* p. 318 (1989).
149. Schmidbaur, H., Schier, A., and Schubert, U., *Chem. Ber.* **116,** 1938 (1983).
150. Armstrong, D. R., Barr, D., Clegg, W., Mulvey, R. E., Reed, D., Snaith, R., and Wade, K., *J. Chem. Soc., Chem. Commun.* p. 869 (1986).
151. Wittig, G., and Hesse, A., *Org. Synth.* **50,** 66 (1970).
152. Rathke, M. W., and Lindert, A., *J. Am. Chem. Soc.* **93,** 2318 (1971).
153. Olofson, R. A., and Dougherty, C. M., *J. Am. Chem. Soc.* **95,** 581, 582 (1973).
154. Corey, E. J., and Gross, W., *Tetrahedron Lett.* **25,** 495 (1984).
155. Cliffe, I. A., Crossley, R., and Shepherd, R. B., *Synthesis* p. 1138 (1985).
156. Rannenberg, M., Hausen, H.-D., and Weidlein, J., *J. Organomet. Chem.* **376,** C27 (1989).
157. Barr, D., Clegg, W., Mulvey, R. E., and Snaith, R. unpublished observations.
158. Hitchcock, P. B., Lappert, M. F., and Smith, S. J., *J. Organomet. Chem.* **320,** C27 (1987).
159. Hitchcock, P. B., Lappert, M. F., Power, P. P., and Smith, S. J., *J. Chem. Soc., Chem. Commun.* p. 1669 (1984).
160. Andrew, P. C., Armstrong, D. R., Mulvey, R. E., and Reed, D., *J. Am. Chem. Soc.* **110,** 5235 (1988).
161. Grüning, R., and Atwood, J. L., *J. Organomet. Chem.* **137,** 101 (1977).
162. Williard, P. G., *Acta Crystallogr., Sect. C* **C44,** 270 (1988).
163. Barr, D., Clegg, W., Mulvey, R. E., Snaith, R., and Wright, D. S., *J. Chem. Soc., Chem. Commun.* 716 (1987).
164. Snaith, R., Barr, D., Wright, D. S., Clegg, W., Hodgson, S. M., Lamming, G. R., Scott, A. J., and Mulvey, R. E., *Angew. Chem.* **101,** 1279 (1989); *Angew. Chem., Int. Ed. Engl.* **28,** 1241 (1989).

165. Sapse, A.-M., Kaufmann, E., Schleyer, P. v.R., and Gleiter, R., *Inorg. Chem.* **23,** 1569 (1984).
166. Hodošček, M., and Šolmajer, T., *J. Am. Chem. Soc.* **106,** 1854 (1984).
166a. Kaufmann, E., Clark, T., and Schleyer, P. v.R., *J. Am. Chem. Soc.* **106,** 1856 (1984).
167. Armstrong, D. R., Perkins, P. G., and Walker, G. T., *J. Mol. Struct. (Theochem.)* **122,** 189 (1985).
168. Gregory, K., and Schleyer, P. v.R., unpublished results.
169. Raghavachari, K., Sapse, A.-M., and Jain, D. C., *Inorg. Chem.* **27,** 3862 (1988).
170. Kaufmann, E., Tidor, B., and Schleyer, P. v.R., *J. Comput. Chem.* **7,** 334 (1986).
171. Kolos, W., *Theor. Chim. Acta* **51,** 219 (1979).
172. Boys, S. F., and Bernardi, F., *Mol. Phys.* **19,** 553 (1970).
173. Clark, T., Chandrasekhar, J., Spitznagel, G., and Schleyer, P. v.R., *J. Comput. Chem.* **4,** 294 (1983).
174. Spitznagel, G., Clark, T., Chandrasekhar, J., and Schleyer, P.v.R., *J. Comput. Chem.* **3,** 363 (1982).
175. Chandrasekhar, J., Andrade, J. G., and Schleyer, P. v.R., *J. Am. Chem. Soc.* **103,** 5609 (1981).
176. Frisch, M. J., Pople, J. A., and Binkley, J. S., *J. Chem. Phys.* **80,** 3265 (1984).
177. Clegg, W., Snaith, R., and Wade, K., *Inorg. Chem.* **27,** 3861 (1988).
178. Armstrong, D. R., Perkins, P. G., and Stewart, J. J. P., *J. Chem. Soc., Dalton Trans.* p. 2277 (1973).
179. Durst, T., *in* "Comprehensive Carbanion Chemistry," Part B (E. Buncel and T. Durst, eds.) Elsevier, Amsterdam, 1984.
180. Normant, H., *Angew. Chem., Int. Ed. Engl.* **6,** 1046 (1967).
181. Mukhopadhyay, T., and Seebach, D., *Helv. Chim. Acta* **65,** 385 (1982).
182. Fraser, R. R., and Mansour, T. S., *Tetrahedron Lett.* **27,** 331 (1986).
183. Hey, E., Hitchcock, P. B., Lappert, M. F., and Rai, A. K., *J. Organomet. Chem.* **325,** 1 (1987).
184. Jones, R. A., Stuart, A. L., and Wright, T. C., *J. Am. Chem. Soc.* **105,** 7459 (1983).
185. Engelhardt, L. M., Jolly, B. S., Junk, P. C., Raston, C. L., Skelton, B. W., and White, A. H., *Aust. J. Chem.* **39,** 1337 (1986).
186. Çetinkaya, B., Hitchcock, P. B., Lappert, M. F., Misra, M. C., and Thorne, A. J., *J. Chem. Soc., Chem. Commun.* p. 148 (1984).
187. Bartlett, R. A., Chen, H., Dias, H. V. R., Olmstead, M. M., and Power, P. P., *J. Am. Chem. Soc.* **110,** 446 (1988).
188. Atwood, J. L., Bott, S. G., Hawkins, S. M., and Lappert, M. F., unpublished results.
189. Boese, R., and Klingebiel, U., *J. Organomet. Chem.* **315,** C17 (1986).
190. Bremer, M., Flock, R., and Schleyer, P.v.R., unpublished results.
191. Bartlett, R. A., Feng, X., Olmstead, M. M., Power, P. P., and Weese, K. J., *J. Am. Chem. Soc.* **109,** 4851 (1987).
192. Chen, H., Bartlett, R. A., Olmstead, M. M., Power, P. P., and Shoner, S. C., *J. Am. Chem. Soc.* **112,** 1048 (1990).
193. Paetzold, P., Pelzer, C., and Boese, R., *Chem. Ber.* **121,** 51 (1988).
194. Power, P. P., *Acc. Chem. Res.* **21,** 147 (1988).
195. Atwood, J. L., Lappert, M. F., Leung, W.-P., and Zhang, H., unpublished results.
196. Chen, H., Bartlett, R. A., Dias, H. V. R., Olmstead, M. M., and Power, P. P., *J. Am. Chem. Soc.* **111,** 4338 (1989).
197. Power, P. P., and Xiaojie, X., *J. Chem. Soc., Chem. Commun.* p. 358 (1984).
198. Bartlett, R. A., Dias, H. V. R., Hope, H., Murray, B. D., Olmstead, M. M., and Power, P. P., *J. Am. Chem. Soc.* **108,** 6921 (1986).
199. Bartlett, R. A., and Power, P. P., *J. Am. Chem. Soc.* **109,** 6509 (1987).

200. Kimura, B. Y., and Brown, T. L., *J. Organomet. Chem.* **26,** 57 (1971).
201. Jackman, L. M., and Scarmoutzos, L. M., *J. Am. Chem. Soc.* **109,** 5348 (1987).
202. Jackman, L. M., Scarmoutzos, L. M., and DeBrosse, C. W., *J. Am. Chem. Soc.* **109,** 5355 (1987).
203. Jackman, L. M., and DeBrosse, C. W., *J. Am. Chem. Soc.* **105,** 4177 (1983).
204. Jackman, L. M., and Smith, B. D., *J. Am. Chem. Soc.* **110,** 3829 (1988).
205. Kallman, N., and Collum, D. B., *J. Am. Chem. Soc.* **109,** 7466 (1987).
206. Galiano-Roth, A. S., Michaelides, E. M., and Collum, D. B., *J. Am. Chem. Soc.* **110,** 2658 (1988).
207. Seebach, D., Bauer, W., Hansen, J., Laube, T., Schweizer, W. B., and Dunitz, J. D., *J. Chem. Soc., Chem. Commun.* p. 853 (1984).
208. DePue, J. S., and Collum, D. B., *J. Am. Chem. Soc.* **110,** 5518 (1988).
209. DePue, J. S., and Collum, D. B., *J. Am. Chem. Soc.* **110,** 5524 (1988).
210. Galiano-Roth, A. S., and Collum, D. B., *J. Am. Chem. Soc.* **111,** 6772 (1989).
211. Seebach, D., and Bauer, W., *Helv. Chim. Acta* **67,** 1972 (1984).